On natural convection flow of micropolar fluid

A THESIS SUBMITTED TO THE DEPARTMENT OF MATHEMATICS IN PARTIAL FULFILLMENT OF THE REQUIREMENTS FOR THE DEGREE OF DOCTOR OF PHILOSOPHY

Submitted by

Md. Mosharof hossain

Registration No: 76

Session: 2017-2018

To

Department of Mathematics

University of Dhaka

Dhaka-1000

Dedicated

to

My beloved parents

Certificate:

This is to certify that the thesis entitled

"**On natural convection flow of micropolar fluid**"

is submitted by Md. Mosharof Hossain in May, 2019 in partial fulfillment of the requirements for the degree of Doctor of Philosophy in the department of Mathematics, University of Dhaka. This work is absolutely based upon his own work under my supervision and neither this thesis nor any part of it has been submitted for any degree/diploma or any other academic award anywhere before.

Professor Amulya Chandra Mandal
Department of Mathematics
University of Dhaka
Dhaka-1000, Bangladesh.

Abstract

The aim of our study, which consists of six chapters, is to study some problems on heat transfer with convection in the micropolar fluids. In the following, a brief discussion of the chapters is given.

Chapter Two contains a brief overview of research works on the boundary layer flow of a micropolar fluid along a vertical plate. The literature review exposes the necessity of investigation of this problem. It also gives the step by step development of the problem. Although there are numerous studies on the boundary layer characteristics of micropolar fluid along a vertical plate, nevertheless further investigation needs to be done.

In Chapte Three, an analysis is performed to study the shear stress, the couple-stress and heat transfer characteristics of a laminar mixed convection boundary layer flow of a micropolar fluid past an isothermal permeable plate. The governing nonsimilar boundary layer equations are analyzed using the (i) series solution for small ξ, (ii) asymptotic solution for large ξ and (iii) primitive-variable formulation and the stream function formulation are being used for all ξ. The effects of the material parameters, such as, the vortex viscosity parameter, K, and the transpiration parameter, s, on the shear stress, the couple-stress and heat transfer have been investigated. The agreement between the solutions obtained from the stream-function formulation and the primitive-variable formulation is found to be excellent.

The unsteady free convection boundary layer flow of a thermo-micropolar fluid along a vertical plate with effect of micropolar heat conduction has been investigated inChapter Four. The governing equations are transformed into a new form using a method of transformed coordinates. We then use an explicit finite difference scheme to solve the transformed equations. Here, the governing equations have been reduced to the forms that are valid for entire, small and large time regimes, by using stream-function formulation. The results obtained for the above mentioned three time regimes are compared and found in excellent agreement. Moreover, the effects of the physical parameters such as the viscosity parameter, K, and the heat conduction parameter, α^*, are presented in terms of the transient shear stress, couple stress and surface heat transfer coefficient as well as transient velocity profiles, angular velocity profiles and temperature profiles.

In Chapte Five, the unsteady free convection boundary layer flow of a thermo-micropolar fluid along a vertical plate has been investigated in this paper. The temperature of the plate is assumed to be oscillating about a mean temperature, $\theta_w(x)$, with small amplitude ε. The governing boundary layer equations are analyzed using straight forward finite difference method. The effects of the material parameters such as micropolar heat conduction parameter, N^*, the vortex viscosity parameter, K, on the shear stress, τ_ω, surface heat transfer, q_ω, and the couple-stress, m_ω, have been investigated.

Chapter Six concerns the boundary layer characteristics of the free convection flow of a thermo-micropolar fluid from a vertical surface with the effect of stream wise sinusoidal variation of the surface temperature. The dimensionless boundary layer equations are solved using the straight forward finite difference method. Results are presented in terms of the skin friction, couple stress and heat transfer coefficients with the variation of the micropolar heat conduction parameter, the vortex viscosity parameter andthe amplitude of surface temperature. We also discussed the effects of these parameters on the streamlines, isoclines of angular velocity and isoclines of temperature.

Acknowledgement

At first, I earnestly thank to my creator for his blessing to complete this thesis. I would like to express my profound gratitude and appreciation to Dr. Amulya Chandra Mandal, Professor, Department of Mathematics, University of Dhaka, Bangladesh for his proper guidance and supervision. I also like to thank Dr. Md. Anwar hossain, Professor Department of Mathematics, who always eagerly monitored my thesis work and used to suggest me where necessary. From the very beginning I have known him and he is always an inspiration for me. The reflection of his tireless mentoring, resourceful instructions and innovative remark could be found throughout this work.

I am grateful to my parents and specially to my beloved mother who is no longer among us for her incessant inspirations and sacrificing help to pursue my studies effortlessly. She was and will remain an encouraging and motivating character for the rest of my life.

I express my gratitude to the chairman of the Department of Mathematics, Professor Dr. Amal Krishna Halder for his helpful support and providing me the computer lab facilities. I would also like to express my deep gratitude to my honorable teachers of the department for their caring suggestion and inspirations. I cordially thank all the staffs in the Department.

I would like to convey many thanks to Dr. Nepal Chandra Roy and Dr. Md. Kamrujjaman for their cooperation in all respects. I would also like to thank other faculty members of this Department. Last but not the least, I would like to thank all my relatives, batchmates and friends for their encouragements and good wishes all the time.
Finally, I am grateful to my family members for their patience and helps.

Md. Mosharof hossain

Contents

Nomenclature

a = amplitude of oscillation

B = dimensionless modified Grashof number

c_p = specific heat capacity

f = dimensionless stream function

g = the acceleration due to gravity

g = dimensionless micro rotation

G = dimensionless component of micro rotation

G = dimensionless angular velocity

Gr = Grashof number

j = micro inertia per unit mass

j_o = reference value (L^2)

K = vortex viscosity parameter (κ/μ)

L = characteristic length

m = couple-stress

m_ω = couple-stress

n = a real number

$\bar{N}$ = dimensional angular velocity

$\bar{N}$ = component of micro rotation

N =dimensionless angular velocity

N^* = micropolar heat conduction parameter

Nu = Nusselt number

Pr = Prandtl number (ν/α)

q = surface heat flux

Re =Reynolds number ($U_0 L / \nu$)

$\bar{T}$ = dimensional temperature

T = temperature of the fluid in the boundary layer region

$\bar{T}_\infty$ = dimensional temperature of the ambient fluid

s = transpiration parameter

t = time

U_0 = free stream velocity

$\bar{T}_w$ = dimensional temperature of the fluid at the surface $T_w > T_\infty$

V_0 = surface mass flux

u = dimensionless velocity components to the *x* co-ordinates

v = dimensionless velocity components to the *y* co-ordinates

$\bar{u}, \bar{v}$ = velocity components

$\bar{u}, \bar{v}$ = dimensional velocity components along the $\bar{x}, \bar{y}$ axes

u, v = dimensionless fluid velocities components along the *x*, *y* axes

U, V = fluid velocities in the *X*- and *Y*-direction respectively

$\bar{x}, \bar{y}$ = dimensional stream wise and cross-stream Cartesian coordinate

x, y = stream wise and cross-stream Cartesian coordinates

X, Y = non dimensional stream wise and cross-stream Cartesian coordinates

η similarity variable

κ = thermal conductivity

ψ = stream function

θ = dimensionless temperature in the boundary layer

μ = dynamic viscosity of the fluid/ dynamic viscosity

α = thermal diffusivity (κ/ρ)

β = coefficient of volume expansion

α_c = the micropolar conductivity

α^* = micro polar heat conduction parameter

ν = viscosity coefficient (μ/ρ)

ρ = density of the fluid (m/ V)

τ = the shear stress the surface shear stress

γ = gyro viscosity coefficient(spin-gradient viscosity) $(\mu + \kappa/2)\, j$

τ = non-dimensional, reduced time

τ_ω = surface shear stress

θ, Θ dimensionless temperature

List of Figures

List of Tables

Chapter One
Introduction

The concept of micropolar fluids introduced by Eringen [1] deals with a class of fluids, which exhibit certain microscopic effects arising from the local structure and micromotions of the fluid elements. These fluids contain dilute suspensions of rigid micromolecules with individual motions, which support stress and body moments and are influenced by spin-inertia. The theory of micropolar fluid and its extension to thermomicropolar fluids [2] may form suitable non Newtonian fluid models which can be used to analyze the behavior of exotic lubricants [3, 4], colloidal suspensions or polymeric fluids [5], liquid crystals [6, 7], and animal blood [8]. Kolpashchikov et al. [9] have derived a method to measure micropolar parameters experimentally. A thorough review of this subject and application of micropolar fluid mechanics has been provided by Ariman et al. [10, 11]. On the other hand, Rees and Bassom [12] investigated the Blasius boundary-layer flow of a micropolar fluid over a flat plate. In this investigation, detailed numerical results and an asymptotic analysis for large distances from the leading edge have been presented.

Studies of heat convection in micropolar fluids have been focused on a flat plate [13–17] and on a wavy surface [18]. Hossain and Chowdhury [19] investigated the effect of material parameters on the mixed convection flow of thermomicropolar fluid from a vertical as well as a horizontal heat surface taking into consideration that the spin-gradient viscosity is non-uniform. Later, Hossain et al. [20] investigated the problem for a viscous incompressible thermomicropolar fluid with uniform spin gradient over a flat plate with a small inclination to the horizontal.

The importance of suction and blowing in controlling the boundary layer thickness and the rate of heat transfer has motivated many researchers to investigate its effects on forced and free convection flows. Eichhorn [21] considered power law variations in the plate temperature and transpiration velocity and found similarity solutions of the problem. Sparrow and Cess [22] discussed the case of constant plate temperature and transpiration velocity and obtained series expansions for temperature and velocity distributions in powers of $x^{1/2}$, where x is the distance in the stream-wise direction measured from the leading edge. Later, Merkin [23, 24] and Perikh et al. [25] presented numerical solutions for free convection heat transfer with blowing along an isothermal vertical flat plate. Hartnett and Eckert [26] and Sparrow

and Starr [27] reported the characteristics of heat transfer and skin-friction for pure forced convection with blowing; the former was dealt with a non-similar case. Local non-similar solutions for convection flow with arbitrary transpiration velocity were obtained by Kao [28, 29] applying GoÈrtler-Meksin transformations. Free convection flow along a vertical plate with arbitrary blowing and wall temperature has also been investigated by Vedhanayagam et al. [30]. With this understanding, Yucel [31] investigated mixed convection micropolar fluid flow over horizontal plate with uniform surface mass flux blowing and suction through the surface. Recently, Attia [32] investigated the steady laminar flow of an incompressible micropolar fluid over a porous flat plate considering the heat generation. Recently, the MHD boundary-layer flow of a micropolar fluid past a wedge with variable wall temperature has been discussed by Ishak et al. [33]. In addition to, mixed convection flow of a micropolar fluid from an isothermal vertical plate has been investigated by Jena and Mathur [34].

Apart from permeable flat plate, the surface condition, buoyancy force and thermal conductivity of the micropolar fluid play an important role in the flow and heat transfer. Hossain et al. [19, 35] investigated two-dimensional mixed convection and natural convection flow of a viscous incompressible thermomicropolar fluid with uniform spin-gradient over a flat plate. Later, Jena and Mathur [13–14] studied the similarity solutions for the steady laminar free convection boundary layer flow of a thermomicropolar fluid past a non-isothermal vertical flat plate. Recently, a model on natural convection flow of a thermomicropolar fluid along a porous vertical surface has been studied by Mosharof et al. [36]. But all the above studies pertain to steady flows.

However, Gorla and Takhar [37] examined the effect of buoyancy force on an unsteady incompressible micropolar fluid in the vicinity of the lower stagnation point of a circular cylinder. More or less recent studies on transient boundary layer flow of micropolar fluid without or with buoyancy effect have been done by Kumari and Nath [38], Lok et al. [39] and Xu et al. [40]. Unsteady mixed convection flow of thermomicropolar fluid along a vertical thin cylinder and a vertical wavy surface have been investigated in [41–45]. Very recently, Mahfooz et al. [46] have studied the fluctuating free convection boundary layer flow of a thermo-micropolar fluid along a vertical plate considering the small amplitude temperature oscillations about a variable surface temperature.

In this regard, an important thermal condition which can significantly affect the boundary layer characteristics is the oscillating surface temperature about a mean temperature with small amplitude.

It is worth mentioning that unsteady laminar boundary layer theory, one area of study, which has received much attention in the past deals with boundary layer responses to

imposed oscillations. Lighthill [47] was the first to study the unsteady forced flow of a viscous incompressible fluid past a flat plate and a circular cylinder with small amplitude oscillation in free stream. The corresponding problem of unsteady free convection flow along a vertical plate with oscillating surface temperature was studied by Nanda and Sharma [48] and Eshghy et al. [49]. In consideration of this class of problems, Muhuri and Maiti [50] and Verma [51] analysed the effect of oscillation of the surface temperature on the unsteady free convection along a horizontal plate. All the above investigations are based on the assumption that the surface temperature oscillates with small amplitude about the uniform mean temperature and they were carried out employing the Karman-Pohlhausen approximate integral method. Based on the linearized theory, Kelleher and Yang [52] have studied the heat transfer responses of a laminar free convection boundary layer along a vertical heated plate to surface temperature oscillations, when the mean surface temperature $T_\omega(x)$ is proportional to x^n, where x is the distance measured from the leading edge of the plate. This study had been extended by Hossain et al [53, 54] for magnetohydrodynmic flows for variable mean surface temperature and surface heat flux. Recent investigation on fluctuating hydro-magnetic natural convection flow of an optically gray fluid past a magnetized vertical surface with effect of thermal radiation has been made by Ashraf et al. [55]. On the other hand, Jaman et al. [56] extend the problem posed by Kelleher and Yang [57] for the case of the flow past a circular cylinder.

Above all, the streamwise variation of the surface temperature might have considerable influence on the skin friction and heat transfer along a vertical surface.

Jena and Mathur [13] have focused on the laminar free convection boundary layer flow of a thermomicropolar fluid past a non-isothermal vertical flat plate. They obtained the similarity solutions of the problem assuming the variation in the temperature of the plate as a linear function of the distance. Authors also examined the influence of suction/injection in the laminar free convection flow of a thermomicropolar fluid subject to a nonuniform heating along the vertical flat plate [14]. Numerical solutions were presented in terms of the velocity, microrotation and temperature fields and the heat transfer coefficient with variation of the boundary condition parameter and suction/injection parameter. Gorla et al. [58] investigated the magnetohydrodynamic boundary layer characteristics for the steady free convection of a thermomicropolar fluid. They have presented the influences of the material properties and the Prandtl number. Hossain et al. [20] performed numerical simulation for the laminar free convection flow of a thermomicropolar fluid while an isothermal plate is taken to be inclined

at a small angle to the horizontal. Recently, Mosharof et al. [44, 59] analyzed the unsteady boundary layer characteristics for free convection flow considering fluctuating surface temperature and a non-uniformly heated vertical plate, respectively. However there are a number of studies [60–62] dealt with the free convection along a vertical plate with the stream wise variations of surface temperature.

In the present dissertation, some problems on free convection flow of thermomicropolar fluid from vertical plate have been investigated. Details discusses are given in the following problems [63] free convection flow of thermomicropolar fluid along a verticall plate with non-uniform surface temperature and surface heat flux, [64] natural convection of thermomicropolar fluid from an isothermal surface inclined at a small angle to the horizontal, [65] mixed convection flow of micropolar fluid with variable spin gradient viscosity along an isothermal vertical plate, and [66] mixed convection flow of a micropolar fluid over a horizontal plate with variable spin gradient viscosity.

1.1 Outline of Thesis

The problem considered in Chapter Three is concerned with the boundary layer flow and heat transfer from a permeable flat surface with uniform surface temperature and uniform surface mass flux. So far the authors concern, this has not been discussed in the literature. The transformed boundary layer equations are solved numerically near to and far from the leading edge, using extended series solutions and asymptotic series solutions. Solutions for intermediate locations are obtained using the primitive-variable formulation as well as by the stream-function formulation. In this investigation, we have considered only the suction case and the effects of the material parameters such as the vortex viscosity parameter, K, the transpiration parameter, s, on the shear stress, the couple-stress and heat transfer are presented graphically. The results illustrate the different behavior that occurs when these parameters are varied.

In Chapter Four, we propose to study the unsteady free convection boundary layer flow of a thermo-micropolar fluid along a heated vertical plate, considering the presence of micropolar heat conduction the reduced governing equations that are valid for entire time regimes are solved using explicit finite difference method. Asymptotic solutions for small and large time are also obtained. The results thus obtained are comparered and found in excellent agreement. We further have studied the effect of the physical parameters, such as, the vortex viscosity parameter, K, and the heat conduction parameter, α^*, in terms of the transient shear stress, couple stress and surface heat transfer coefficients as well as transient velocity profiles, angular velocity profiles and temperature profiles.

The unsteady free convection boundary layer flow of a thermomicropolar fluid along a vertical plate has been investigated in Chapter Five considering that the surface temperature is oscillating about a mean temperature $\theta_w(x)$ with a small amplitude ε as posed by Kelleher and Yang [57]. With author's best knowledge, this problem has not been discussed in the literature.

Chapter Six deals with the boundary layer characteristics of the free convection flow of a thermomicropolar fluid along a vertical plate with the effect of streamwise sinusoidal variation of the surface temperature. We solve the dimensionless governing equations employing the straight forward finite difference method. The effects of the physical parameters are discussed in terms of skin friction, couple stress and heat transfer coefficients. Moreover the variations of streamlines, isolines of angular velocity and isolines of temperature with the change of the parameters are presented.

Chapter Two
Governing Equations

2.1 Introduction

This theory includes the effects of local rotary inertia and couple stresses which are not present in the theory of Newtonian fluids. The micropolar model has been proposed to study flows of fluids made up of large molecules and flows of suspensions.

In the present chapter the boundary layers equations for a micropolar fluids are developed. Which are appropriate for the thermomicropolar fluids. As proposed by Peddieson and Nitt.

2.2 The boundary layer equations for thermomicropolar fluids

The mass, momentum, angular momentum and energy balance equations for the incompressible fluid as prescribed Peddieson and Nitt are given below.

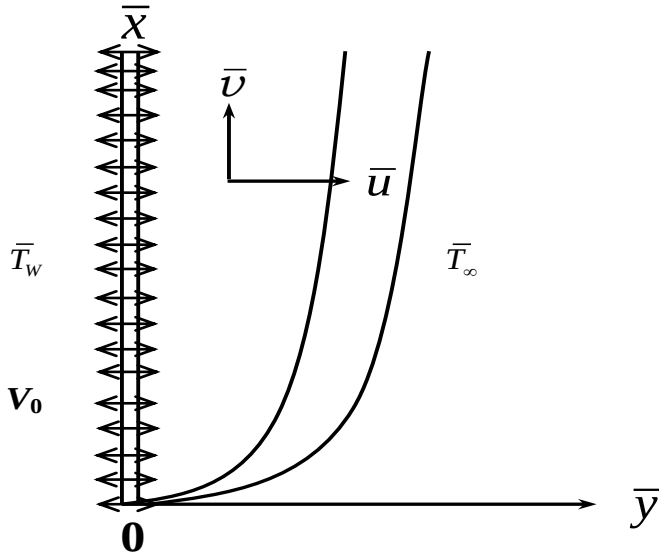

Fig. 2.1: The flow configuration and the coordinate system

Continuity equation

$$\nabla \cdot \boldsymbol{V} = 0 \tag{2.1}$$

Momentum equation

$$\rho_0 \frac{d\boldsymbol{V}}{dt} = -\nabla p + (\mu + \kappa)\nabla^2 \boldsymbol{V} + \kappa \nabla \times \boldsymbol{N} + \rho \boldsymbol{g} \tag{2.2}$$

Angular momentum equation

$$\rho_0 j \frac{d\boldsymbol{N}}{dt} = (\varepsilon + \beta')\nabla(\nabla.\boldsymbol{V}) + \gamma \nabla^2 \boldsymbol{N} + \kappa \nabla \times \boldsymbol{V} - 2\kappa \boldsymbol{N} \tag{2.3}$$

Energy equation

$$\rho_0 c_v \frac{dT}{dt} = k_T \nabla^2 T + \alpha_c (\nabla \times \boldsymbol{N}).\nabla T \tag{2.4}$$

Where ∇, neblla vector, ∇^2, laplacian operatore, $\boldsymbol{V}$, velocity vector, ρ_0, reference density, ρ, density, p, pressure, μ, dynamic viscosity, κ, thermal conductivity, $\boldsymbol{N}$, the components of the gyration vector to the x, y, z plane, $\boldsymbol{g}$, gravitational acceleration vector, j, microinertia constant, ε, β' and γ stands for micropolar coefficients of viscosity, c_v, specific heat at constant volume, and α_c, coefficient giving account of the coupling between the spin flux and the heat flux which is also micropolar thermal conductivity, T, temperature.

$$\boldsymbol{V} = \hat{i}\,u + \hat{j}\,v + \hat{k}w,\ \boldsymbol{N} = \hat{i}N_1 + \hat{j}N_2 + \hat{k}N_3,\ \boldsymbol{g} = \hat{i}g_x + \hat{j}g_y + \hat{k}g_z$$

$\boldsymbol{u}$, $\boldsymbol{v}$, $\boldsymbol{w}$ are the vectors components of $\boldsymbol{V}$

$\frac{d}{dt} = \frac{\partial}{\partial t} + u\frac{\partial}{\partial x} + v\frac{\partial}{\partial y} + w\frac{\partial}{\partial z}$ is the material derivatives

$$\nabla = \hat{i}\frac{\partial}{\partial x} + \hat{j}\frac{\partial}{\partial y} + \hat{k}\frac{\partial}{\partial z},\ \nabla^2 = \frac{\partial^2}{\partial x^2} + \frac{\partial^2}{\partial y^2} + \frac{\partial^2}{\partial z^2} \tag{2.5}$$

Where $\hat{i}$, $\hat{j}$ and $\hat{k}$ are unit vectors in x, y and z directions

Divergence of the velocity vector $\boldsymbol{V}$

$$\nabla.\boldsymbol{V} = = \frac{\partial u}{\partial x} + \frac{\partial v}{\partial y} + \frac{\partial w}{\partial z} \tag{2.6}$$

Curl $\boldsymbol{N}$ is unit of the angular velocity vector

$$\nabla \times \boldsymbol{N} = = i\left(\frac{\partial N_3}{\partial y} - \frac{\partial N_2}{\partial z}\right) - j\left(\frac{\partial N_3}{\partial x} - \frac{\partial N_1}{\partial z}\right) + k\left(\frac{\partial N_2}{\partial x} - \frac{\partial N_1}{\partial y}\right) \tag{2.7}$$

The gyration vector $\boldsymbol{N}$ is defined by

$$\boldsymbol{N} = \nabla \times \boldsymbol{V} = i\left(\frac{\partial w}{\partial y} - \frac{\partial v}{\partial z}\right) - j\left(\frac{\partial w}{\partial x} - \frac{\partial u}{\partial z}\right) + k\left(\frac{\partial v}{\partial x} - \frac{\partial u}{\partial y}\right) \tag{2.8}$$

$$\nabla \boldsymbol{T} = \left(\hat{i}\frac{\partial T}{\partial x} + \hat{j}\frac{\partial T}{\partial y} + \hat{k}\frac{\partial T}{\partial z}\right)$$

2.3 For three dimensional flows the equations can be

Under the above assumptions, the governing boundary layer equations are:

Continuity equation

$$\frac{\partial \bar{u}}{\partial \bar{x}} + \frac{\partial \bar{v}}{\partial \bar{y}} + \frac{\partial \bar{w}}{\partial \bar{z}} = 0 \tag{2.9}$$

Momentum equation

$$\rho_0 \left(\frac{\partial \bar{u}}{\partial \bar{t}} + \bar{u} \frac{\partial \bar{u}}{\partial \bar{x}} + \bar{v} \frac{\partial \bar{u}}{\partial \bar{y}} + \bar{w} \frac{\partial \bar{u}}{\partial \bar{z}} \right) = -\frac{\partial \bar{p}}{\partial \bar{x}} + (\mu + \kappa) \left(\frac{\partial^2 \bar{u}}{\partial \bar{x}^2} + \frac{\partial^2 \bar{u}}{\partial \bar{y}^2} + \frac{\partial^2 \bar{u}}{\partial \bar{z}^2} \right) + \kappa \left(\frac{\partial \bar{N}_3}{\partial \bar{y}} - \frac{\partial \bar{N}_2}{\partial \bar{z}} \right) + \rho g_x \tag{2.10}$$

y linear momentum equation

$$\rho_0 \left(\frac{\partial \bar{v}}{\partial \bar{t}} + \bar{u} \frac{\partial \bar{v}}{\partial \bar{x}} + \bar{v} \frac{\partial \bar{v}}{\partial \bar{y}} + \bar{w} \frac{\partial \bar{v}}{\partial \bar{z}} \right) = -\frac{\partial \bar{p}}{\partial \bar{y}} + (\mu + \kappa) \left(\frac{\partial^2 \bar{v}}{\partial \bar{x}^2} + \frac{\partial^2 \bar{v}}{\partial \bar{y}^2} + \frac{\partial^2 \bar{v}}{\partial z^2} \right) - \kappa \left(\frac{\partial \bar{N}_3}{\partial \bar{x}} - \frac{\partial \bar{N}_1}{\partial \bar{z}} \right) + \rho g_y \tag{2.11}$$

z linear momentum equation

$$\rho_0 \left(\frac{\partial \bar{w}}{\partial \bar{t}} + \bar{u} \frac{\partial \bar{w}}{\partial \bar{x}} + \bar{v} \frac{\partial \bar{w}}{\partial \bar{y}} + \bar{w} \frac{\partial \bar{w}}{\partial \bar{z}} \right) = -\frac{\partial \bar{p}}{\partial \bar{z}} + (\mu + \kappa) \left(\frac{\partial^2 \bar{w}}{\partial \bar{x}^2} + \frac{\partial^2 \bar{w}}{\partial \bar{y}^2} + \frac{\partial^2 \bar{w}}{\partial \bar{z}^2} \right) + \kappa \left(\frac{\partial \bar{N}_2}{\partial \bar{x}} - \frac{\partial \bar{N}_1}{\partial \bar{y}} \right) + \rho g_z \tag{2.12}$$

x angular momentum equation

$$\rho_0 j \left(\frac{\partial \bar{N}_1}{\partial \bar{t}} + \bar{u} \frac{\partial \bar{N}_1}{\partial \bar{x}} + \bar{v} \frac{\partial \bar{N}_1}{\partial \bar{y}} + \bar{w} \frac{\partial \bar{N}_1}{\partial \bar{z}} \right) = (\varepsilon + \beta') \left(\frac{\partial^2 \bar{N}_1}{\partial x^2} + \frac{\partial^2 \bar{N}_2}{\partial x \partial y} + \frac{\partial^2 \bar{N}_3}{\partial x \partial z} \right) + \gamma \left(\frac{\partial^2 \bar{N}_1}{\partial \bar{x}^2} + \frac{\partial^2 \bar{N}_1}{\partial \bar{y}^2} + \frac{\partial^2 \bar{N}_1}{\partial \bar{z}^2} \right) + \kappa \left(\frac{\partial \bar{w}}{\partial \bar{y}} - \frac{\partial \bar{v}}{\partial \bar{z}} \right) - 2\kappa \bar{N}_1 \tag{2.13}$$

y angular momentum equation

$$\rho_0 j \left(\frac{\partial \bar{N}_2}{\partial \bar{t}} + \bar{u} \frac{\partial \bar{N}_2}{\partial \bar{x}} + \bar{v} \frac{\partial \bar{N}_2}{\partial \bar{y}} + \bar{w} \frac{\partial \bar{N}_2}{\partial \bar{z}} \right) = (\varepsilon + \beta') \left(\frac{\partial^2 \bar{N}_1}{\partial y \partial x} + \frac{\partial^2 \bar{N}_2}{\partial y^2} + \frac{\partial^2 \bar{N}_3}{\partial y \partial z} \right) + \gamma \left(\frac{\partial^2 \bar{N}_2}{\partial \bar{x}^2} + \frac{\partial^2 \bar{N}_2}{\partial \bar{y}^2} + \frac{\partial^2 \bar{N}_2}{\partial \bar{z}^2} \right) - \kappa \left(\frac{\partial \bar{w}}{\partial \bar{x}} - \frac{\partial \bar{u}}{\partial \bar{z}} \right) - 2\kappa \bar{N}_2 \tag{2.14}$$

z angular momentum equation

$$\rho_0 j\left(\frac{\partial \bar{N}_3}{\partial \bar{t}}+\bar{u}\frac{\partial \bar{N}_3}{\partial \bar{x}}+\bar{v}\frac{\partial \bar{N}_3}{\partial \bar{y}}+\bar{w}\frac{\partial \bar{N}_3}{\partial \bar{z}}\right)=(\varepsilon+\beta')\left(\frac{\partial^2 \bar{N}_1}{\partial z\partial x}+\frac{\partial^2 \bar{N}_2}{\partial z\partial y}+\frac{\partial^2 \bar{N}_3}{\partial z^2}\right)$$
$$+\gamma\left(\frac{\partial^2 \bar{N}_3}{\partial \bar{x}^2}+\frac{\partial^2 \bar{N}_3}{\partial \bar{y}^2}+\frac{\partial^2 \bar{N}_3}{\partial \bar{z}^2}\right)+\kappa\left(\frac{\partial \bar{v}}{\partial \bar{x}}-\frac{\partial \bar{u}}{\partial \bar{y}}\right)-2\kappa \bar{N}_3 \tag{2.15}$$

Energy equation

$$\rho_0 c_v\left(\frac{\partial \bar{T}}{\partial \bar{t}}+\bar{u}\frac{\partial \bar{T}}{\partial \bar{x}}+\bar{v}\frac{\partial \bar{T}}{\partial \bar{y}}+\bar{w}\frac{\partial \bar{T}}{\partial \bar{z}}\right)=\kappa_T\left(\frac{\partial^2 \bar{T}}{\partial \bar{x}^2}+\frac{\partial^2 \bar{T}}{\partial \bar{y}^2}+\frac{\partial^2 \bar{T}}{\partial \bar{z}^2}\right)$$
$$+\alpha_c\left[\left(\frac{\partial T}{\partial x}\frac{\partial N_3}{\partial y}-\frac{\partial T}{\partial x}\frac{\partial N_2}{\partial z}\right)-\left(\frac{\partial T}{\partial y}\frac{\partial N_3}{\partial x}-\frac{\partial T}{\partial y}\frac{\partial N_1}{\partial z}\right)+\left(\frac{\partial T}{\partial z}\frac{\partial N_2}{\partial x}-\frac{\partial T}{\partial z}\frac{\partial N_1}{\partial y}\right)\right] \tag{2.16}$$

2.4 For two dimensional flows the equations can be

Continuity equation

$$\frac{\partial \bar{u}}{\partial \bar{x}}+\frac{\partial \bar{v}}{\partial \bar{y}}=0 \tag{2.17}$$

x linear momentum equation

$$\rho_0\left(\frac{\partial \bar{u}}{\partial \bar{t}}+\bar{u}\frac{\partial \bar{u}}{\partial \bar{x}}+\bar{v}\frac{\partial \bar{u}}{\partial \bar{y}}\right)=-\frac{\partial \bar{p}}{\partial \bar{x}}+(\mu+\kappa)\left(\frac{\partial^2 \bar{u}}{\partial \bar{x}^2}+\frac{\partial^2 \bar{u}}{\partial \bar{y}^2}\right)+\kappa\frac{\partial \bar{N}_3}{\partial \bar{y}}+\rho g_x \tag{2.18}$$

y linear momentum equation

$$\rho_0\left(\frac{\partial \bar{v}}{\partial \bar{t}}+\bar{u}\frac{\partial \bar{v}}{\partial \bar{x}}+\bar{v}\frac{\partial \bar{v}}{\partial \bar{y}}\right)=-\frac{\partial \bar{p}}{\partial \bar{y}}+(\mu+\kappa)\left(\frac{\partial^2 \bar{v}}{\partial \bar{x}^2}+\frac{\partial^2 \bar{v}}{\partial \bar{y}^2}\right)-\kappa\frac{\partial \bar{N}_3}{\partial \bar{x}}+\rho g_y \tag{2.19}$$

z angular momentum equation

$$\rho_0 j\left(\frac{\partial \bar{N}_3}{\partial \bar{t}}+\bar{u}\frac{\partial \bar{N}_3}{\partial \bar{x}}+\bar{v}\frac{\partial \bar{N}_3}{\partial \bar{y}}\right)=\gamma\left(\frac{\partial^2 \bar{N}_3}{\partial \bar{x}^2}+\frac{\partial^2 \bar{N}_3}{\partial \bar{y}^2}\right)+\kappa\left(\frac{\partial \bar{v}}{\partial \bar{x}}-\frac{\partial \bar{u}}{\partial \bar{y}}\right)-2\kappa \bar{N}_3 \tag{2.20}$$

Energy equation

$$\rho_0 c_v\left(\frac{\partial \bar{T}}{\partial \bar{t}}+\bar{u}\frac{\partial \bar{T}}{\partial \bar{x}}+\bar{v}\frac{\partial \bar{T}}{\partial \bar{y}}\right)=\kappa_T\left(\frac{\partial^2 \bar{T}}{\partial \bar{x}^2}+\frac{\partial^2 \bar{T}}{\partial \bar{y}^2}\right)+\alpha_c\left(\frac{\partial T}{\partial x}\frac{\partial N_3}{\partial y}-\frac{\partial T}{\partial y}\frac{\partial N_3}{\partial x}\right) \tag{2.21}$$

Now, we introduce the following dimensionless variables

$$x=\frac{\bar{x}}{L},\quad y=\frac{\bar{y}}{L},\quad u=\frac{\bar{u}}{U_0},\quad v=\frac{\bar{v}}{U_0}, \tag{2.22a}$$

$$\bar{N} = \frac{U_0}{L} N,\ \theta = \frac{\bar{T} - \bar{T}_\infty}{\bar{T}_W - \bar{T}_\infty},\quad p = \frac{\bar{p}}{\rho {U_0}^2},\quad t = \frac{U_0}{L}\bar{t}\,. \tag{2.22b}$$

Continuity equation

$$\frac{\partial u}{\partial x} + \frac{\partial v}{\partial y} = 0 \tag{2.23}$$

x linear momentum equation

$$\frac{\partial u}{\partial t} + u\frac{\partial u}{\partial x} + v\frac{\partial u}{\partial y} = -\frac{\rho}{\rho_0}\frac{\partial p}{\partial x} + \frac{1}{\mathrm{Re}}(1+K)\left(\frac{\partial^2 u}{\partial x^2} + \frac{\partial^2 u}{\partial y^2}\right) + \frac{1}{\mathrm{Re}}K\frac{\partial N}{\partial y} + \frac{\rho}{\rho_0}\frac{L}{{U_0}^2}g_x \tag{2.24}$$

2.5 Order of magnitude analysis

Consider flow past a plane wall coincident with the *x* axis. If

$$\begin{aligned} &x = O(1),\ y = O(\delta),\ u = O(1),\ v = O(\delta),\quad t = O(1)\,, p = O(1),\\ &\mu = O(\delta^2),\ \kappa = O(\delta),\ \mu + \kappa = O(\delta),\ N_3 = O(1),\ \nu = O(\delta^2),\\ &\mathrm{Re} = \frac{1}{\delta},\ T = O(1),\quad \gamma = O(\delta),\ \delta \prec\prec 1, \end{aligned} \tag{2.25}$$

This results for two dimensional flows the equations can be

Continuity equation

$$\begin{aligned} &\frac{\partial \bar{u}}{\partial \bar{x}} + \frac{\partial \bar{v}}{\partial \bar{y}} = 0\\ &\frac{1}{1} \quad \frac{\delta}{\delta} \end{aligned} \tag{2.26}$$

x linear momentum equation

$$\begin{aligned} &\rho_0\left(\frac{\partial \bar{u}}{\partial \bar{t}} + \bar{u}\frac{\partial \bar{u}}{\partial \bar{x}} + \bar{v}\frac{\partial \bar{u}}{\partial \bar{y}}\right) = -\frac{\partial \bar{p}}{\partial \bar{x}} + (\mu+\kappa)\left(\frac{\partial^2 \bar{u}}{\partial \bar{x}^2} + \frac{\partial^2 \bar{u}}{\partial \bar{y}^2}\right) + \kappa\frac{\partial \bar{N}_3}{\partial \bar{y}} + \rho g_x\\ &\rho_0\left(\frac{1}{1} \quad 1.\frac{1}{1} \quad \delta.\frac{1}{\delta}\right) \quad \frac{1}{1} \qquad \delta\left(\frac{1}{1} \qquad \frac{1}{\delta^2}\right) \quad \delta\frac{1}{\delta} \qquad \rho g_x \end{aligned} \tag{2.27}$$

y linear momentum equation

$$\begin{aligned} &\rho_0\left(\frac{\partial \bar{v}}{\partial \bar{t}} + \bar{u}\frac{\partial \bar{v}}{\partial \bar{x}} + \bar{v}\frac{\partial \bar{v}}{\partial \bar{y}}\right) = -\frac{\partial \bar{p}}{\partial \bar{y}} + (\mu+\kappa)\left(\frac{\partial^2 \bar{v}}{\partial \bar{x}^2} + \frac{\partial^2 \bar{v}}{\partial \bar{y}^2}\right) - \kappa\frac{\partial \bar{N}_3}{\partial \bar{x}} + \rho g_y\\ &\rho_0\left(\frac{\delta}{1} \quad 1.\frac{\delta}{1} \quad \delta.\frac{\delta}{\delta}\right) \quad \frac{1}{\delta} \qquad \delta\left(\frac{\delta}{1} \quad \frac{\delta}{\delta^2}\right) \quad \delta\frac{1}{1} \quad \rho g_y \end{aligned} \tag{2.28}$$

z angular momentum equation

$$\rho_0 j\left(\frac{\partial \bar{N}_3}{\partial \bar{t}}+\bar{u}\frac{\partial \bar{N}_3}{\partial \bar{x}}+\bar{v}\frac{\partial \bar{N}_3}{\partial \bar{y}}\right)=\gamma\left(\frac{\partial^2 \bar{N}_3}{\partial \bar{x}^2}+\frac{\partial^2 \bar{N}_3}{\partial \bar{y}^2}\right)+\kappa\left(\frac{\partial \bar{v}}{\partial \bar{x}}-\frac{\partial \bar{u}}{\partial \bar{y}}\right)-2\kappa \bar{N}_3$$
$$\rho_0 j\left(\frac{1}{1}\quad 1.\frac{1}{1}\quad \delta.\frac{1}{\delta}\right)\delta\left(\frac{1}{1}\quad \frac{1}{\delta^2}\right)\quad \delta\left(\frac{\delta}{1}\quad \frac{1}{\delta}\right)\quad 2.\delta.1 \tag{2.29}$$

Energy equation

$$\rho_0 c_v\left(\frac{\partial \bar{T}}{\partial \bar{t}}+\bar{u}\frac{\partial \bar{T}}{\partial \bar{x}}+\bar{v}\frac{\partial \bar{T}}{\partial \bar{y}}\right)=\kappa_T\left(\frac{\partial^2 \bar{T}}{\partial \bar{x}^2}+\frac{\partial^2 \bar{T}}{\partial \bar{y}^2}\right)+\alpha_c\left(\frac{\partial T}{\partial x}\frac{\partial N_3}{\partial y}-\frac{\partial T}{\partial y}\frac{\partial N_3}{\partial x}\right)$$
$$\rho_0 c_v\left(\frac{1}{1}\quad 1.\frac{1}{1}\quad \delta\frac{1}{\delta}\right)\quad \kappa_T\left(\frac{1}{1}\quad \frac{1}{\delta^2}\right)\quad \alpha_c\left(\frac{1}{1}\frac{1}{\delta}\quad \frac{1}{\delta}\frac{1}{1}\right) \tag{2.30}$$

Evaluating from equations (3.23) - (3.27) gives the final form of the two dimensional flows. All the governing equations are summarized below.

Continuity equation

$$\frac{\partial \bar{u}}{\partial \bar{x}}+\frac{\partial \bar{v}}{\partial \bar{y}}=0 \tag{2.31}$$

x linear momentum equation

$$\rho_0\left(\frac{\partial \bar{u}}{\partial \bar{t}}+\bar{u}\frac{\partial \bar{u}}{\partial \bar{x}}+\bar{v}\frac{\partial \bar{u}}{\partial \bar{y}}\right)=-\frac{\partial \bar{p}}{\partial \bar{x}}+(\mu+\kappa)\frac{\partial^2 \bar{u}}{\partial \bar{y}^2}+\kappa\frac{\partial \bar{N}_3}{\partial \bar{y}}+\rho g_x \tag{2.32}$$

y linear momentum equation

$$0=-\frac{\partial \bar{p}}{\partial \bar{y}}+\rho g_y \tag{2.33}$$

z angular momentum equation

$$\rho_0 j\left(\frac{\partial \bar{N}_3}{\partial \bar{t}}+\bar{u}\frac{\partial \bar{N}_3}{\partial \bar{x}}+\bar{v}\frac{\partial \bar{N}_3}{\partial \bar{y}}\right)=\gamma\frac{\partial^2 \bar{N}_3}{\partial \bar{y}^2}-\kappa\left(\frac{\partial \bar{u}}{\partial \bar{y}}+2\bar{N}_3\right) \tag{2.34}$$

Energy equation

$$\rho_0 c_v\left(\frac{\partial \bar{T}}{\partial \bar{t}}+\bar{u}\frac{\partial \bar{T}}{\partial \bar{x}}+\bar{v}\frac{\partial \bar{T}}{\partial \bar{y}}\right)=\kappa_T\frac{\partial^2 \bar{T}}{\partial \bar{y}^2}+\alpha_c\left(\frac{\partial T}{\partial x}\frac{\partial N_3}{\partial y}-\frac{\partial T}{\partial y}\frac{\partial N_3}{\partial x}\right) \tag{2.35}$$

Chapter Three
Boundary layer flow and heat transfer in a micropolar fluid past a permeable flat plate

3.1 Introduction

An analysis is performed to study the shear stress, the couple-stress and heat transfer characteristics of a laminar mixed convection boundary layer flow of a micropolar fluid past an isothermal permeable plate. The governing nonsimilar boundary layer equations are analyzed using the (i) series solution for small ξ, (ii) asymptotic solution for large ξ and (iii) primitive-variable formulation and the stream function formulation are being used for all ξ. The effects of the material parameters, such as, the vortex viscosity parameter, K, and the transpiration parameter, s, on the shear stress, the couple-stress and heat transfer have been investigated. The agreement between the solutions obtained from the stream-function formulation and the primitive-variable formulation is found to be excellent.

3.2 Mathematical Formalisms

A two-dimensional steady, laminar boundary layer flow of a micropolar fluid along a permeable vertical flat plate is considered. The temperature of the ambient fluid is assumed to be uniform at $\bar{T}_\infty$ and that of the surface at T_W. The coordinate system and the flow configuration are shown in Fig. 4. 1.

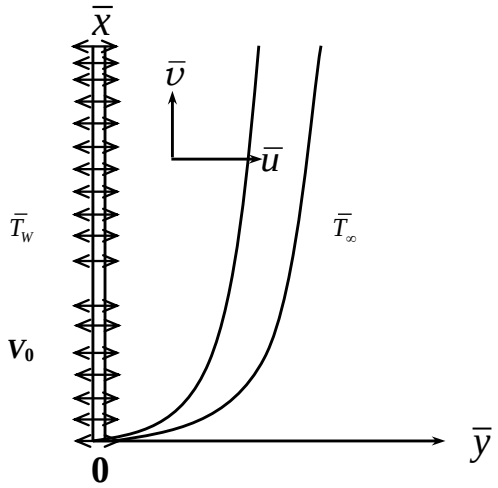

Fig. 3.1: The flow configuration and the coordinate system.

Under the usual boundary layer approximation, following Ahmadi [11] and Ress and Bossom [12], the equations of conservation of mass, momentum and energy that govern the flow are given as below:

$$\frac{\partial \bar{u}}{\partial \bar{x}} + \frac{\partial \bar{v}}{\partial \bar{y}} = 0 \tag{3.1}$$

$$\bar{u}\frac{\partial \bar{u}}{\partial \bar{x}} + \bar{v}\frac{\partial \bar{u}}{\partial \bar{y}} = \frac{\mu + \kappa}{\rho}\frac{\partial^2 \bar{u}}{\partial \bar{y}^2} + \frac{\kappa}{\rho}\frac{\partial \bar{N}}{\partial \bar{y}} \tag{3.2}$$

$$\bar{u}\frac{\partial \bar{N}}{\partial \bar{x}} + \bar{v}\frac{\partial \bar{N}}{\partial \bar{y}} = \frac{\gamma}{\rho j}\frac{\partial^2 \bar{N}}{\partial \bar{y}^2} - \frac{\kappa}{\rho j}\left(2\bar{N} + \frac{\partial \bar{u}}{\partial \bar{y}}\right) \tag{3.3}$$

$$\bar{u}\frac{\partial \bar{T}}{\partial \bar{x}} + \bar{v}\frac{\partial \bar{T}}{\partial \bar{y}} = \alpha\frac{\partial^2 \bar{T}}{\partial \bar{y}^2} \tag{3.4}$$

Here, $\bar{x}, \bar{y}$ are the coordinates parallel with and perpendicular to the flat surface, $\bar{u} - \bar{v}$ are the velocity component, $\bar{p}$ the pressure, $\bar{N}$ the component of the gyration vector normal to the $\bar{x} - \bar{y}$ plane, and j is the microinertia density. Further, ρ is the fluid density, μ the dynamic viscosity, κ vortex viscosity and γ is the spin-gradient viscosity given by $\gamma = \left(\mu + \kappa/2\right) j$ (see [11]). We follow the work of many recent authors by assuming that j is a constant and therefore it shall be set equal to a reference value, j_0; consequently the equation for the microinertia density (3.3) is trivially satisfied.

The boundary conditions to be satisfied by equations (4.1)-(4.4) are

$$\begin{aligned} &\bar{u} = 0, \quad \bar{v} = -V_0, \quad \bar{N} = -n\left(\frac{\partial \bar{u}}{\partial \bar{y}}\right), \quad \bar{T} = \bar{T}_w \text{ at } \bar{y} = 0 \\ &\bar{u} \to U_0, \quad \bar{v} \to 0, \quad \bar{N} \to 0, \quad \bar{T} \to \bar{T}_\infty \quad \text{as } \bar{y} \to \infty \end{aligned} \tag{3.5}$$

where V_0 represents the suction velocity of the fluid through the surface of the plate. In this study we shall consider only the suction case (rather than blowing) and therefore V_0 is taken as positive throughout. Furthermore, n is a constant, $0 \le n \le 1$. The case n=0 corresponds to the strong concentration of micro-elements. This indicates $\bar{N} = 0$ near the wall other hand, indicates the vanishing of anti-symmetric part of the stress tensor and denotes weak suggesting that the concentration of the particles is strong enough so that the micro-elements near the walls are unable to rotate because of this concentration. The case, n=1/2, on the concentration. The case n=1 may be used for the modeling of turbulent boundary layer flows ([16]).

Now we introduce the following dimensionless dependent and independent variables:

$$x=\frac{\bar{x}}{L},\ \ y=\frac{\bar{y}}{L}\mathrm{Re}^{1/2},\ \ u=\frac{\bar{u}}{U_0},\ \ \bar{v}=\frac{\nu}{L}\mathrm{Re}^{1/2}v$$
$$\bar{N}=\frac{U_0}{L}\mathrm{Re}^{1/2}N,\quad \theta=\frac{\bar{T}-\bar{T}_\infty}{\bar{T}_W-\bar{T}_\infty},\ \ s=\frac{V_0L}{\nu}\mathrm{Re}^{-1/2}\ . \tag{3.6}$$

In the above set of equations, where x, y are the non dimensional coordinate axis, u, v the non dimensional velocity components, L is reference length, N is the non dimensional angular momentum, and θ is the non dimensional temperature.

Thus the equations (3.1)–(3.4) take the following form:

$$\frac{\partial u}{\partial x}+\frac{\partial v}{\partial y}=0 \tag{3.7}$$

$$u\frac{\partial u}{\partial x}+v\frac{\partial u}{\partial y}=(1+K)\frac{\partial^2 u}{\partial y^2}+K\frac{\partial N}{\partial y} \tag{3.8}$$

$$u\frac{\partial N}{\partial x}+v\frac{\partial N}{\partial y}=\left(1+\frac{K}{2}\right)\frac{\partial^2 N}{\partial y^2}-K\left(2N+\frac{\partial u}{\partial y}\right) \tag{3.9}$$

$$u\frac{\partial \theta}{\partial x}+v\frac{\partial \theta}{\partial y}=\frac{1}{\mathrm{Pr}}\frac{\partial^2 \theta}{\partial y^2} \tag{3.10}$$

In equation (3.6) $\mathrm{Re}\left(=U_0L/\nu\right)$ is the Reynolds number, $K\left(=\kappa/\mu\right)$, appeared in equations (3.8) and (3.9), is termed as the vortex viscosity parameter and in equation (3.10) $Pr\left(=\nu/\alpha\right)$ is the Prandtl number. We also use $j_0=L^2$ in equation (3.9).

The boundary conditions now become

$$\begin{aligned} &u=0,\ \ v=s,\ \ N=-n\frac{\partial u}{\partial y},\ \ \theta=1 \quad \ at\ y=0\\ &u\to 1,\ \ v\to 0,\ \ N\to 0,\ \ \theta\to 0\ \ as\ y\to\infty \end{aligned} \tag{3.11}$$

From application point of view, we need to find the values of shear stress, $\bar{\tau}$, the couple-stress, $\bar{m}$, and rate of heat transfer, $\bar{q}$, at the surface of the plate, that may be obtained by the relations given below:

$$\bar{\tau}=\left((\mu+\kappa)\frac{\partial \bar{u}}{\partial \bar{y}}\right)_{\bar{y}=0},\ \bar{m}=\gamma\left(\frac{\partial \bar{N}}{\partial \bar{y}}\right)_{\bar{y}=0},\ \bar{q}=-k\left(\frac{\partial \bar{T}}{\partial \bar{y}}\right)_{\bar{y}=0} \tag{3.12}$$

Using the relation (3.6) on (3.12), we obtain

$$\tau=\left[1+(1-n)K\right]\left(\frac{\partial u}{\partial y}\right)_{y=0},\ \ m=\left(1+\frac{K}{2}\right)\left(\frac{\partial N}{\partial y}\right)_{y=0},\ \ q=-\left(\frac{\partial \theta}{\partial y}\right)_{y=0} \tag{3.13}$$

where τ, m and q are dimensionless shear stress, the couple-stress and rate of heat transfer, respectively, which are define by

$$\tau = \frac{\bar{\tau} L \,\mathrm{Re}^{-1/2}}{\mu U_0}, \quad m = \frac{\bar{m}}{\rho U_0^{\,2} L}, \quad q = \frac{\bar{q} L \,\mathrm{Re}^{-1/2}}{k\left(T_w - T_\infty\right)}$$

3.3 Methods of solution

To Investigate the present problem we have employed two formulations, namely, the primitive-variable formulation and the stream-function formulation, method of solution of which are presented in the following sections.

3.3.1 Primitive-variable transformation

To get the set of equations (3.7)-(3.10) in convenient form for integration, we define the following one parameter group of transformation for the dependent and the independent variables:

$$u = U, \quad v = x^{-1/2}\left(V + s\xi\right), \quad N = x^{-1/2}G, \quad \theta = \Theta, \quad \xi = x^{1/2}, Y = x^{-1/2}y \tag{3.14}$$

Thus the equations (3.7)-(3.10) are transformed to

$$\frac{1}{2}\xi\frac{\partial U}{\partial \xi} - \frac{1}{2}Y\frac{\partial U}{\partial Y} + \frac{\partial V}{\partial Y} = 0 \tag{3.15}$$

$$\frac{1}{2}\xi U\frac{\partial U}{\partial \xi} + \left(V + s\xi - \frac{1}{2}YU\right)\frac{\partial U}{\partial Y} = \left(1+K\right)\frac{\partial^2 U}{\partial^2 Y} + K\frac{\partial G}{\partial Y} \tag{3.16}$$

$$-\frac{1}{2}UG + \frac{1}{2}\xi U\frac{\partial G}{\partial \xi} + \left(V + s\xi - \frac{1}{2}YU\right)\frac{\partial G}{\partial Y} = \left(1+\frac{K}{2}\right)\frac{\partial^2 G}{\partial^2 Y} - K\xi^2\left(2G + \frac{\partial U}{\partial Y}\right) \tag{3.17}$$

$$\frac{1}{2}\xi U\frac{\partial \Theta}{\partial \xi} + \left(V + s\xi - \frac{1}{2}YU\right)\frac{\partial \Theta}{\partial Y} = \frac{1}{\mathrm{Pr}}\frac{\partial^2 \Theta}{\partial Y^2} \tag{3.18}$$

Appropriate boundary conditions are

$$\begin{aligned} &U = 0, \;\; V = 0, \quad G = -n\frac{\partial U}{\partial Y}, \quad \Theta = 1 \quad at \quad Y = 0 \\ &U = 1, \;\; V = 0, \quad G = 0, \quad \Theta = 0 \qquad as \quad Y \to \infty \end{aligned} \tag{3.19}$$

Once we know the values of U, V, G and Θ and their derivatives, we are at position to find the values of shear stress, τ, the couple-stress, m, and rate of heat transfer, q, from the following relations obtained from (3.13):

$$\tau = \left[1 + \left(1-n\right)K\right]\xi^{-1}\left(\frac{\partial U}{\partial Y}\right)_{Y=0}, \; m = \left(1+\frac{K}{2}\right)\xi^{-2}\left(\frac{\partial G}{\partial Y}\right)_{Y=0}, \; q = -\xi^{-1}\left(\frac{\partial \Theta}{\partial Y}\right)_{Y=0} \tag{3.20}$$

3.3.2 Stream function formulation

To get the set of equations (3.7)-(3.10) in convenient form for integration, we define the following one parameter group of transformation for the dependent and the independent variables:

$$\psi = x^{1/2}\left[f\left(\xi,Y\right)+s\xi \right],\ N=\xi^{-1/2}g\left(\xi,Y\right),\ \theta=h\left(\xi,Y\right),$$
$$\xi = x^{1/2} \text{ and } Y = x^{-1/2}y \tag{3.21}$$

Here Y is the pseudo-similarity variable and ψ is the stream function that satisfies equation (3.7) and is defined by

$$u=\frac{\partial\psi}{\partial y},\ \ v=-\frac{\partial\psi}{\partial x} \tag{3.22}$$

Equations (3.8), (3.9) and (3.10) thus reduce to

$$\left(1+K\right)f'''+\frac{1}{2}ff''+Kg'+s\xi f''=\frac{1}{2}\xi\left(f'\frac{\partial f'}{\partial\xi}-f''\frac{\partial f}{\partial\xi}\right) \tag{3.23}$$

$$\left(1+K/2\right)g''+\frac{1}{2}\left(fg'+gf'\right)-K\xi^2\left(2g+f''\right)+s\xi g'=\frac{1}{2}\xi\left(f'\frac{\partial g}{\partial\xi}-g'\frac{\partial f}{\partial\xi}\right) \tag{3.24}$$

$$\frac{1}{\Pr}h''+\frac{1}{2}fh'+s\xi h'=\frac{1}{2}\xi\left(f'\frac{\partial h}{\partial\xi}-h'\frac{\partial f}{\partial\xi}\right) \tag{3.25}$$

Boundary conditions take the form

$$f\left(\xi,0\right)=f'\left(\xi,0\right)=0,\ \ g\left(\xi,0\right)=-nf''\left(\xi,0\right),\ \ h\left(\xi,0\right)=1,$$
$$f'\left(\xi,\infty\right)=1,\quad g\left(\xi,\infty\right)=0,\quad h\left(\xi,\infty\right)=0. \tag{3.26}$$

In these equations, primes denote differentiation of the functions with respect to Y. Here solution of the set of equations (3.23)-(3.25) is obtained by implicit finite difference method together with the Keller-box elimination technique (also known as Keller box method), introduced by Keller and Cebeci [35] and described in more detail in Cebeci and Bradshaw [36]. In this case, the expressions for the shear stress, the couple-stress and rate of heat transfer given in [13] becouse

$$\tau=\left[1+\left(1-n\right)\right]\xi^{-1}f''\left(\xi,0\right),\ m=\left(1+\frac{K}{2}\right)\xi^{-2}g'\left(\xi,0\right),\ q=-\xi^{-1}h'\left(\xi,0\right) \tag{3.27}$$

3.4 Asymptotic solutions

3.4.1 Solutions for small ξ

Near the leading edge, or equivalently for small ξ, we expand the functions f, g and h in powers of ξ as given below:

$$f(\xi,Y)=\sum_{i=0}^{\infty}\xi^i f_i(Y),\quad g(\xi,Y)=\sum_{i=0}^{\infty}\xi^i g_i(Y),\quad h(\xi,Y)=\sum_{i=0}^{\infty}\xi^i h_i(Y). \tag{3.28}$$

Substituting these into equations (3.23)-(3.25) and then equating the terms of like powers of ξ to zero, we get the following pairs of ordinary differential equations for the functions f_i, g_i and h_i:

$$(1+K)f_0'''+\frac{1}{2}f_0f_0''+Kg_0'=0 \tag{3.29}$$

$$(1+K/2)g_0''+\frac{1}{2}(f_0g_0'+g_0f_0')=0 \tag{3.30}$$

$$\frac{1}{\Pr}h_0''+\frac{1}{2}f_0h_0'=0 \tag{3.31}$$

The boundary conditions appropriate to this set of equations are

$$f_0(0)=f_0'(0)=0,\quad g_0(0)=-nf_0''(0),\quad h_0(0)=1,$$

$$f_0'(\infty)=1,\quad g_0(\infty)=0,\quad h_0(\infty)=0. \tag{3.32}$$

The higher order equations, for $i \geq 1$, are as follows:

$$(1+K)f_i'''+sf_{i-1}''+Kg_i'=\frac{1}{2}\sum_{r=0}^{i}\{rf_r'f_{i-r}'-(1+r)f_rf_{i-r}''\} \tag{3.33}$$

$$\left(1+\frac{K}{2}\right)g_i''+sg_{i-1}'-K(2g_{i-2}+f_{i-2}'')=\frac{1}{2}\sum_{r=0}^{i}\{(r-1)g_rf_{i-r}'-(1+r)f_rg_{i-r}'\} \tag{3.34}$$

$$\frac{1}{\Pr}h_i''+sh_{i-1}'=\frac{1}{2}\sum_{r=0}^{i}\{rf_r'h_{i-r}-(1+r)f_rh_{i-r}'\} \tag{3.35}$$

The boundary conditions are as follows:

$$f_i(0)=f_i'(0)=0,\quad g_i(0)=-nf_i''(0),\quad h_i(0)=1,$$

$$f_i'(\infty)=0,\quad g_i(\infty)=0,\quad h_i(\infty)=0. \tag{3.36}$$

for $i = 1, 2, 3, \ldots$.

In the above equations the functions f_0, g_0 and h_0 are the well-known free convection similarity solutions for flow around a constant temperature semi-infinite vertical plate and the functions f_i, g_i and h_i $(i = 1,2,3, \ldots)$ are effectively first and higher order corrections to the flow due to the effect of the transpiration of the fluid through the surface of the plate, Further the equations for each $i \geq 1$) are linear, but coupled, and may be found by pair-wise sequential solution. These pair of equations has been integrated using an implicit Runge-Kutta-Butcher (Butcher [37] initial value solver together with the iteration scheme of Nachtsheim and Swigert [38]. In the present investigation, solutions of 10 sets of equations have been obtained.

The solution of the above equations enables the calculation of the various flow parameters near the leading edge, such as the values of shear stress, τ , the couple-stress, m , and rate of heat transfer, q . Using the relation given in (3.27), the quantities τ, m and q can now be calculated respectively from the following expressions:

$$\tau = \left[1+(1-n)\right]\xi^{-1} f''(\xi,0)\,,\ m = \left(1+\frac{K}{2}\right)\xi^{-2} g'(\xi,0),\ q = -\xi^{-1} h'(\xi,0) \tag{3.37}$$

3.4.2 Asymptotic solution for large ξ

In this section attention has been given to the solution of equations (3.23)-(3.25) when ξ is large. The order of magnitude analysis of various terms in (3.23)-(3.25) shows that the largest terms are f''' and $\xi f''$ in (3.23), g'' and $\xi g'$ in (3.24), and h'' and $\xi h'$ in (3.25). In the respective equations both the terms have to be balanced in magnitude and the only way to do this is to assume that Y be small and hence derivatives are large. Given that $h = O(1)$ as $\xi \to \infty$, it is essential to find appropriate scaling for f and Y. On balancing f''' and $\xi f''$ in (3.23), it is found that $Y = O\left(\xi^{-1}\right)$ and $f = O\left(\xi^{-1}\right)$ as $\xi \to \infty$. Therefore the following transformation may be introduced:

$$f = \xi^{-1} F(\xi,\eta),\ \ g = \xi G(\xi,\eta),\ \ h = H(\xi,\eta),\ \ \eta = \xi Y \tag{3.38}$$

Equations (3.23)-(3.25) together with the transformations given in (3.38) then become

$$(1+K)F''' + KG' + sF'' = \frac{1}{2}\xi^{-1}\left(F'\frac{\partial F'}{\partial \xi} - F''\frac{\partial F}{\partial \xi}\right) \tag{3.39}$$

$$\left(1+\frac{K}{2}\right)G'' - K(2G+F'') + sG' = \frac{1}{2}\xi^{-1}\left(F'\frac{\partial G}{\partial \xi} - G'\frac{\partial F}{\partial \xi}\right) \tag{3.40}$$

$$\frac{1}{\Pr}H'' + sH'' = \frac{1}{2}\xi^{-1}\left(F'\frac{\partial H}{\partial \xi} - H'\frac{\partial F}{\partial \xi}\right) \tag{3.41}$$

For sufficiently large ξ, we can write the above equations as follows

$$(1+K)F''' + KG' + sF'' = 0 \tag{3.42}$$

$$\left(1+\frac{K}{2}\right)G'' - K(2G+F'') + sG' = 0 \tag{3.43}$$

$$\frac{1}{\Pr}\bar{H}'' + s\bar{H}' = 0 \tag{3.44}$$

Boundary conditions take the form

$$\begin{aligned} &F(\xi,0) = F'(\xi,0) = 0, \quad G(\xi,0) = -nF''(\xi,0), \quad H(\xi,0) = 1, \\ &F'(\xi,\infty) = 1, \quad G(\xi,\infty) = 0, \quad H(\xi,\infty) = 0. \end{aligned} \tag{3.45}$$

The various flow parameters such as the shear stress, the couple-stress and rate of heat transfer may be calculated from the following relations:

$$\tau = \left[1+(1-n)K\right]F''(\xi,0)\,,\ m = \left(1+\frac{K}{2}\right)G'(\xi,0),\ q = -H'(\xi,0) \tag{3.46}$$

Numerical values of τ, m and q thus obtained are compared with that obtained from primitive variable formulation through figures 3.2 and 3.3.

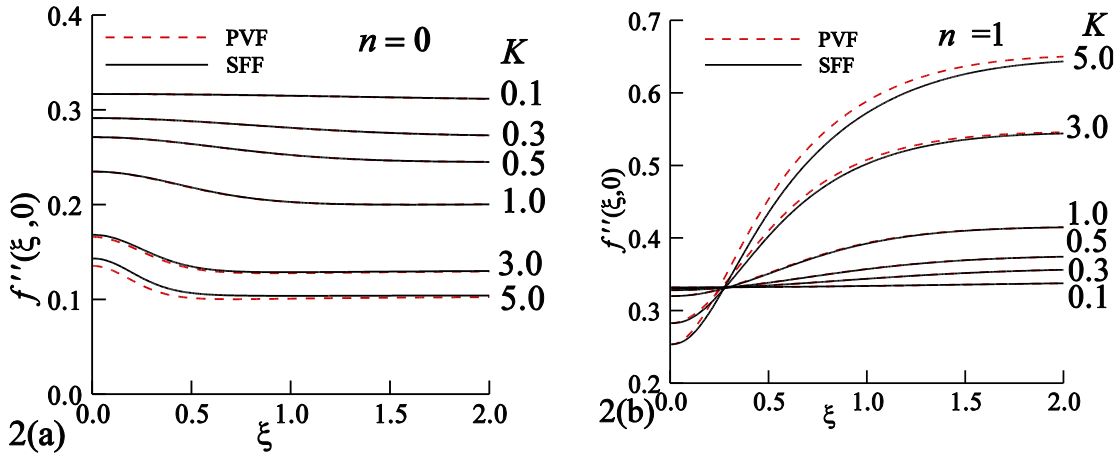

Fig. 3.2: Development of wall shear stress $f''(\xi,0)$ as a function of ξ for (a) n = 0 and (b) n = 1 and for various values of K. The solid lines represent primitive variable formulation and the dotted lines represent the stream-function formulation.

3.5 Results and discussions

Numerical computation were carried out mainly for fluid having a Prandtl number, Pr = 10.0 while the value of the vortex viscosity parameter, K = 0.0, 2.0 and 5.0 and the transpiration parameter, s = 0.5, 1.5 and 3.0.

Representative numerical values of $X^{-1/2}g'(100,0)$ obtained from the present integration of equation (3.23) are entered into the Table1 for comparison with those of Rees and Bossom [12].

Table 3.1

Numerical values of $X^{-1/2}g'$ at $X = 100$ and $Y=0$ for $n = 0$ and different values of K.

K	Rees et al. [8]	Present
0.1	-0.06895	-0.06908
0.3	-0.1050	-0.10518
0.5	-0.1211	-0.12124
1.0	-0.1354	-0.13555
3.0	-0.1285	-0.12859
5.0	-0.1145	-0.11455

From this table it may be seen that the present solutions are in excellent agreement with Rees and Bossom [12]. Further, throughout figures 3.2 to 3.5 the solid lines represent solutions from primitive variable formulation (PVF) and the dotted are from stream-function formulation (SFF).

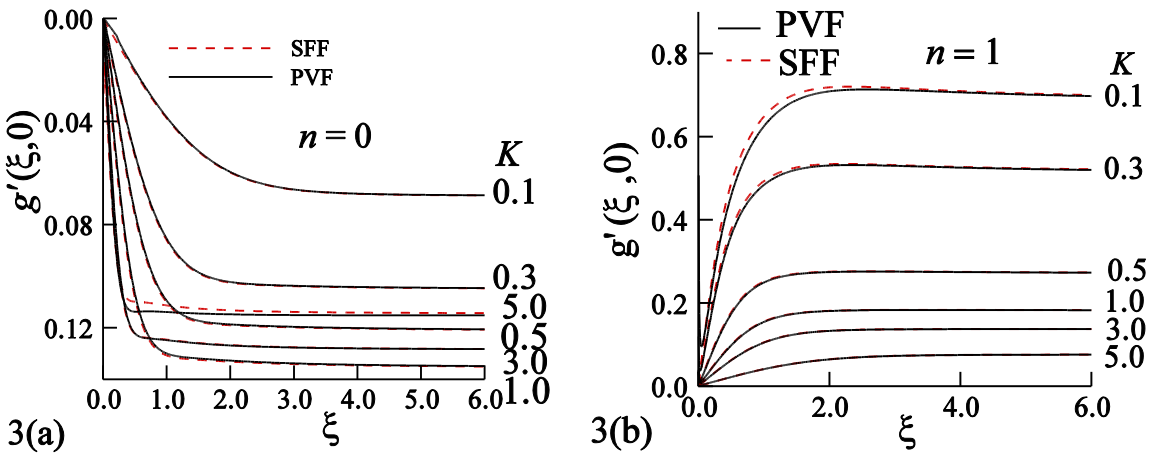

Fig. 3.3: Development of change of the gyration component at the wall, $g'(\xi,0)$ as a function of ξ for (a) $n = 0$ and (b) $n =1$ and for various values of K. The solid lines represent primitive variable formulation and the dotted lines represent the stream-function formulation.

In Fig. 3.2 and 3.3 we have shown a comparison between the stream-function formulation and the primitive-variable formulation of the variations of both the shear stress and of the rate of change of the gyration component at the solid boundary with considering s = 0.0, Pr = 10.0 and a range of values of K with n fixed. The agreement between these formulations is seen to be extremely good. We further observe that these figures are exactly similar to that of Rees *et al.* [12].

A comparison between the results obtained by the stream-function formulation and the primitive-variable formulation is shown in Fig. 3.4 and 3.5. From the figures, it is evident that there is an excellent agreement between these two results hence rest of the results presented and discussed here is based on primitive-variable formulation.

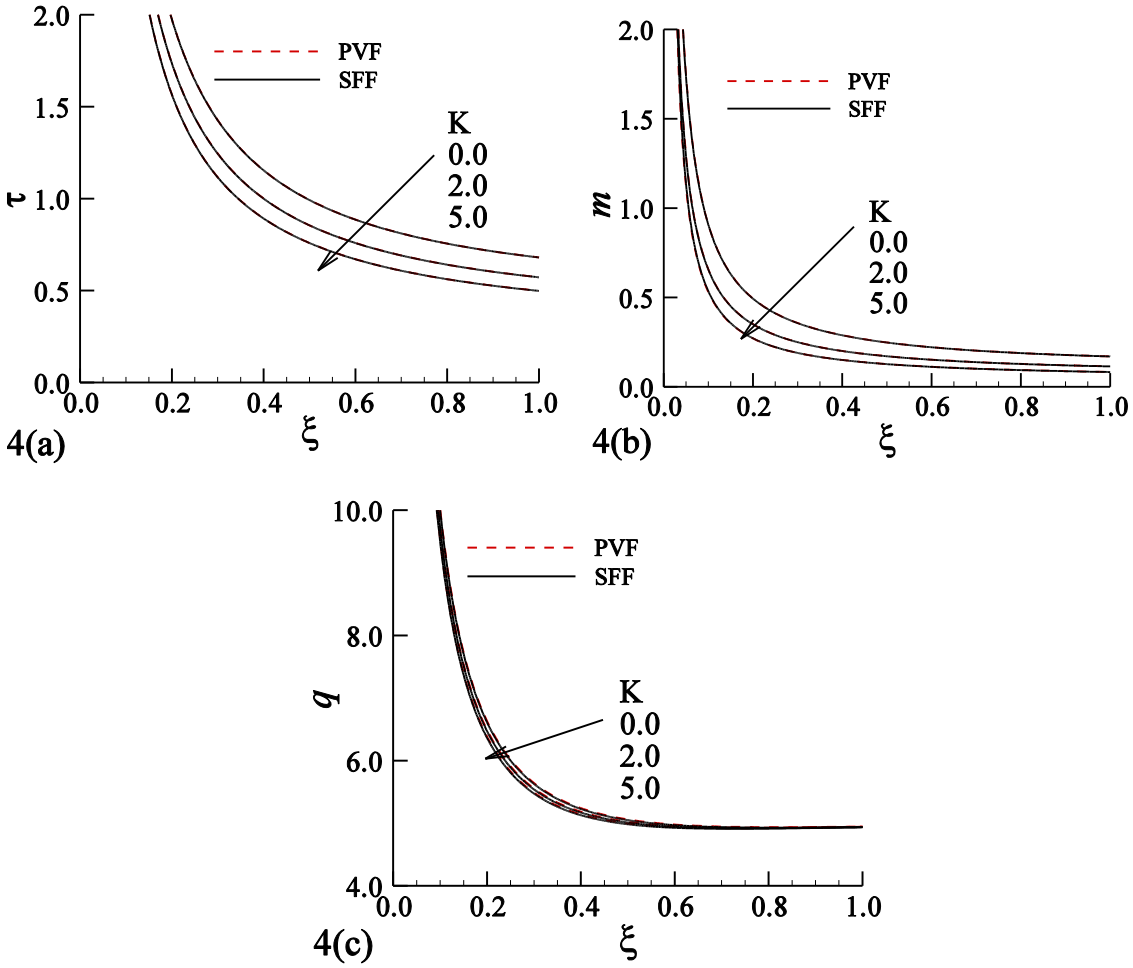

Fig. 3.4: The surface shear stress, τ, the couple-stress, m, and the heat transfer, q, for n = 0.5, s = 1.0, Pr = 10.0 and for various values of K. The solid lines represent primitive variable formulation and the dotted lines represent the stream- function formulation.

In Fig. 3.6, we depict the values of local shear stress, τ, the local heat transfer, q, at the surface and the distribution of the local couple-stress, m, in the boundary layer for different

values of the vortex viscosity parameter K (= 0.0, 2.0 and 5.0) while the Prandtl number, Pr = 10, the transpiration parameter, s = 1.0, and the temperature gradient parameter, n = 0.5.

In these figures the curves marked by solid, broken and dotted curves represent respectively, the results obtained by the finite difference method, the series solution method and the asymptotic method. From these figures it may be seen that an increase in the value of the vortex viscosity parameter K leads to an increase in the value of the local shear stress, the local heat transfer and the local couple-stress.

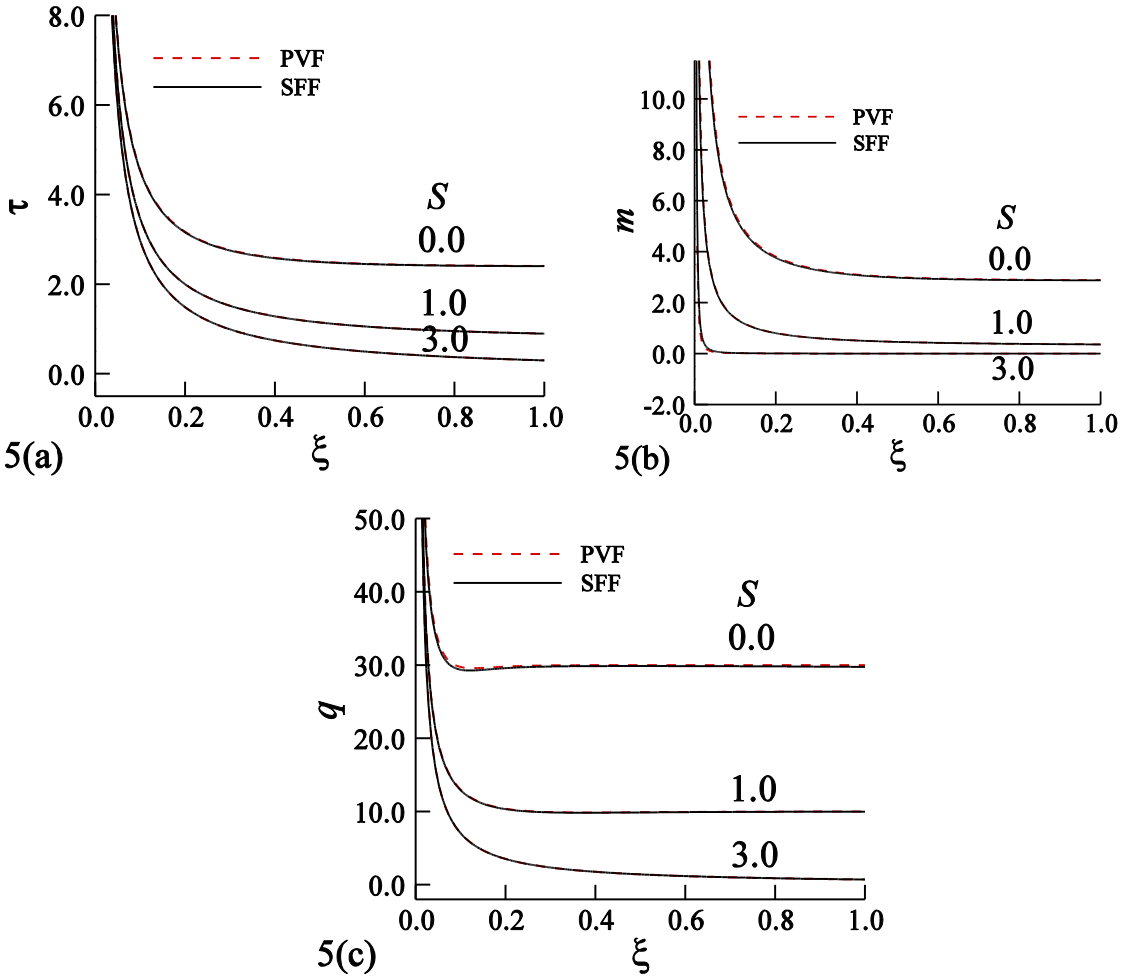

Fig. 3.5: The surface shear stress, τ, the couple-stress, m, and the heat transfer, q, for n = 0.5, K = 0.5, Pr = 10.0 and for various values of s. The solid lines represent primitive variable formulation and the dotted lines represent the stream-function formulation.

We further observe that for any selected value of the vortex viscosity parameter K, values of the shear stress, heat transfer and the couple-stress reach the respective asymptotic values smoothly. The heat transfer reaches its asymptotic values at smaller ξ; whereas the shear stress and the couple-stress does so at comparatively larger value of ξ. We further observe

that as the value of K increases, the shear stress, the heat transfer and the couple-stress reach their asymptotic values faster.

Finally, it may be concluded that the values of the shear stress, the heat transfer and the couple-stress obtained by the three methods are in excellent agreement with each other when the value of K is large.The effect of the transpiration parameter, s, on the local shear stress, the heat transfer and the couple-stress are presented graphically in Fig. 3.7.

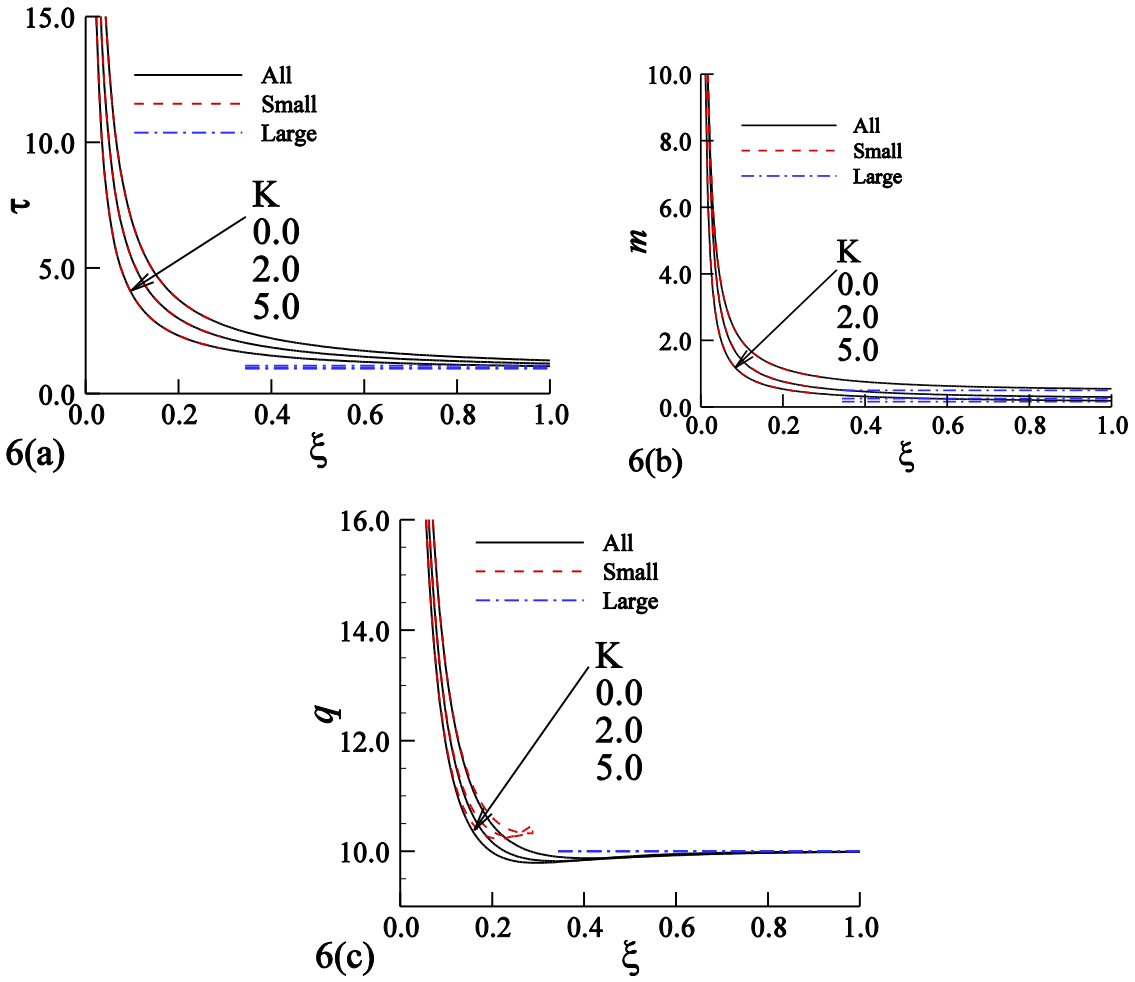

Fig. 3.6: The surface shear stress, τ, the couple-stress, m, and the heat transfer, q, for n = 0.5, s = 1.0, Pr = 10.0 and for various values of K.

It is observed from these figures that an increase in the value of s increases the value of the shear stress, the heat transfer and the couple-stress. We also observe that for any selected value of s, values of the shear stress, the heat transfer and the couple-stress tend to their respective asymptotic values. As the value of s increases, the shear stress, the heat transfer

and the couple-stress reach their asymptotic values faster In this case we also found that the results from the three methods are in excellent agreement.

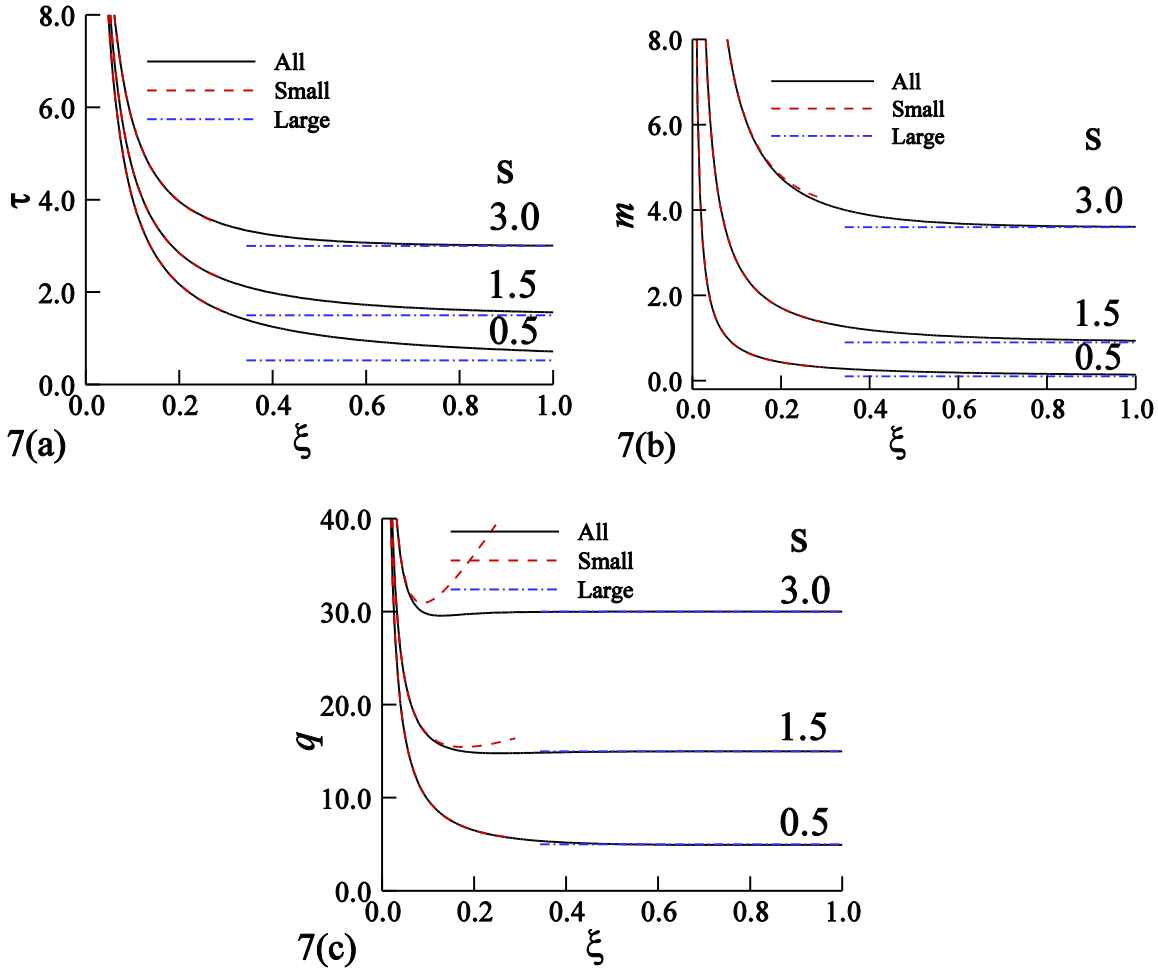

Fig. 3.7: The surface shear stress, τ, the couple-stress, m, and the heat transfer, q, for $n = 0.5$, $K = 0.5$, Pr = 10.0 and for various values of s.

Chapter Four

Transient natural convection flow of thermo-micropolar fluid of micropolar thermal conductivity along a non-uniformly heated vertical surface

4.1 Introduction

In this paper, the unsteady free convection boundary layer flow of a thermo-micropolar fluid along a vertical plate with effect of micropolar heat conduction has been investigated. The governing equations are transformed into a new form using a method of transformed coordinates. We then use an explicit finite difference scheme to solve the transformed equations. Here, the governing equations have been reduced to the forms that are valid for entire, small and large time regimes, by using stream-function formulation. The results obtained for the above mentioned three time regimes are compared and found in excellent agreement. Moreover, the effects of the physical parameters such as the viscosity parameter, K, and the heat conduction parameter, α^*, are presented in terms of the transient shear stress, couple stress and surface heat transfer coefficient as well as transient velocity profiles, angular velocity profiles and temperature profiles.

4.2 Mathematical Formalisms

A two-dimensional unsteady laminar boundary layer flow of a thermo-micropolar natural convection incompressible fluid along a permeable vertical flat plate is considered. The flow configuration and the coordinate system is shown in Fig. 4.1.The dimensionless equations of continuity, momentum, angular velocity and energy that govern the flow are given as (Jena and Mathur [10], Hossain et. at. [13], [22]),

$$\frac{\partial u}{\partial x}+\frac{\partial v}{\partial y}=0 \tag{4.1}$$

$$\frac{\partial u}{\partial t}+u\frac{\partial u}{\partial x}+v\frac{\partial u}{\partial y}=\left(1+K\right)\frac{\partial^2 u}{\partial y^2}+K\frac{\partial G}{\partial y}+\theta \tag{4.2}$$

$$\frac{\partial G}{\partial t}+u\frac{\partial G}{\partial x}+v\frac{\partial G}{\partial y}=\left(1+\frac{K}{2}\right)\frac{\partial^2 G}{\partial y^2}-K\left(2G+\frac{\partial u}{\partial y}\right) \tag{4.3}$$

$$\frac{\partial \theta}{\partial t}+u\frac{\partial \theta}{\partial x}+v\frac{\partial \theta}{\partial y}=\frac{1}{\Pr}\frac{\partial^2 \theta}{\partial y^2}+\alpha^*\left(\frac{\partial \theta}{\partial x}\frac{\partial G}{\partial y}-\frac{\partial \theta}{\partial y}\frac{\partial G}{\partial x}\right) \tag{4.4}$$

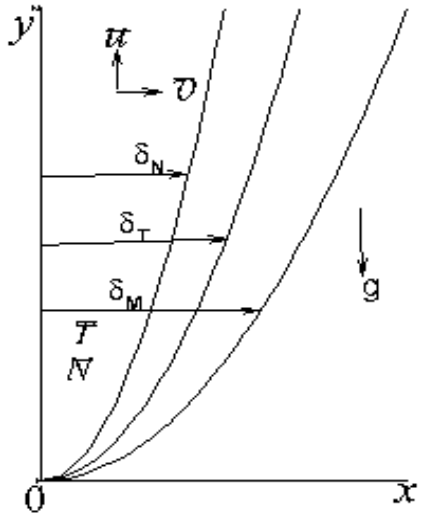

Fig. 4.1: Flow configuration and coordinate system.

The set of equations (4.1)-(4.4) are dimensionless which are based on the following dimensionless dependent and independent variables

$$x=\frac{\bar{x}}{L},\quad y=\frac{\bar{y}}{L},\quad \bar{u}=\frac{\nu}{L}u,\quad \bar{v}=\frac{\nu}{L}v$$

$$\bar{N}=\frac{\nu}{L^2}G,\quad t=\frac{\nu}{L^2}\bar{t},\quad \theta=\frac{g\beta\left(\bar{T}-T_\infty\right)L^3}{\nu^2}. \tag{4.5}$$

Here, $(\bar{x},\bar{y})$ are the co-ordinates parallel with and perpendicular to the flat surface respectively, $(\bar{u},\bar{v})$ are the velocity components, t, time, $\bar{N}$, the angular velocity, θ, dimensionless temperature, j, the micro-inertia per unit mass, ρ, the density of the fluid, g the acceleration due to gravity, κ, the thermal conductivity of the fluid, $\gamma = (\mu + \kappa/2)j$, the gyro-viscosity coefficient and α^*, the micropolar heat conduction coefficient. Following Jena and Mathur [10], it is assumed that micro-inertia, j, is a constant and, therefore, it is set equal to a reference value, $j_0 = L^2$. Further, L is the characteristic length, $K = (\kappa/\mu)$ is vortex viscosity parameter, μ the dynamic viscosity, $Pr = (\nu/\alpha)$ is the Prandtl number that gives the ratio of

momentum diffusivity to thermal diffusivity, ν, viscosity coefficient, $\alpha^*= (N^*/L^2)$ is the micropolar heat conduction parameter. Corresponding boundary conditions are

$$\begin{aligned} u=0,\ v=0,\ G=-n\frac{\partial u}{\partial y},\quad \theta=\theta_w(x)\ \text{at}\ y=0 \\ u=0,\ \ \text{G=0},\ \ \theta=0\quad \text{as}\quad y\to\infty \end{aligned} \tag{4.6}$$

In the above equation $\theta_w(x)$ is the prescribed surface temperature. Here we have considered that $\theta_w(x) = x$.

In the worthwhile Jena and Mathur [11-12] studied the same model for steady laminar free convection flow of a thermomicropolar fluid past a non-isothermal vertical flat plate as well as for non-uniformly heated porous vertical flat plate.

The values of the physical quantities namely, the shear stress, τ_ω, the couple-stress, m_ω, and the rate of heat transfer, q_ω, at the surface of the plate, which are important from the experimental point of view are readily obtained

$$\tau_\omega=(1+K)\left(\frac{\partial u}{\partial y}\right)_{y=0},\ m_\omega=\left(1+\frac{K}{2}\right)\left(\frac{\partial G}{\partial y}\right)_{y=0},\ q_\omega=-\left(\frac{\partial \theta}{\partial y}\right)_{y=0} \tag{4.7}$$

4.3 Methods of solution

Here we are investigating the present problem in three time regimes, namely, (i) entire, (ii) small and (iii) large time regimes. The method of solutions discussed in the following section has been adopted by Hossain et al. [23] and Mahfooz et al. [24] while analyzing the problems on unsteady mixed-convection boundary layer flow of viscous incompressible fluid along a symmetric wedge with variable surface temperature as well as on the radiation effects on transient magneto-hydrodynamic natural convection flow with heat generation.

4.3.1 Solutions for entire time regime (all τ)

To get the solutions for entire time regime here we introduce the following group of transformations ([23, 24]:

$$\psi=x\left(1-e^{-\tau}\right)^{\frac{3}{2}} f(\eta,\tau),\ \ \bar{\theta}=x\theta(\eta,\tau),\ \ \eta=y\left(1-e^{-\tau}\right)^{-\frac{1}{2}},\ \tau=x^{-\frac{1}{2}}t \tag{4.8}$$

In equation (5.1) η is the similarity variable and ψ *is* the stream function defined by

$$u = \frac{\partial \psi}{\partial \eta}, \quad v = -\frac{\partial \psi}{\partial x} \tag{4.9}$$

that satisfies the equation of continuity (4.1).

Now, equations (4.1)–(4.4) together with the boundary conditions (4.6) and the transformations (4.8) are reduced to:

$$(1+K) f''' + \left(1-e^{-\tau}\right)^2 \left(ff'' - f'^2 \right) + Kg' + \theta - e^{-\tau} \left(f' - \frac{1}{2} \eta f'' \right) = \left(1-e^{-\tau}\right) \frac{\partial f'}{\partial \tau} \tag{4.10}$$

$$\left(1+\frac{K}{2}\right) g'' + \left(1-e^{-\tau}\right)^2 \left(fg' - f'g \right) - K\left(1-e^{-\tau}\right)\left(2g + f''\right) - e^{-\tau} \frac{1}{2}\left(g - \eta g'\right) = \left(1-e^{-\tau}\right) \frac{\partial g}{\partial \tau} \tag{4.11}$$

$$\frac{1}{\Pr} \theta'' + \left(1-e^{-\tau}\right)^2 \left(f\theta' - f'\theta \right) + \alpha^* \left(1-e^{-\tau}\right)\left(g'\theta - g\theta' \right) + \frac{1}{2} e^{-\tau} \eta \theta' = \left(1-e^{-\tau}\right) \frac{\partial \theta}{\partial \tau} \tag{4.12}$$

The corresponding boundary conditions are

$$\begin{aligned} &f(0,\tau) = 0, \;\; f'(0,\tau) = 0, \;\; g(0,\tau) = -\frac{1}{2} f''(0,\tau), \;\; \theta(0,\tau) = 1 \;\; at \;\; \eta = 0 \\ &f'(\infty,\tau) = 0, \;\; g(\infty,\tau) = 0, \quad \theta(\infty,\tau) = 0 \quad \forall\, 0 \le \tau \le \infty \end{aligned} \tag{4.13}$$

Where, (') primes denote the differentiation with respect to η.

The starting point to obtain the solutions of the equations (4.10)-(4.12) is the set of the finite-difference equations obtained by spatial discretization of the transformed equations (4.10)–(4.12). The first-order central difference approximation is used for the first-order derivative with respect to η, and the second-order central difference approximation is used for the second-order derivative with respect to η. The forward differences are used for the time derivative. This discretization results in the following tridiagonal algebraic system of equations:

$$A_k \Omega_{i-1,j} + B_k \Omega_{i,j} + C_k \Omega_{i+1,j} = D_k \tag{4.14}$$

In the above equations, the subscripts k (= 1, 2, and 3) represent the functions U, θ, and φ, respectively. i (= 1, 2,.... ,M) and j (= 1, 2, ..., N) correspond to the grid points in η and τ directions, respectively. The coefficients A_k, B_k, C_k, and D_k may be obtained easily. These block tridiagonal systems for k = 1, 2, and 3 are solved by a block matrix version of the well-known Thomas algorithm. Once the function $U = f'(\eta)$ is known, the function f may be found explicitly from the following relation:

$$f_{i,j} = f_{i-1,j} + \Delta\eta U_{i,j} \tag{4.15}$$

The computation is started at $\tau = 0.0$, and then marches forward until it reaches a steady state. The convergence criteria for detecting the steady state solutions are set in such a way that the difference between the values of the function $f(\eta, \tau)$ obtained in two consecutive time steps is less than 10^{-4}. The computational domain is discretized in the (τ, η) space by using the step sizes of $\Delta\tau$ and $\Delta\eta$. After some experimentation, the final mesh sizes are chosen to be $\Delta\eta = 0.005$ and $\Delta\tau = 0.02$.

Solutions thus obtained are used to get the values of non-dimensional shear stress, the couple-stress, and the rate of heat transfer, from equations (4.5) are then transformed to

$$\frac{\tau_\omega}{x} = (1+K)\left(1-e^{-\tau}\right)^{\frac{1}{2}} f''(0,\tau)\ ,\ \frac{m_\omega}{x} = \left(1+\frac{K}{2}\right) g'(0,\tau)\ ,\ \frac{q_\omega}{x} = -\left(1-e^{-\tau}\right)^{-\frac{1}{2}} \theta'(0,\tau) \tag{4.16}$$

Numerical values of the coefficients of shear stress, the couple-stress, and the rate of heat transfer are presented in tabular form as well as graphically in the following sections.

In the next subsections, we will discuss the asymptotic solutions for small and large time τ.

4.3.2 Asymptotic solutions for small time ($\tau << 1$) regime

For small time regime we consider $\tau << 1$. Consequently, the value of $e^{-\tau} \approx 1$ and $1-e^{-\tau} \approx \tau$. Thus equations (4.17)–(4.19) must now be written in the following form, which are more convenient for analysis at small times:

$$(1+K) f''' + \tau^2 \left(ff'' - f'^2 \right) + \left(\frac{1}{2}\eta f'' - f' \right) + Kg' + \theta - \tau \frac{\partial f'}{\partial \tau} = 0 \tag{4.17}$$

$$\left(1+\frac{K}{2}\right) g'' + \tau^2 \left(fg' - f'g \right) - \tau K \left(f'' + 2g \right) + \frac{1}{2}\left(\eta g' - g \right) - \tau \frac{\partial g}{\partial \tau} = 0 \tag{4.18}$$

$$\frac{1}{\mathrm{Pr}} \theta'' + \tau^2 \left(f\theta' - f'\theta \right) + \alpha^* \tau \left(g'\theta - g\theta' \right) + \frac{1}{2}\eta\theta' - \tau \frac{\partial \theta}{\partial \tau} = 0 \tag{4.19}$$

The boundary conditions (4.13) becomes

$$\begin{aligned} &f(0,\tau) = f'(0,\tau) = 0,\ g(0,\tau) = -\frac{1}{2} f''(0,\tau),\ \theta(0,\tau) = 1 \\ &f'(\infty,\tau) = g'(\infty,\tau) = \theta'(\infty,\tau) = 0 \quad \forall 0 \le \tau \le 1 \end{aligned} \tag{4.20}$$

By knowing the functions *f*, *g* and θ and their derivatives we can readily get the values of the shear stress, the couple-stress, and the rate of heat transfer, *q*, from the following relations:

At small values of τ (τ<<1), it can easily be verified that the solutions of equations (4.17)–(4.19) take the following form:

$$f(\eta,\tau)=\sum_{i=0}^{n}\tau^{i} f_i(\eta)\ \ ,\ \ g(\eta,\tau)=\sum_{i=0}^{n}\tau^{i} g_i(\eta),\ \ \theta(\eta,\tau)=\sum_{i=0}^{n}\tau^{i}\theta_i(\eta) \tag{4.21}$$

Now, substituting the series expressions given in (4.21) into the equations (4.17)–(4.19) and picking up the terms up to the o(τ^2), we get the following sets of boundary value problems:

Equations of O(τ^0)

$$(1+K)\, f_0''' + \frac{1}{2}\eta\, f_0'' - f_0' + K g_0' + \theta_0 = 0 \tag{4.22}$$

$$\left(1+\frac{K}{2}\right) g_0'' + \frac{1}{2}\left(\eta g_0' - g_0\right) = 0 \tag{4.23}$$

$$\frac{1}{\Pr}\theta_0'' + \frac{1}{2}\eta\theta_0' = 0 \tag{4.24}$$

Corresponding boundary conditions (4.20) becomes

$$\begin{gathered} f_0(0,\tau) = f_0'(0,\tau) = 0,\ \ g_0(0,\tau) = -\frac{1}{2} f_0''(0,\tau),\ \ \theta_0(0,\tau) = 1 \\ f_0'(\infty,\tau) = g_0(\infty,\tau) = \theta_0(\infty,\tau) = 0 \qquad \forall\, \tau \ge 0 \end{gathered} \tag{4.25}$$

Equations of O(τ^1)

$$(1+K)\, f_1''' + \frac{1}{2}\eta\, f_1'' - 2 f_1' + K g_1' + \theta_1 = 0 \tag{4.26}$$

$$\left(1+\frac{K}{2}\right) g_1'' - K\left(2g_1 + f_1''\right) + \frac{1}{2}\left(\eta g_1' - g_1\right) = 0 \tag{4.27}$$

$$\frac{1}{\Pr}\theta_1'' + \frac{1}{2}\eta\theta_1' + \alpha^{*}\left(g_0'\theta_0 - g_0\theta_0'\right) - \theta_1 = 0 \tag{4.28}$$

Corresponding boundary conditions (4.25) becomes

$$\begin{gathered} f_1(0,\tau) = f_1'(0,\tau) = 0,\quad g_1(0,\tau) = -\frac{1}{2} f_1''(0),\ \ \theta_1(0,\tau) = 0 \\ f_1'(\infty,\tau) = g_1(\infty,\tau) = \theta_1(\infty,\tau) = 0 \quad \forall 0 \le \tau \le \infty \end{gathered} \tag{4.29}$$

Equations of O(τ^2)

$$(1+K)\,f_2''' + \frac{1}{2}\eta\, f_2'' - 3f_2' + f_0 f_0'' - f_0'^2 + Kg_2' + \theta_2 = 0 \tag{4.30}$$

$$\left(1+\frac{K}{2}\right)g_2'' + \frac{1}{2}\eta g_2' - \frac{5}{2}g_2 + f_0 g_0' - f_0' g_0 - K\left(f_1'' + 2g_1\right) = 0 \tag{4.31}$$

$$\frac{1}{\Pr}\theta_2'' + \frac{1}{2}\eta\theta_2' + f_0\theta_0' - f_0'\theta_0 + \alpha^*\left(g_0'\theta_1 + g_1'\theta_0 - g_0\theta_1' - g_1\theta_0'\right) - 2\theta_2 = 0 \tag{4.32}$$

Corresponding boundary conditions (4.29) becomes

$$\begin{gathered} f_2(0,\tau) = f_2'(0,\tau) = 0, \quad g_2(0,\tau) = -\frac{1}{2} f_2''(0), \ \theta_2(0,\tau) = 0 \quad \text{at} \ \ \eta = 0 \\ f_2'(\infty,\tau) = g_2(\infty,\tau) = \theta_2(\infty,\tau) = 0 \ \ \forall 0 \le \tau \le \infty \end{gathered} \tag{4.33}$$

The set of equations (4.22)-(4.24), (4.26)-(4.28) and (4.30)-(4.32) are linear by nature which, although are solvable analytically, are solved numerical employing the linear shooting method (or the method of superposition). Results thus obtained for $f_i''(0)$, $g_i'(0)$ and $\theta_i'(0)$, i = 0,2 are used in obtaining the values of the shear stress, the couple-stress, and the rate of heat transfer, from

$$\frac{\tau_\omega}{x} = (1+K)\tau^{1/2}\sum_{i=0}^{2} f_i''(0) \ , \ \frac{m_\omega}{x} = \left(1+\frac{K}{2}\right)\sum_{i=0}^{2} g_i'(0) \ , \ \frac{q_\omega}{x} = -\tau^{-1/2}\sum_{i=0}^{2}\theta_i'(0) \tag{4.34}$$

For example we have obtained the solutions of the above sets of equations for K= 1 while Pr = 9.0 and α*= 0.25, for which we have the following expressions for shear stress, τ_ω/x, couple stress, m_ω/x, and surface heat transfer, q_ω/x:

$$\begin{aligned} \frac{\tau_\omega}{x} &= (1+K)\tau^{1/2}\left(0.17551 + 0.00775\tau - 0.00547\tau^2 + \right) \ , \\ \frac{m_\omega}{x} &= \left(1+\frac{K}{2}\right)\left(0.06352 + 0.05055\tau - 0.01803\tau^2 + \right), \\ \frac{q_\omega}{x} &= \tau^{-1/2}\left(1.69440 + 0.04697\tau + 0.01640\tau^2 \right) \end{aligned} \tag{4.35}$$

Numerical values obtained from the above expressions for shear stress, couple stress and surface heat transfer entered in the Table 2 for comparison with other solutions obtained by the method discussed in forgoing section.

4.3.3 Asymptotic solutions for large time (τ >>1) regime

Now for large time regime equations (4.10)-(4.12) can be reduced to following form:

$$(1+K)f''' + ff'' - f'^2 + Kg' + \theta - \tau^{-1}\left(f' - \frac{1}{2}\eta f''\right) = \frac{\partial f'}{\partial \tau} \tag{4.36}$$

$$(1+K/2)g'' + fg' - f'g - \frac{1}{2}\tau^{-1}(g - \eta g') - K(f'' + 2g) = \frac{\partial g}{\partial \tau} \tag{4.37}$$

$$\frac{1}{\Pr}\theta'' + f\theta' - f'\theta + \frac{1}{2}\tau^{-1}\eta\theta' + \alpha^*(g'\theta - g\theta') = \frac{\partial \theta}{\partial \tau} \tag{4.38}$$

Corresponding boundary conditions are obtained as follows:

$$f(0,\tau) = 0,\ \ f'(0,\tau) = 0,\ \ g(0,\tau) = -\frac{1}{2}f'',\ \ \theta(0,\tau) = 1 \quad \text{at} \quad \eta = 0 \tag{4.39}$$

Expanding the functions involving the set of equations (4.36)-(4.39) in powers of τ^{-1} as given below:

$$f(\eta,\tau) = \sum_{i=0}^{n}\tau^{-i}F_i(\eta), \quad g(\eta,\tau) = \sum_{i=0}^{n}\tau^{-i}G_i(\eta), \quad \theta(\eta,\tau) = \sum_{i=0}^{n}\tau^{-i}\Phi_i(\eta) \tag{4.40}$$

Now using the functions given in (4.40) into the equations (4.36)–(4.39) and taking the terms up to the $O(\tau^{-1})$ we get

Equations of O(τ^0)

$$(1+K)F_0''' + F_0F_0'' - F_0'^2 + KG_0' + \Phi_0 = 0 \tag{4.41}$$

$$(1+K/2)G_0'' + F_0G_0' - F_0'G_0 - K(F_0'' + 2G_0) = 0 \tag{4.42}$$

$$\frac{1}{\Pr}\Phi_0'' + F_0\Phi_0' - F_0'\Phi_0 + \alpha^*(G_0'\Phi_0 - G_0\Phi_0') = 0 \tag{4.43}$$

Corresponding boundary conditions are obtained as follows (4.39)

$$\begin{aligned} &F_0(0,\tau) = 0,\ \ F_0'(0,\tau) = 0,\ \ G_0(0,\tau) = -\frac{1}{2}F_0'',\ \Phi_0(0,\tau) = 1 \\ &F_0'(\infty,\tau) = 0,\ \ G_0(\infty,\tau) = 0,\ \ \Phi_0(\infty,\tau) = 0 \quad \forall 0 \le \tau \le \infty \end{aligned} \tag{4.44}$$

Equations of O(τ^{-1})

$$(1+K)F_1''' + F_0F_1'' + F_1F_0'' - 2F_0'F_1' + KG_1' + \Phi_1 - \left(f_0' - \frac{1}{2}\eta f_0''\right) = 0 \tag{4.45}$$

$$(1+K/2)G_1''+F_0G_1'+F_1G_0'-(F_0'G_1+F_1'G_0)-K(F_1''+2G_1)-\frac{1}{2}(g_0-\eta g_0')=0 \tag{4.46}$$

$$\frac{1}{\Pr}\Phi_1''+F_0\Phi_1'+F_1\Phi_0'-F_0'\Phi_1-F_1'\Phi_0+\frac{1}{2}\eta\theta_0' + \alpha^*\left[(G_0'\Phi_1+G_1'\Phi_0)-\left(G_0\Phi_1'+G_1\Phi_0'\right)\right]=0 \tag{4.47}$$

Corresponding boundary conditions are obtained as follows (4.44)

$$\begin{aligned} &F_1(0,\tau)=0,\ F_1'(0,\tau)=0,\ G_1(0,\tau)=-\frac{1}{2}F_1'',\ \Phi_1(0,\tau)=0 \\ &F_1'(\infty,\tau)=0,\ G_1(\infty,\tau)=0,\ \Phi_1(\infty,\tau)=0 \quad \forall 0\le\tau\le\infty \quad \text{at}\ \ \eta=0 \end{aligned} \tag{4.48}$$

Equations (4.41) to (4.43) are the leading order equations and represent the steady state flow at large τ. The same set of equations were obtained by Hossain *et al.* [22] as the steady mean part of the fluctuating flow of the thermomicropolar fluid past a flat surface that was maintained at small amplitude oscillating temperature about a non-uniform steady mean temperature. We should further mention that, Jena and Mathur [10] in studying the laminar free convective flow of a thermomicropolar fluid past a non-isothermal vertical flat plate obtained the same set of that given above. It should be noted that the set of equations (4.41) to (4.43) are nonlinear. Hence solutions of these equations are obtained numerically by employing the non-linear shooting method. Typical values of $F''(0)$, $G'(0)$ and $\Phi'(0)$ thus obtained are compare with that of Jena and Mathur [10] in Table-4.1.

Table-4.1: Numerical values of the coefficients of shear stress, surface heat transfer and couple-stress for K = 0.1 and 0.25 while Pr = 9.0 and α^*= 1.0 a comparison.

Comparison	K= 0.1			K = 0.25		
	$F''(0)$	$-G'(0)$	$-\theta'(0)$	$F''(0)$	$-G'(0)$	$-\theta'(0)$
Jena and Mathur [10]	0.1558	0.0365	0.3675	0.1480	0.0389	0.3561
Present	0.15574	0.03652	0.36764	0.14829	0.03883	0.35787

Here we have obtained the solutions of equations upto the $O(\tau^{-1})$ using the non-linear shooting method. Once we know the values of $F_i''(0)$, $G_i'(0)$ and $\Phi_i'(0)$ for i = 0,1 we may obtain the

numerical values of the coefficients of shear stress, couple stress and surface heat transfer from the expressions are given below:

$$\frac{\tau_\omega}{x}=(1+K)\sum_{i=0}^{1}\tau^{-i}F_i''(0)\ ,\ \frac{m_\omega}{x}=\left(1+\frac{K}{2}\right)\sum_{i=0}^{1}\tau^{-i}G_{ii}'(0)\ ,\ \frac{q_\omega}{x}=-\sum_{i=0}^{1}\tau^{-i}\Phi_i'(0) \tag{4.49}$$

For example, taking K =1.0, Pr = 9.0 and α^* = 0.25, we get the following expressions for shear stress, τ_ω/x, couple stress, m_ω/x, and surface heat transfer, q_ω/x:shear stress, couple stress and surface heat transfer:

$$\frac{\tau_\omega}{x}=(1+K)\left(0.34516-0.34155\tau^{-1}+\right)\ ,\ \frac{m_\omega}{x}=\left(1+\frac{K}{2}\right)\left(0.13937-0.03245\tau^{-1}+\right),\quad \frac{q_\omega}{x}=-\left(-1.09407-0.33523\tau^{-1}+\right) \tag{4.50}$$

Numerical values thus obtained for shear stress, τ_ω/x, couple stress, m_ω/x, and surface heat transfer, q_ω/x, are entered in the Table-4.2 for values of τ while K =1.0 and α^*=0.25. This table also contained the asymptotic values of the above physical quantities for comparison. The comparison shows excellent agreement with the perturbation solutions for smaller value of τ up to 1.48 and for large value of τ from 40.0 that obtained for all τ.

Table-4.2: Numerical values of shear stress, τ_ω/x, couple stress, m_ω/x, and surface heat transfer, q_ω/x, while K =1.0 and α^*= 0.25 against τ.

τ	τ_ω/x		m_ω/x		q_ω/x	
	All τ	Asymptotic	All τ	Asymptotic	All τ	Asymptotic
0.01	0.03428	0.03512^s	0.09375	0.09604^s	17.21207	16.94869^s
0.02	0.04851	0.04968^s	0.09449	0.09679^s	12.17307	11.98789^s
0.05	0.07681	0.07866^s	0.09667	0.09901^s	7.70340	7.58826^s
0.10	0.10887	0.11146^s	0.10020	0.10260^s	5.45267	5.37353^s
0.20	0.15459	0.15817^s	0.10692	0.10937^s	3.86422	3.81126^s
0.4	0.22004	0.22482^s	0.11907	0.12129^s	2.74688	2.71293^s
0.6	0.27066	0.27514^s	0.12974	0.13182^s	2.25728	2.26240^s
1.0	0.35052	0.35557^s	0.14740	0.14407^s	1.77750	1.7577^s
1.50	0.42721	0.42823^s	0.16417	0.14819^s	1.49132	1.47113^s

1.86	0.47167	0.46641^{s}	0.17345	0.14278^{s}	1.34835	1.34805^{s}
20.0	0.68453	0.65616^{l}	0.20662	0.14273^{l}	1.11083	1.55191^{l}
30.0	0.68454	0.66755^{l}	0.20613	0.20743^{l}	1.09406	1.10524^{l}
40.0	0.68455	0.67324^{l}	0.20613	0.20784^{l}	1.09410	1.10245^{l}
50.0	0.68455	0.67666^{l}	0.20613	0.20808^{l}	1.09410	1.10077^{l}
60.0	0.68455	0.67893^{l}	0.20824	0.20739^{l}	1.20824	1.09965^{l}
70.0	0.68455	0.68056^{l}	0.20613	0.20836^{l}	1.09410	1.09886^{l}
80.0	0.68455	0.68178^{l}	0.20613	0.20845^{l}	1.09410	1.09826^{l}
90.0	0.68455	0.68273^{l}	0.20613	0.20851^{l}	1.09410	1.09779^{l}
100.0	0.68455	0.68349^{l}	0.20613	0.20857^{l}	1.09410	1.09742^{l}

s stands for small time and *l* stands for large time.

4.4 Results and discussion

In the above sections, we have analyzed the problem of unsteady natural convection laminar boundary layer flow of thermo-micropolar viscous incompressible fluid along a non-uniformly heated vertical surface. The governing dimensionless boundary layer equations are transformed into suitable forms appropriate for entire, small and large time regimes. Solutions of the resulting equations are then obtained numerically and the results are depicted in terms of the transient shear stress, τ_ω/x, couple stress, m_ω/x, and surface heat transfer, q_ω/x. Here we have discussed the effects of the physical parameters, such as, the micropolar heat conduction parameter, α^*, and the vortex viscosity parameter, K, τ_ω/x, m_ω/x, and q_ω/x against the time variable τ. The present analysis of the problem has been carried out considering the fluid for which Pr = 9.0 (Jena and Mathur [10]). Further results have been presented and discussed in terms of axial velocity, angular velocity and the temperature profiles with effect of the aforementioned physical parameters.

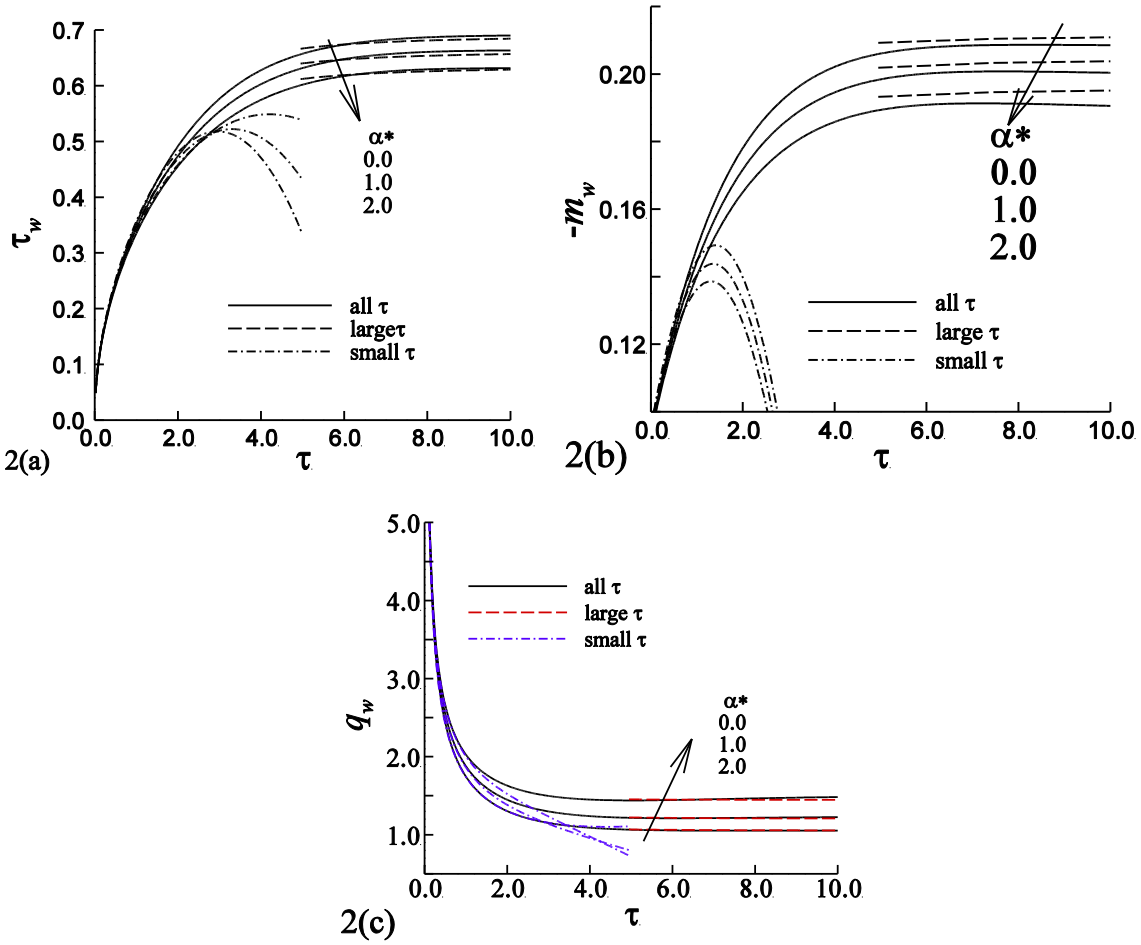

Fig. 4.2: Numerical values of (a) shear stress (b) couple-stress and (c) surface heat transfer coefficient for different values of α^* against values of τ while Pr = 9.0, K =1.0.

4.4.1 Effect of micropolar heat conduction parameter, α^* on transient shear stress, couple stress coefficients and surface heat transfer

The effects of the micropolar heat conduction parameter, α^*, on the transient shear stress, τ_ω/x, the couple stress, m_ω/x, and the surface heat transfer coefficient, q_ω/x are presented, respectively, in figures 4.2(a) to 4.2(c) taking value of the vortex viscosity parameter, K, equal to 1.0. It is seen from these figures that as the micropolar heat conduction, α^* leads to decrease the value of the shear stress as well as the heat transfer; whereas, there is increase in the couple stress. These happen due to the fact that increase in the value of micropolar thermal conductivity enhances the fluid's thermal conductivity. These figures also contain the representative values of τ_ω/x, m_ω/x, and q_ω/x obtained from the asymptotic solution for

different values of α^*. One can claim that the asymptotic values in the smaller and larger time regimes agree excellently with all time solutions. This claims that the results presented here for all time regime are accurate and hence may be useful for the experimentalists.

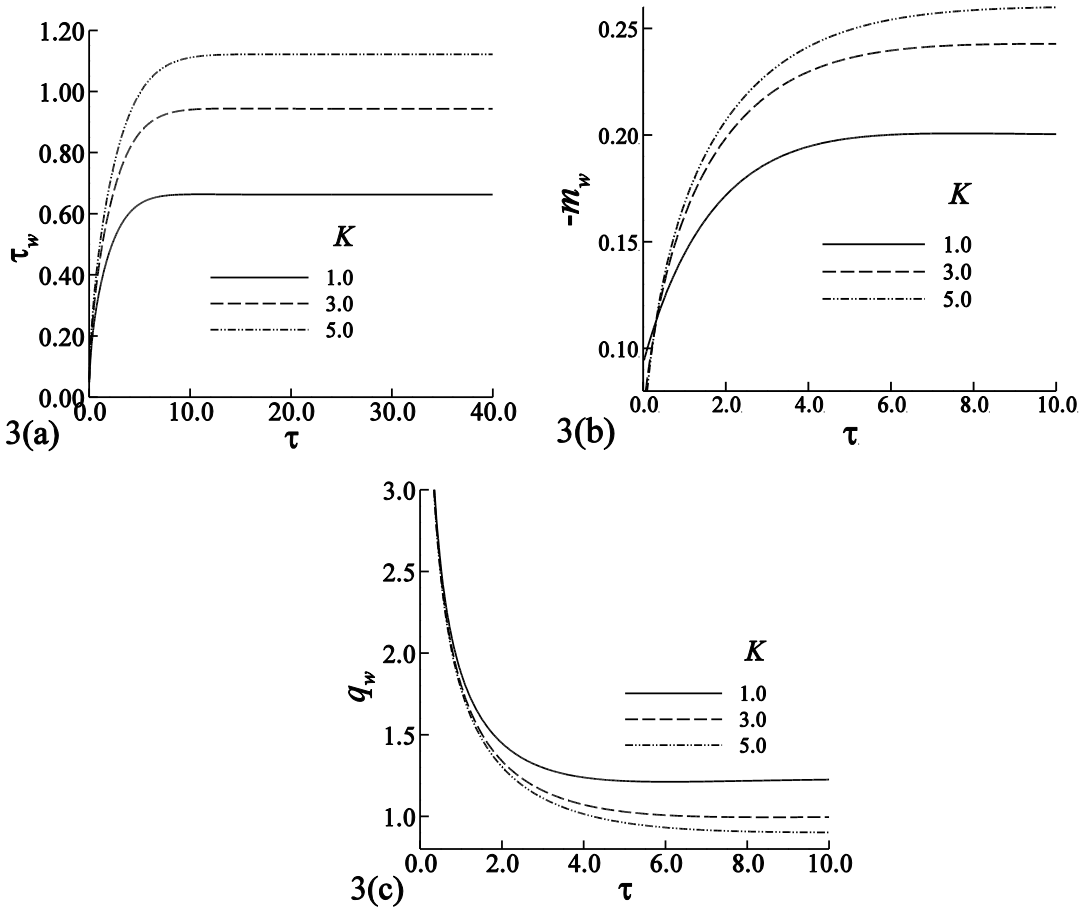

Fig. 4.3: Numerical values of (a) shear stress (b) couple-stress and (c) surface heat transfer coefficient for different values of K against values of τ while α^* =1.0.

4.4.2 Effect of vortex viscosity parameter, *K*, on transient shear stress, couple stress coefficients and surface heat transfer

Now we show the effect of the vortex viscosity parameter, K, on the transient shear stress, τ_ω/x, couple stress, m_ω/x, and surface heat transfer coefficient, q_ω/x. Fig 4.3(a)-(c) depict the values of τ_ω/x, m_ω/x, and q_ω/x for K=1.0, 3.0 and 5.0 while α^* =1 against τ. From these figures one can see that an increase in the value of the vortex-viscosity leads to increase in shear

stress but decrease the couple stress the surface heat transfer. This is expected because increasing value of the vortex viscosity will increase the total viscosity of the fluid.

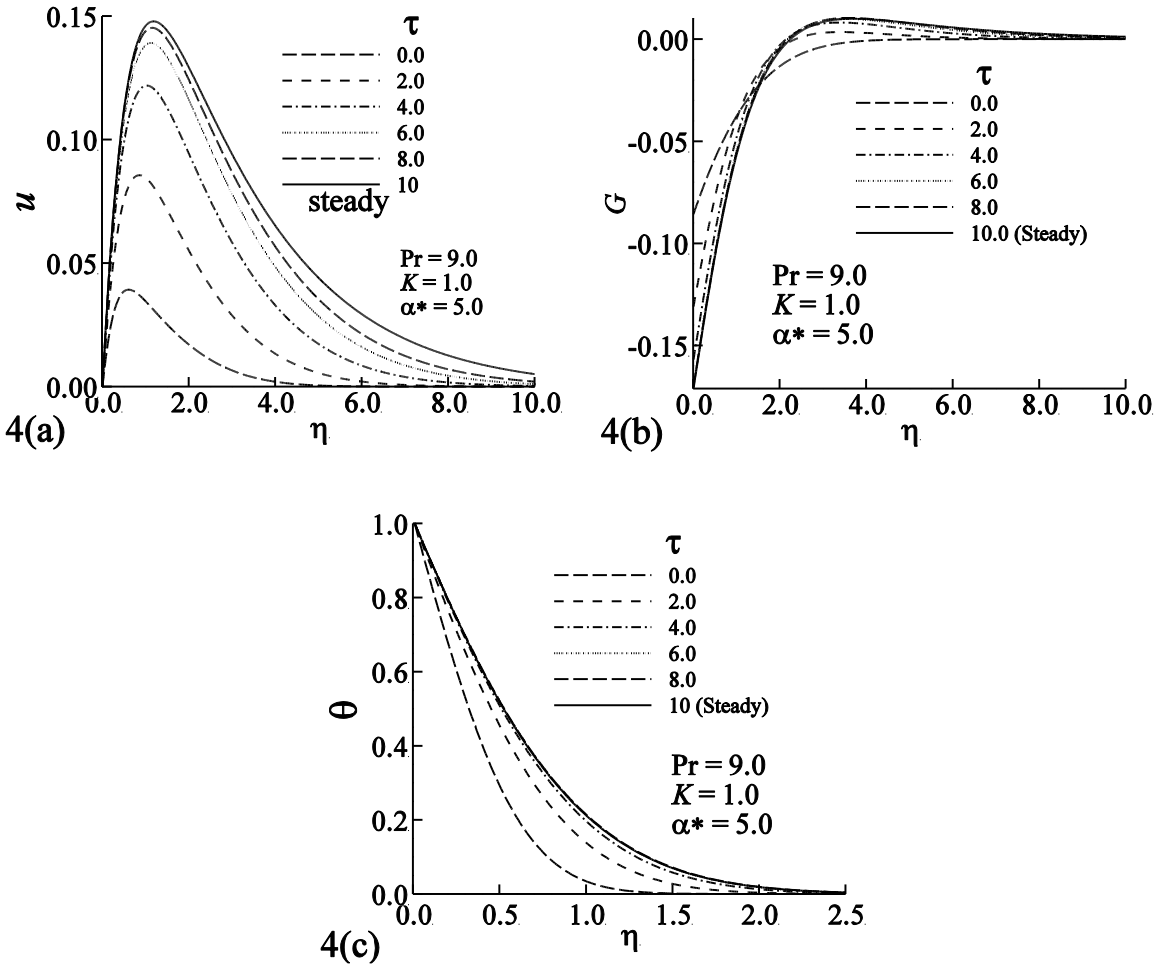

Fig. 4.4: Numerical values of (a) velocity profiles (b) angular velocity profiles and (c) temperature profiles for different values of τ against η when Pr = 9.0, K =1.0.

4.4.3 Transient axial velocity, angular velocity and temperature profiles for different time (τ):

The transient axial velocity, angular velocity and temperature profiles are shown in Figs 4.4(a)-(c) against η for values of τ in [0, 8] while vortex-viscosity parameter K=1 and micropolar thermal conductivity parameter α^*= 5.0. It is seen from figs 4.4(a) and 4.4(c) that the axial velocity and the temperature profiles increase with the increase of time which leads to increase in both the momentum boundary thickness. On the other hand, one can also see

that in the vicinity of the surface, i.e., in the region $\eta \leq 2$ (approximately) the angular velocity profile decrease, whereas these profiles increase with the increase of time in the region $\eta > 2$. Further we notice that all the profiles reach to the asymptotic profile (or the steady state profile at larger value to time parameter τ. In this case we found the maximum value of τ to be 8 to reach the profiles at steady state.

4.4.4 Effect of micropolar heat conduction parameter, α^* on axial and angular velocity and temperature profiles

Here we show the effect of micropolar thermal conductivity, α^*, on the transient axial velocity, angular velocity and the temperature profiles at τ =2.0 while K=1.0 through figures

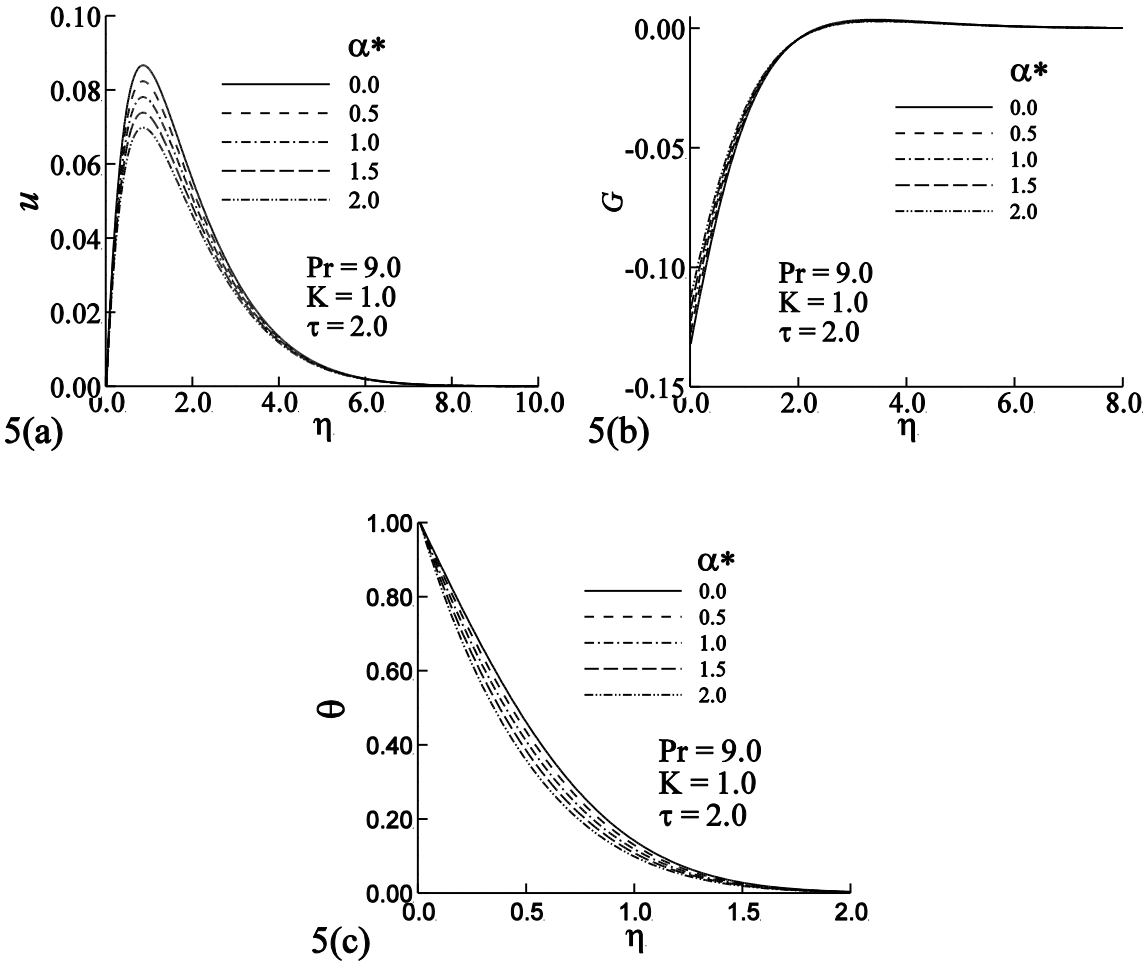

Fig. 4.5: (a) Axial velocity profiles (b) angular velocity profiles and (c) temperature profiles for different values of α^* against η at τ = 2 when Pr = 9.0, K =1.0.

4.5(a) to (c), respectively. In this case α^* = 0.0, 0.5, 1.0, 1.5, and 2.0. It is clear from these figures that the axial velocity, angular velocity and temperature profiles increase due to increase in micropolar thermal conductivity, α^*. But, owning to increase in the heat conduction parameter, no significant effect on the angular velocity profile is observed.

4.4.5 Effect of vortex viscosity parameter, *K* on axial velocity, angular velocity and temperature profiles

The effect of increasing values of the vortex viscosity parameter, *K*, on the transient axial velocity, angular velocity and temperature profiles are depicted in Figs 4.6(a)-(c) at τ = 2.0 and α^*= 0.25.

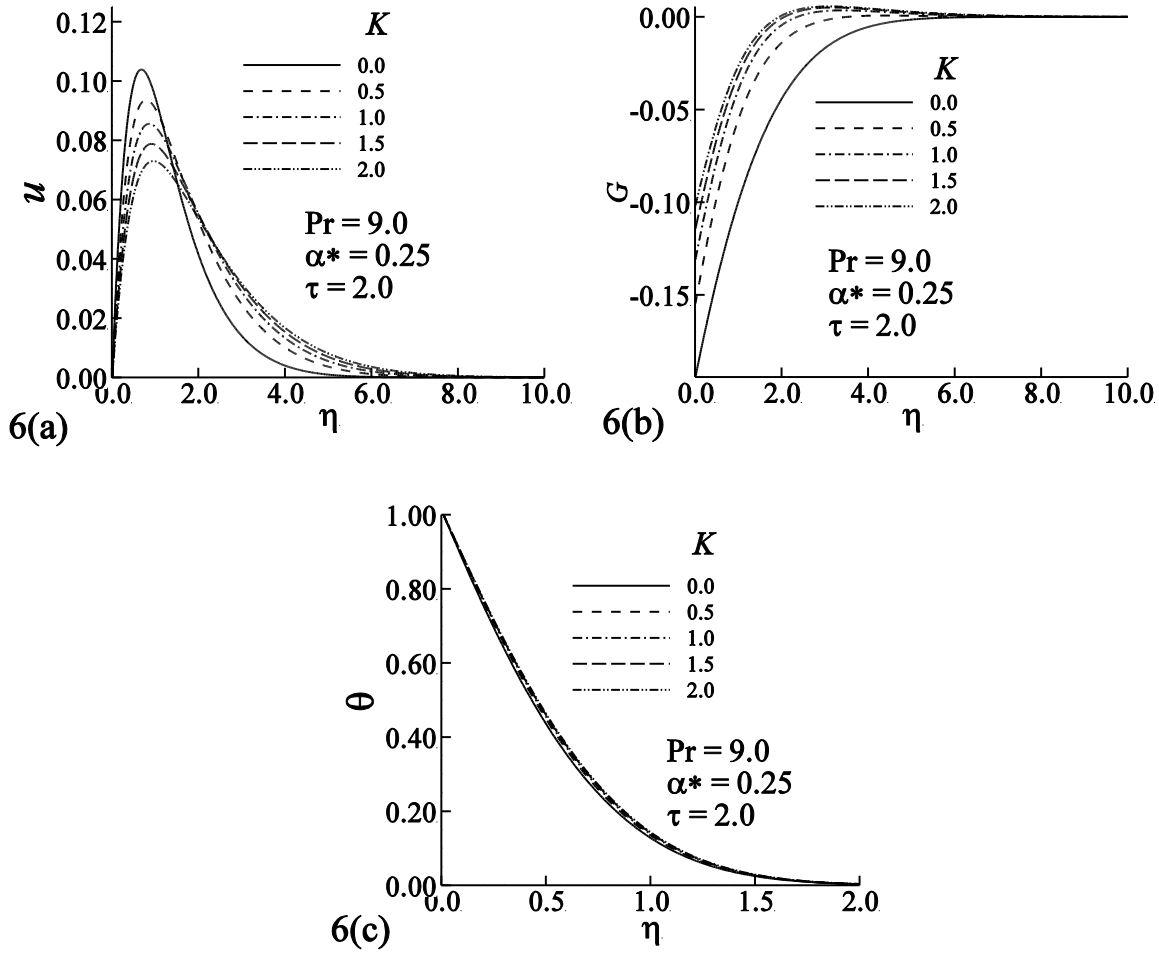

Fig. 4.6: Numerical values of (a) velocity profiles (b) angular velocity profiles and (c) temperature profiles for different values of *K* against η at τ = 2 when *Pr* = 9.0, α^*= 0.25.

From Fig. 4.6(a) it can be seen that within the region $\eta < 1.8$, the velocity profile increases due to increase in the value of the vortex-viscosity of the fluid; whereas, this leads to decrease the velocity profile in the region $\eta > 1.8$. This implies that increase in the vortex viscosity leads to decrease in the momentum boundary layer thickness. We further observe that the angular velocity profile decreases owing to increase in the value of K which leads to that this reduces the angular momentum boundary layer thickness. Finally, one can see that there is no significant contribution to the temperature profile due to increase in the vortex viscosity parameter K.

Chapter Five
Fluctuating Flow of Thermomicropolar Fluid past a Vertical Surface

5.1 Introduction

The unsteady free convection boundary layer flow of a thermo-micropolar fluid along a vertical plate has been investigated in this paper. The temperature of the plate is assumed to be oscillating about a mean temperature, $\theta_w(x)$, with small amplitude ε. The governing boundary layer equations are analyzed using straight forward finite difference method. The effects of the material parameters such as micropolar heat conduction parameter, N^*, the vortex viscosity parameter, K, on the shear stress, τ_ω, surface heat transfer, q_ω, and the couple-stress, m_ω, have been investigated.

5.2 Mathematical Formalisms

A two-dimensional unsteady laminar boundary layer flow of a thermo-micropolar fluid along a permeable vertical flat plate is considered. The temperature of the ambient fluid and the surface are assumed to be T_∞ and T_W respectively. The co-ordinate system and the flow configuration are shown in Fig. 5.1.

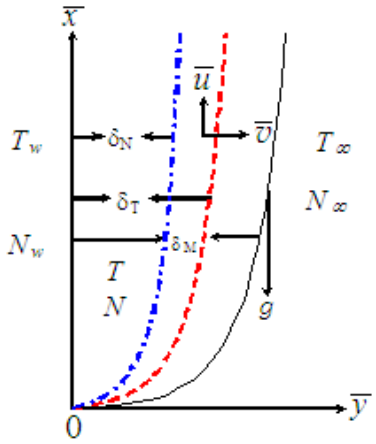

Fig. 5.1: Flow configuration and coordinate system.

Under the usual Boussinesq approximation the dimensionless equations of conservation of mass, momentum, angular velocity and energy that govern the flow are given as (see Jena and Mathur (1981)),

$$\frac{\partial u}{\partial x}+\frac{\partial v}{\partial y}=0 \tag{5.1}$$

$$\frac{\partial u}{\partial t}+u\frac{\partial u}{\partial x}+v\frac{\partial u}{\partial y}=\left(1+K\right)\frac{\partial^2 u}{\partial y^2}+K\frac{\partial N}{\partial y}+\theta \tag{5.2}$$

$$\frac{\partial N}{\partial t}+u\frac{\partial N}{\partial x}+v\frac{\partial N}{\partial y}=\left(1+\frac{K}{2}\right)\frac{\partial^2 N}{\partial y^2}-K\left(2N+\frac{\partial u}{\partial y}\right) \tag{5.3}$$

$$\frac{\partial \theta}{\partial t}+u\frac{\partial \theta}{\partial x}+v\frac{\partial \theta}{\partial y}=\frac{1}{\Pr}\frac{\partial^2 \theta}{\partial y^2}+N^*\left(\frac{\partial \theta}{\partial x}\frac{\partial N}{\partial y}-\frac{\partial \theta}{\partial y}\frac{\partial N}{\partial x}\right) \tag{5.4}$$

which are based on the following dimensionless dependent and independent variables

$$\begin{aligned} &x=\frac{\bar{x}}{L},\ y=\frac{\bar{y}}{L},\ \bar{u}=\frac{\nu}{L}u,\ \bar{v}=\frac{\nu}{L}v \\ &\bar{N}=\frac{\nu}{L^2}N,\ t=\frac{\nu}{L^2}\bar{t},\ \theta=\frac{g\beta\left(\bar{T}-\bar{T}_\infty\right)L^3}{\nu^2}. \end{aligned} \tag{5.5}$$

Here, $(\bar{x},\bar{y})$ are the co-ordinates parallel with and perpendicular to the flat surface respectively, $(\bar{u},\bar{v})$ are the velocity components, t, time, $\bar{N}$, the angular velocity, θ, dimensionless temperature, j, the micro-inertia per unit mass, ρ, the density of the fluid, g the acceleration due to gravity, κ, the thermal conductivity of the fluid, $\gamma = (\mu + \kappa/2)j$, the gyro-viscosity coefficient and α^*, the micropolar heat conduction coefficient.

Following Jena and Mathur (1981), it is assumed that micro-inertia, j, is a constant and, therefore, it is set equal to a reference value, $j_0 = L^2$. Further, L is the characteristic length, $K=(\kappa/\mu)$ is vortex viscosity parameter, μ, the dynamic viscosity, $Pr = (\nu/\alpha)$ is the Prandtl number that gives the ratio of momentum diffusivity to thermal diffusivity, ν, viscosity coefficient, $N^* = (\alpha^*/L^2)$ is the micropolar heat conduction parameter and ε is the amplitude of oscillation.

The corresponding boundary conditions are

$$\begin{aligned} &u = 0, \quad v = 0, \quad N = -n\frac{\partial u}{\partial y}, \quad \theta = \theta_w(x)(1 + \varepsilon\cos(\tau)) \text{ at } y = 0 \\ &u = 0, \quad \theta = 0 \quad \text{as} \quad y \to \infty \end{aligned} \tag{5.6}$$

Where n is a constant such that $0 \le n \le 1$. The case $n = 0$ corresponds to the strong concentration of microelements. Thus equation (5.6) suggests that when $n = 0$ (i.e., $N = 0$) near the walls, the concentration of the particles is strong enough so that the micro-elements near the walls are unable to rotate because of its concentration. The case, $n = 1/2$, on the other hand, indicates the vanishing of anti-symmetric part of the stress tensor and denotes weak concentration.

The boundary condition for $\theta(\tau, 0)$ given in (5.6) suggests the solutions of equations (5.1)-(5.4) of the following form:

$$\begin{aligned} &u = u_0 + \varepsilon\exp(i\tau)u_1, \quad v = v_0 + \varepsilon\exp(i\tau)v_1 \\ &N = N_0 + \varepsilon\exp(i\tau)N_1, \quad \theta = \theta_0 + \varepsilon\exp(i\tau)\theta_1 \end{aligned} \tag{5.7}$$

where, $\omega t = \tau$. Further, u_0, v_0, N_0 and θ_0 represent the flow variables for the steady mean flow and u_1, v_1, N_1 and θ_1 are the fluctuating flow variables. The real parts of the functions defined in (5.7) is our desired solutions.

Now substituting the functions given in (5.7) into Eqs. (5.1)–(5.4) and equating the terms up to $O(\varepsilon)$ one gets

$$\frac{\partial u_0}{\partial x} + \frac{\partial v_0}{\partial y} = 0 \tag{5.8}$$

$$u_0\frac{\partial u_0}{\partial x} + v_0\frac{\partial u_0}{\partial y} = (1+K)\frac{\partial^2 u_0}{\partial y^2} + K\frac{\partial N_0}{\partial y} + \theta_0 \tag{5.9}$$

$$u_0\frac{\partial N_0}{\partial x} + v_0\frac{\partial N_0}{\partial y} = \left(1+\frac{K}{2}\right)\frac{\partial^2 N_0}{\partial y^2} - K\left(2N_0 + \frac{\partial u_0}{\partial y}\right) \tag{5.10}$$

$$u_0\frac{\partial \theta_0}{\partial x} + v_0\frac{\partial \theta_0}{\partial y} = \frac{1}{\Pr}\frac{\partial^2 \theta_0}{\partial y^2} + N^*\left(\frac{\partial \theta_0}{\partial x}\frac{\partial N_0}{\partial y} - \frac{\partial \theta_0}{\partial y}\frac{\partial N_0}{\partial x}\right) \tag{5.11}$$

with boundary conditions

$$\begin{aligned} &u_0 = 0, \quad v_0 = 0, \quad N_0 = -n\frac{\partial u_0}{\partial y}, \quad \theta_0 = \theta_w(x) \quad \text{at} \quad y = 0 \\ &u_0 = 0, \quad \theta_0 = 0 \quad \text{as} \quad y \to \infty. \end{aligned} \tag{5.12}$$

and

$$\frac{\partial u_1}{\partial x}+\frac{\partial v_1}{\partial y}=0 \tag{5.13}$$

$$iu_1+u_0\frac{\partial u_1}{\partial x}+u_1\frac{\partial u_0}{\partial x}+v_0\frac{\partial u_1}{\partial y}+v_1\frac{\partial u_0}{\partial y}=(1+K)\frac{\partial^2 u_1}{\partial y^2}+K\frac{\partial N_1}{\partial y}+\theta_1 \tag{5.14}$$

$$iN_1+u_0\frac{\partial N_1}{\partial x}+u_1\frac{\partial N_0}{\partial x}+v_0\frac{\partial N_1}{\partial y}+v_1\frac{\partial N_0}{\partial y}=\left(1+\frac{K}{2}\right)\frac{\partial^2 N_1}{\partial y^2}-K\left(2N_1+\frac{\partial u_1}{\partial y}\right) \tag{5.15}$$

$$\begin{aligned} i\theta_1+u_0\frac{\partial \theta_1}{\partial x}+u_1\frac{\partial \theta_0}{\partial x}+v_0\frac{\partial \theta_1}{\partial y}+v_1\frac{\partial \theta_0}{\partial y}&=\frac{1}{\Pr}\frac{\partial^2\theta_1}{\partial y^2}\\ &+N^*\left(\frac{\partial\theta_0}{\partial x}\frac{\partial N_1}{\partial y}+\frac{\partial\theta_1}{\partial x}\frac{\partial N_0}{\partial y}-\frac{\partial\theta_0}{\partial y}\frac{\partial N_1}{\partial x}-\frac{\partial\theta_1}{\partial y}\frac{\partial N_0}{\partial x}\right)\end{aligned} \tag{5.16}$$

subject to the boundary conditions

$$\begin{aligned} &u_1=0,\ v_1=0,\ N_1=-n\frac{\partial u_1}{\partial y},\ \theta_1=\theta_w(x)\quad \text{at}\quad y=0\\ &u_1\to 0,\ \theta_1\to 0\quad \text{as}\quad y\to\infty. \end{aligned} \tag{5.17}$$

Here the equations (5.8)–(5.11) are the equations for the steady state flow and those (5.13)-(5.16) are for the fluctuating flow.

5.3 Methods of solution

In this section, emphasis is given to the method of solution which is used to solve the boundary layer equations (5.8)–(5.11) will represent the steady mean flow and those (5.13)–(5.16) the oscillating flow. The numerical solutions are obtained with the help of an efficient finite difference scheme.

To get the similarity equations for the steady state equations (5.8) –(5.11), we introduce the following group of transformations:

$$\psi_0=xf(\eta),\ N_0=xg(\eta),\ \theta_0=x\Theta_0(\eta),\ \eta=y \tag{5.18}$$

where ψ_0 is the stream function for the steady state flow defined by

$$u_0=\frac{\partial\psi_0}{\partial\eta},v_0=-\frac{\partial\psi_0}{\partial x}\cdot \tag{5.19}$$

Thus we have

$$(1+K)f''' + ff'' - f'^2 + Kg' + \Theta_0 = 0 \tag{5.20}$$

$$\left(1+\frac{K}{2}\right)g'' + fg' - f'g - K(f'' + 2g) = 0 \tag{5.21}$$

$$\frac{1}{\Pr}\Theta_0'' + f\Theta_0' - f'\Theta_0 + N^*(\Theta_0 g' - \Theta_0' g) = 0. \tag{5.22}$$

The boundary conditions to be satisfied by the above equations are

$$\begin{aligned} &f = 0,\ f' = 0,\ g = -nf'',\ \Theta_0 = 1 \text{ at } y \to 0 \\ &f'(0) = 0,\ \Theta_0 = 0 \text{ at } y \to \infty. \end{aligned} \tag{5.23}$$

Here $'$ denotes differentiation with respect to η.

Equations (5.20)–(5.22) are considered by Jena and Mathur (1981). Representative numerical values of shear stress, surface heat transfer and couple stress obtained from the present investigation of these equations are entered in Table 1, for comparison with those of Jena and Mathur (1981). From this table it is seen that the present solutions are in excellent agreement with those of Jena and Mathur (1981).

Table 5.1: The effect of variation of *K* on shear stress, surface heat transfer and couple-stress when *Pr* = 9.0 and N^*= 1.0.

Comparison	K= 0.1			K = 0.25		
	$F''(0)$	$-G'(0)$	$-\theta'(0)$	$F''(0)$	$-G'(0)$	$-\theta'(0)$
Jena and Mathur (1981)	0.1558	– 0.0365	0.3675	0.1480	– 0.0389	0.3561
Present	0.15574	– 0.03652	0.36764	0.14829	– 0.03883	0.35787

Again, to get the similarity equations for the unsteady state equations (5.13)–(5.16), we introduce the following group of transformations:

$$\psi_1 = xF(\eta),\ N_1 = xG(\eta),\ \theta_1 = x\Theta_1(\eta),\ \eta = y \tag{5.24}$$

where ψ_1 is the stream function for the unsteady flow defined by

$$u_1 = \frac{\partial \psi_1}{\partial \eta}, \quad v_1 = -\frac{\partial \psi_1}{\partial x}. \tag{5.25}$$

Thus equations (5.13)–(5.16) then reduce to

$$iF' + 2f'F' - fF'' - f''F = (1+K)F''' + KG' + \Theta_1 \tag{5.26}$$

$$iG + f'G - fG' + F'g - Fg' = \left(1+\frac{K}{2}\right)G'' - K\left(F'' + 2G\right) \tag{5.27}$$

$$i\Theta_1 + f'\Theta_1 - f\Theta_1' + F'\Theta_0 - F\Theta_0' = \frac{1}{\Pr}\Theta_1'' + N^*\left(\Theta_0 G' + \Theta_1 g' - \Theta_0' G - \Theta_1' g\right) \tag{5.28}$$

and the boundary conditions become

$$\begin{aligned} &F = 0,\ F' = 0,\ G = -nF'',\ \ \Theta_1 = 1 \quad \text{at} \quad y = 0 \\ &F \to 0,\ F' \to 0,\ \Theta_1 \to 0 \quad \text{as} \quad y \to \infty. \end{aligned} \tag{5.29}$$

The set of equations (5.20)–(5.22) and (5.26)–(5.28) together with the boundary conditions (5.23) and (5.29) can be integrated by straight forward finite difference method. Before going to apply the aforementioned method we first set $f = V_0$, $f' = U_0$, $F = V$ and $F' = U$ so that the equations (5.20)–(5.22) reduce to

$$(1+K)U_0'' + V_0U_0' - (U_0)^2 + Kg' + \Theta_0 = 0 \tag{5.30}$$

$$\left(1+\frac{K}{2}\right)g'' + V_0 g' - U_0 g - K\left(\frac{\partial U_0}{\partial \eta} + 2g\right) = 0 \tag{5.31}$$

$$\frac{1}{\Pr}\Theta_0'' + V_0\Theta_0' - U_0\Theta_0 + N^*\left(\Theta_0 g' - \Theta_0' g\right) = 0. \tag{5.32}$$

with boundary conditions

$$\begin{aligned} &V_0 = 0,\ U_0 = 0,\ \ g = -nU_0',\ \ \Theta_0 = 1 \quad \text{at} \quad \eta = 0 \\ &U_0 = 0,\ \Theta_0 = 0 \text{ at } \eta \to \infty. \end{aligned} \tag{5.33}$$

and the equations (5.26)–(5.28) take the form

$$iU + 2U_0U - V_0U' - VU_0' = (1+K)U'' + KG' + \Theta_1 \tag{5.34}$$

$$iG + GU_0' - VG' + U'g - Vg' = \left(1+\frac{K}{2}\right)G'' - K\left(U' + 2G\right) \tag{5.35}$$

$$i\Theta_1 + U_0'\Theta_1 - V\Theta_1' + U\Theta_0 - V\Theta_0' = \frac{1}{\Pr}\Theta_1'' + N^*\left(\Theta_0 G' + \Theta_1 g' - \Theta_0' G - \Theta_1' g\right) \tag{5.36}$$

Now equations (5.30)–(5.32) are discretised by a simple numerical scheme, in which we use central-difference for diffusion terms and convection terms and thus, for example, (5.30) gives

$$\left\{\frac{1+K}{\Delta\eta^2}+\frac{(V_0)_j}{2\Delta\eta}\right\}(U_0)_{j+1}+\left\{\frac{1+K}{\Delta\eta^2}-\frac{(V_0)_j}{2\Delta\eta}\right\}(U_0)_{j-1}-\left\{\frac{2(1+K)}{\Delta\eta^2}-(U_0)_j\right\}(U_0)_j$$
$$=-K\left(\frac{g_{j+1}-g_{j-1}}{2\Delta\eta}\right)-\Theta_j \tag{5.37}$$

Equation (5.37) can be rewritten in the form

$$A_j(U_0)_{j+1}+B_j(U_0)_j+C_j(U_0)_{j-1}=D_j \tag{5.38}$$

where $A_j=\frac{1+K}{\Delta\eta^2}+\frac{(V_0)_j}{2\Delta\eta}$, $B_j=-\left\{\frac{2(1+K)}{\Delta\eta^2}-(U_0)_j\right\}$, $C_j=\frac{1+K}{\Delta\eta^2}-\frac{(V_0)_j}{2\Delta\eta}$

and $D_j=-K\left(\frac{g_{j+1}-g_{j-1}}{2\Delta\eta}\right)-\Theta_j$.

Similarly, the equations (5.31)–(5.32) can be rendered in the form (5.38). The resulted tri-diagonal algebraic system is solved by Gaussian elimination technique. The computation is started at η = 0, and then marches downstream implicitly. The ordinary differential equations governing the upstream condition at η = 0 can be obtained by taking the limit of equations (5.38) that η approaches zero. The associated boundary conditions are equations (5.33) with η = 0.

Now we define the functions

$$U=U_r+iU_i,\quad \Theta_1=\Theta_r+i\Theta_i,\quad G=G_r+iG_i \tag{5.39}$$

Using (5.39) into (5.34)–(5.36) and then separating the real and imaginary parts, we can solve the resulting systems of equations employing the procedure described above.

Again, from the set of relations (5.7) together with the transformations given in and(5.18)–(5.19) and (5.24)–(5.25), we get the expression for the dimensionless axial velocity, temperature and angular velocity functions as given below

$$\begin{aligned}
u(\tau,\eta)/x &= f'+\varepsilon\left[\cos(\tau)U_r-\sin(\tau)U_i\right],\\
\theta(\tau,\eta)/x &= \theta+\varepsilon\left[\cos(\tau)\Theta_r-\sin(\tau)\Theta_i\right],\\
N(\tau,\eta)/x &= g+\varepsilon\left[\cos(\tau)G_r-\sin(\tau)G_i\right].
\end{aligned} \tag{5.40}$$

In equations (5.30)–(5.32), U_r, Θ_r, G_r and U_i, Θ_i, G_i are respectively, the real and imaginary parts of the velocity function, $u_1(\tau,\eta)$, the temperature function, $\Theta_1(\tau,\eta)$ and angular velocity, $G(\tau,\eta)$.

From the application point of view, it is needed to interpret the behavior of physical quantities such as surface shear stress, τ_ω, surface heat flux, q_ω, and the surface couple stress, m_ω, which may be obtained from the following dimensionless relations

$$\bar{\tau} = \left[(\mu + k)\left(\frac{\partial \bar{u}}{\partial \bar{y}}\right) + k\bar{N} \right]_{\bar{y}=0}, \quad \bar{q}_\omega = \left[-k\frac{\partial \bar{T}}{\partial \bar{y}} + \beta_c \frac{\partial \bar{N}}{\partial \bar{x}} \right]_{\bar{y}=0}, \quad \bar{m}_\omega = \left(\gamma \frac{\partial \bar{N}}{\partial \bar{y}} + \alpha_c \frac{\partial \bar{T}}{\partial \bar{x}} \right)_{\bar{y}=0} \tag{5.41}$$

Using the equation (5.6) on equation (5.33) we obtain

$$\tau_\omega = (1+K)\left(\frac{\partial u}{\partial y}\right)_{y=0}, \quad q_\omega = -\left(\frac{\partial \theta}{\partial y}\right)_{y=0}, \quad m_\omega = \left(1+\frac{K}{2}\right)\left(\frac{\partial N}{\partial y}\right)_{y=0}$$
$$\text{where } \tau_\omega = \frac{L^2}{\nu}\bar{\tau}, \quad q_\omega = -\frac{g\beta L^4}{\kappa \nu^2}\bar{q}, \quad m_\omega = \frac{L^3}{\nu}\bar{m}. \tag{5.42}$$

are, respectively, dimensionless surface shear stress, surface heat flux and the surface couple stress.

Once the solutions of the equations (5.20)–(5.22) and (5.26)–(5.28) are known, the values of the physical quantities are readily obtained. These are the shear stress, τ_ω, the rate of heat transfer, q_ω, and the couple-stress, m_ω, at the surface of the plate, which are important from the experimental point of view. Thus we obtain

$$\tau_\omega = (1+K)\, x\left[\frac{\partial u_0}{\partial y} + \varepsilon A_u \cos(\tau + \phi_u)\right], \quad q_\omega = \frac{\partial \theta_0}{\partial y} + \varepsilon A_T \cos(\tau + \phi_T)$$
$$m_\omega = \left(1+\frac{K}{2}\right)\left[\frac{\partial N_0}{\partial y} + \varepsilon A_N \cos(\tau + \phi_N)\right]. \tag{5.43}$$

where $\partial u_0/\partial y$, $\partial \theta_0/\partial y$ and $\partial N_0/\partial y$ are respectively the steady mean shear stress, surface heat transfer and couple stress.

Here it is proposed to express the available solutions in terms of amplitude (A_u, A_T, A_N) and phase (ϕ_u, ϕ_T, ϕ_N) of the shear stress, the heat transfer rate and the couple-stress having the following relations:

$$A_u = \sqrt{\tau_r^2 + \tau_i^2}, \quad A_T = \sqrt{q_r^2 + q_i^2}, \quad A_N = \sqrt{m_r^2 + m_i^2} \tag{5.44}$$

and

$$\phi_u = \tan^{-1}\frac{\tau_i}{\tau_r}, \quad \phi_T = \tan^{-1}\frac{q_i}{q_r}, \quad \phi_N = \tan^{-1}\frac{m_i}{m_r} \tag{5.45}$$

where the real parts of the transverse velocity gradient, temperature gradient, and couple-stress at the surface are τ_r, q_r and m_r respectively and the imaginary parts of those are τ_i, q_i and m_i respectively.

5.4 Results and discussion

In this study, the straight forward finite difference method has been employed in finding the solutions of the equations governing the unsteady natural convection boundary layer flow of a viscous and incompressible fluid along a vertical plate. The results are expressed in terms of transient the shear stress, τ_ω, surface heat transfer, q_ω, and couple stress, m_ω, showing the effects of the physical parameters involved in the flow field, such as, the micropolar heat conduction parameter, N^*, and vortex viscosity parameter, K .

The effect of the vortex viscosity parameter, K, on the amplitude, A_u, and phase, ϕ_u, of the surface shear stress is presented in Fig. 5.2(a) and 5.2(b) respectively. It is evident from the figures that the amplitude and phase of the shear stress decrease as the value of the vortex viscosity parameter, K, increases. This is expected because an increase in the value of the vortex viscosity parameter gives rise to the total viscosity of the fluid flow, which in turn lowers the magnitude of the amplitude and phase of the surface shear stress. Surface heat transfer is the major cause of such reduction in the above mentioned quantities. Thus, micropolar fluids exhibit drag reduction behavior compared to viscous fluids.

Figures 5.3(a) and 5.3(b) depict the effect of the vortex viscosity parameter, K, on the amplitude, A_T, and phase, ϕ_T, of the surface heat transfer.

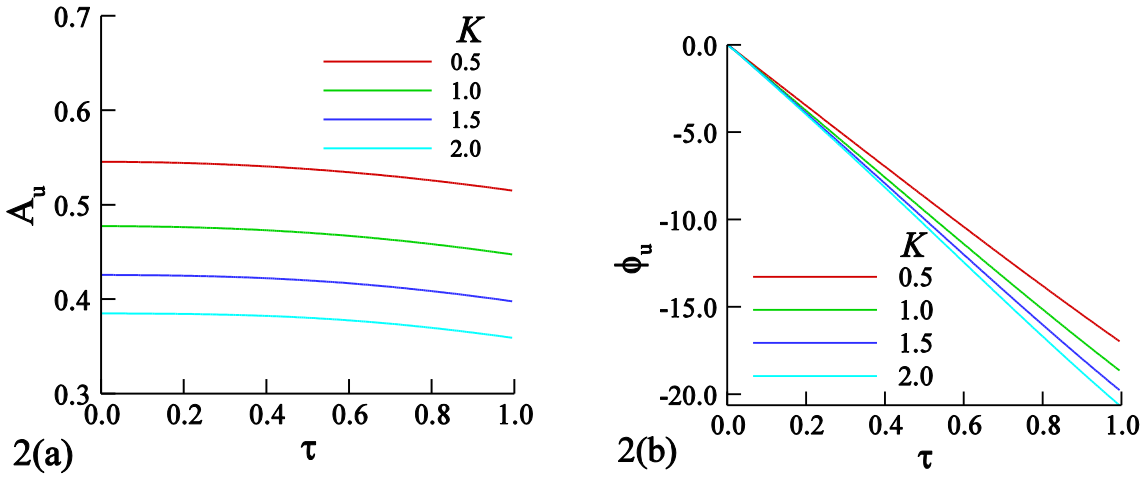

Fig. 5.2: Amplitude and phase of the surface shear stress showing the effect of K when ε = 0.1, Pr = 9.0, N^* = 1.0.

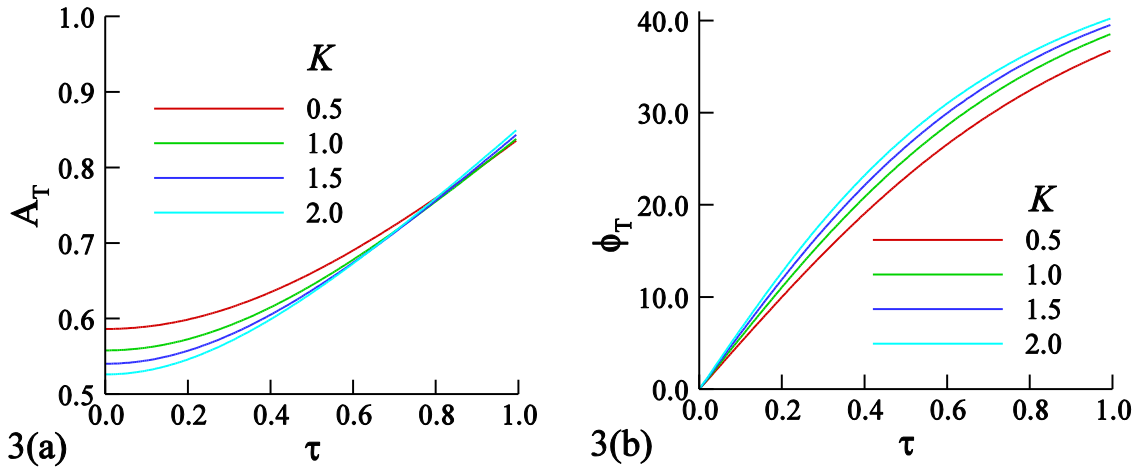

Fig. 5.3: Amplitude and phase of the surface heat transfer showing the effect of K when ε = 0.1, Pr = 9.0, N∗ = 1.0.

From the figures, it is seen that the amplitude of the surface heat transfer decreases while the phase increases when the value of the vortex viscosity parameter, K, is increased. In this case, an increase in the vortex viscosity parameter leads to an increase in the rotation of microelements which decelerates the fluid flow and ultimately diminishes the amplitude of heat transfer. However, the phase of the heat transfer increases which is expected since total viscosity of the fluid increases as K gets stonger and due to fluid friction ϕ_T enhances within the boundary layer region.

The effect of varying the vortex viscosity parameter, K, on the amplitude, A_N, and phase, ϕ_N, of the couple stress is shown in Fig. 5.4(a) and 5.4(b). We observe that the amplitude and phase of the couple stress decrease owing to the increase of the vortex viscosity parameter, K. Here again, an increase in the vortex viscosity parameter gives rise to the rotation of microelements which decelerates the motion of the fluid and ultimately diminishes the amplitude as well as phase of the couple stress

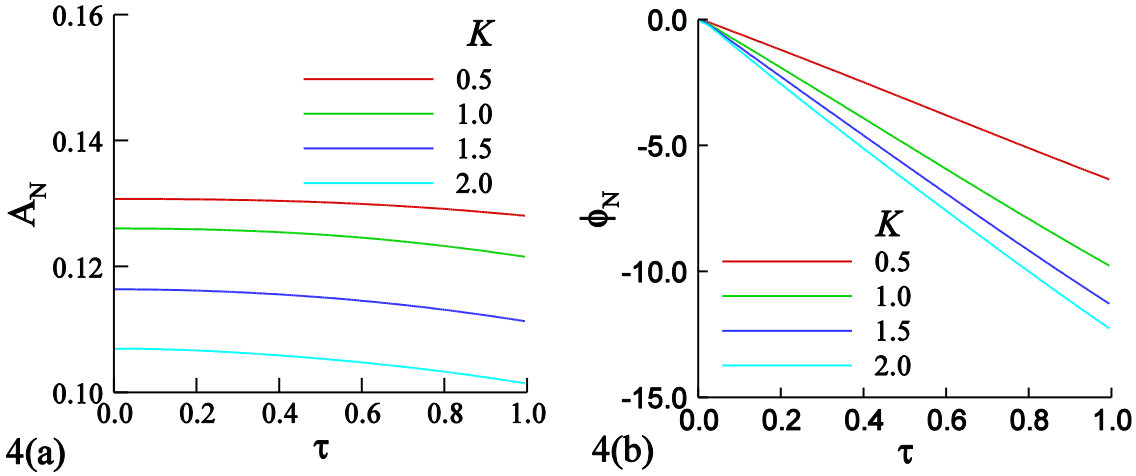

Fig. 5.4: Amplitude and phases of the couple stress showing the effect of K when $\varepsilon = 0.1$, $Pr = 9.0$, $N^* = 1.0$.

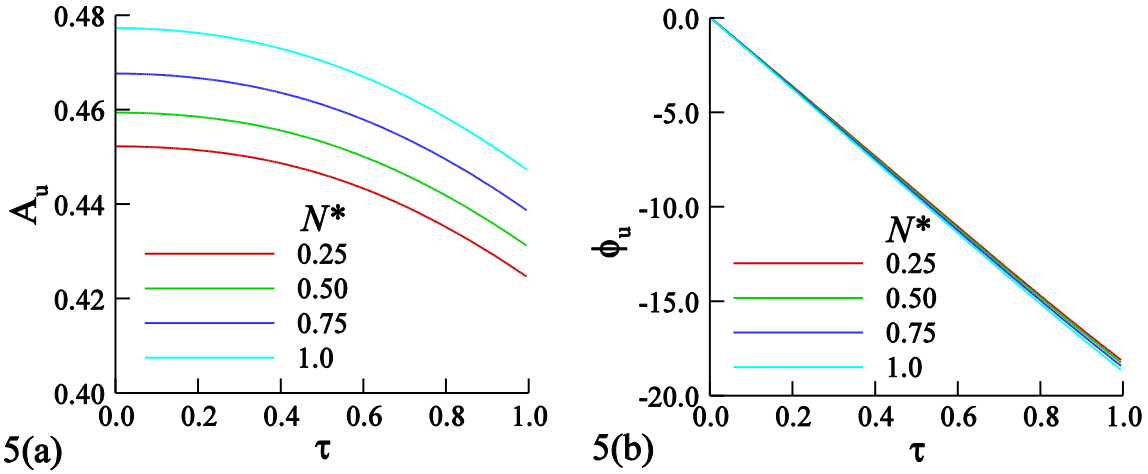

Fig. 5.5: Amplitude and phase of surface shear stress showing the effect of N^* when $\varepsilon = 0.1$, $Pr = 9.0$, $N^*=1.0$.

In Fig. 5.5 the effect of micropolar heat conduction parameter, N^*, is shown for N^*= 0.25, 0.50, 0.75, 1.0 while other parameters are ε = 0.1 and Pr = 9.0. It is observed from this fig. that the amplitude of the surface shear stress enhances due to the increase in the micropolar heat conduction parameter, N^*. However, the phase of the shear stress does not vary much but if we look closely it is anticipated that it slightly diminishes. This result is due to the fact that micropolar fluids offer a greater resistance (resulting from dynamic viscosity and vortex viscosity) to the fluid motion compared to Newtonian fluids.

The influence of micropolar heat conduction parameter, N^* (= 0.25, 0.50, 0.75, 1.0) on amplitude and phase of heat transfer is shown in Fig. 5.6. It can be seen that the amplitude of heat transfer micropolar fluid decreases whereas the phase of heat transfer increases considerably. It happens because the rotation of microelements increases due to an increase in the micropolar heat conduction parameter which results in the decrease in the amplitude of heat transfer while phase of heat transfer increases.

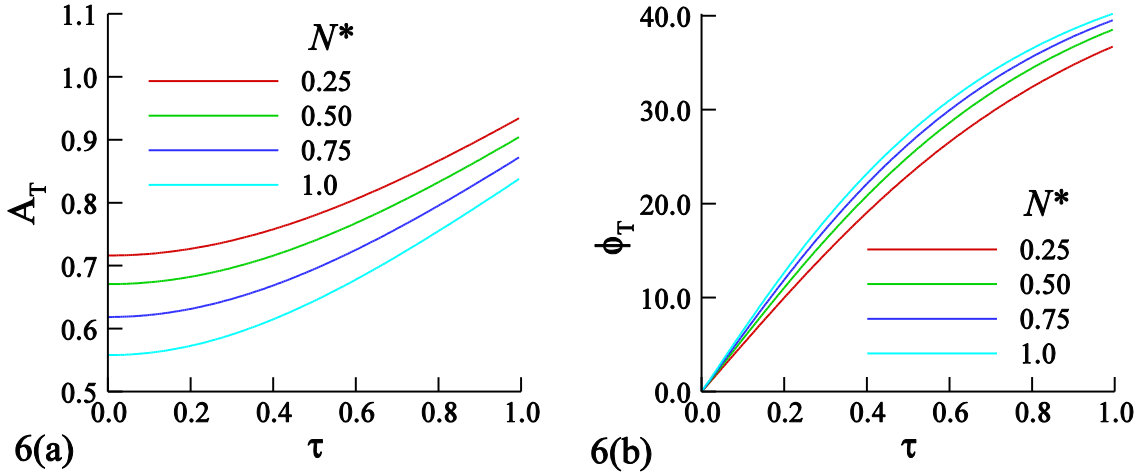

Fig. 5.6: Amplitude and phase of surface heat transfer showing the effect of N^* when ε = 0.1, Pr = 9.0, N^*=1.0.

The effect of micropolar heat conduction parameter, N^*, on the amplitude and phase of couple stress is depicted in Fig. 5.7. The physical parameters are set to be N^*= 0.25, 0.50, 0.75, 1.0, ε = 0.1 and Pr = 9.0. One can find that amplitude of the couple stress increases while phase decreases extensively when micropolar heat conduction parameter enhances from 0.25 to 1.0.

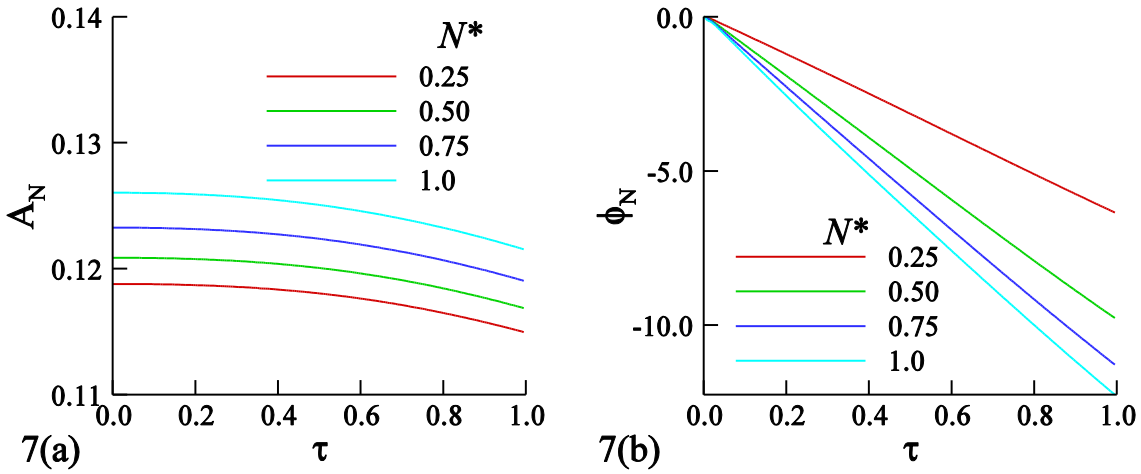

Fig. 5.7: Amplitude and phase of couple stress showing the effect of N^* when $\varepsilon = 0.1$, Pr = 9.0, N^*=1.0.

5.4.1 Effect of micropolar heat conduction parameter, N^* on transient shear stress, surface heat transfer and couple stress coefficients

Attention is now given to see the effect of the micropolar heat conduction parameter N^*(= 0.25, 0.50, 0.75, and 1.0) on the transient shear stress, τ_ω, while Pr = 9.0. These figures display the effect of N^* on shear stress, τ_ω. As N^* increases, the shear stress, τ_ω, increases. In Fig. 5.8(a), for every value of the heat conduction parameter N^*, there exists a local maximum of the shear stress, τ_ω. These maximum values of the shear stress, τ_ω, are recorded to be 0.66683, 0.68414, 0.70324, and 0.72449 at τ = 6.6 for N^* = 0.25, 0.50, 0.75, and 1.0, respectively. For τ = 6.6, the shear stress increases by 2.3%, 5.5% and 8.7%, respectively, as N^* increases from 0.25 to 0.50, 0.75 and 1.0. Fig. 5.8(b) shows the surface heat transfer coefficient, q_ω, against τ for different values of the micropolar heat conduction parameter N^* (= 0.25, 0.50, 0.75, and 1.0) while Pr = 9.0. These figures display the effect of N^* on the heat transfer coefficient, q_ω. As N^* increases, the surface heat transfer coefficient, q_ω, decreases. In the same fig., for all values of the heat conduction parameter N^*, there exists the local maximum of the surface heat transfer coefficient, q_ω, in each case. These maximum values of the surface heat transfer coefficient, q_ω, are seen to be 0.62630, 0.56880, 0.50547, and 0.43516 at τ = 5.7 for N^* = 0.25, 0.50, 0.75, and 1.0, respectively. At τ = 5.7, there are decreases in the heat transfer coefficient, q_ω, by 9.18, 21.24 and 30.51 percent respectively, as N^* increases from 0.25 to 0.50, 0.75 and 1.0. Fig. 5.8(c)

depicts the couple stress coefficient, m_ω, against τ for different values of the heat conduction parameter N^* (= 0.25, 0.50, 0.75 and 1.0) while Pr = 9.0. These figures display the effect of N^* on the couple stress coefficient, m_ω. As N^* increases, the couple stress coefficient, m_ω, increases. This happens because the increase of N^* means that the heat conduction through the fluid increases so that the viscosity of the fluid decreases. Again Fig. 5.8(c) shows that there exists a local maximum of the couple stress coefficient, m_ω, for every values of the heat conduction parameter, N^* .These maximum values of the couple stress coefficient, m_ω, are found to be 0.48063, 0.49328, 0.50724, and 0.52276 at τ = 6.4 for N^* = 0.25, 0.50, 0.75, and 1.0, respectively. At τ = 6.4, the shear stress increases by 2.63, 5.53 and 8.76 percent, respectively, as N^* increases from 0.25 to 0.50, 0.75 and 1.0.

Table 5.2: Amplitudes and phases of oscillation in shear stress, surface heat transfer and couple stress showing the effect of K when ε = 0.1, Pr = 9.0, N^* =1.0.

τ	A_u	A_T	A_N	ϕ_u	ϕ_T	ϕ_N
			K = 0.5			
0.0	0.54433	0.57995	0.13461	0.00000	0.00000	0.00000
0.1	0.54402	0.58307	0.13459	-1.73080	5.07365	-0.50783
0.2	0.54310	0.59256	0.13454	-3.51399	10.09909	-1.12000
0.3	0.54156	0.60811	0.13445	-5.29338	14.86849	-1.74020
0.5	0.53656	0.65521	0.13411	-8.83135	23.29560	-3.00369
0.6	0.53309	0.68538	0.13383	-10.58221	26.87041	-3.64218
0.7	0.52896	0.71900	0.13348	-12.31395	30.01566	-4.28100
0.8	0.52420	0.75541	0.13305	-14.02027	32.75422	-4.91669
0.9	0.51882	0.79401	0.13254	-15.69445	35.11944	-5.54549
1.0	0.51287	0.83427	0.13195	-17.32975	37.14912	-6.16341
			K = 2.0			
0.0	0.38492	0.52198	0.10949	0.00000	0.00000	0.00000
0.1	0.38482	0.52686	0.10944	-1.93426	6.47870	-1.11614
0.2	0.38443	0.54166	0.10923	-4.01690	12.74616	-2.43792
0.3	0.38362	0.56492	0.10890	-6.13324	18.41238	-3.73035

0.5	0.38015	0.63021	0.10794	-10.46187	-10.46187	-6.23926
0.6	0.37727	0.66951	0.10734	-12.64779	31.23695	-7.47043
0.7	0.37356	0.71188	0.10663	-14.82082	34.25848	-8.68800
0.8	0.36904	0.75649	0.10582	-16.95900	36.76954	-9.88685
0.9	0.36377	0.80265	0.10490	-19.04228	38.84107	-11.05924
1.0	0.35784	0.84976	0.10387	-21.05359	40.53872	-12.19679

5.4.2 Effect of vortex viscosity parameter, *K*, on transient shear stress, surface heat transfer and couple stress coefficients

The effect of the vortex viscosity parameter, *K*, on the transient shear stress, τ_ω, surface heat transfer coefficient, q_ω, and coefficient of couple stress, m_ω, are presented in Fig. 5.9 and in Table 5.2. It is evident from the figures and Table 5.2 that the shear stress coefficient, surface heat transfer coefficient and coefficient of couple stress decreases due to an increase in the value of the vortex viscosity parameter, *K*. Fig. 5.9(a) illustrates shear stress, τ_ω, against τ for different values of the vortex viscosity parameter *K* (= 0.5, 1.0, 1.5 and 2.0) while *Pr* = 9.0 . These figures display the effect of *K* on shear stress, τ_ω. As *K* increases, the shear stress, τ_ω, decreases. In the same figure, for all values of the vortex viscosity parameter *K*, we observe a local maximum of the shear stress, τ_ω. These maximum values of the shear stress, τ_ω, are 0.84163, 0.72448, 0.63753, and 0.57104 at τ = 6.6 for *K* = 0.5, 1.0, 1.5 and 2.0, respectively. At τ = 6.6, the shear stress decreases by 13.91, 24.25 and 32.15 percent, respectively, when *K* increases from 0.50 to 1.0, 1.5 and 2.0. Fig. 5.9(b) shows the effect of the surface heat transfer coefficient, q_ω, against τ for different values of the vortex viscosity parameter *K* (= 0.5, 1.0, 1.5, and 2.0) while *Pr* = 9.0. This fig. displays the effect of *K* on the heat transfer coefficient, q_ω. As *K* increases, the surface heat transfer coefficient, q_ω decreases. Again in Fig. 5.9(b), for all values of the vortex viscosity parameter, *K*, there is a local maximum of the heat transfer, q_ω. These maximum values of the heat transfer coefficient, q_ω, are seen to be 0.44791, 0.43549, 0.42693, and 0.41999 at τ = 5.6 for *K* = 0.50, 1.0, 1.5 and 2.0, respectively. At τ = 5.6, the surface heat transfer coefficient, q_ω, decreases by 2.77, 4.68 and 6.23 percent, respectively, as *K* increases from 0.50 to1.0, 1.50 and 2.0. Finally Fig. 5.9(c) depicts the couple stress coefficient, m_ω, against τ for different values of the vortex viscosity parameter *K* (= 0.5, 1.0, 1.5, and 2.0) while *Pr* = 9.0. This figure displays the

effect of K on the couple stress coefficient, m_ω. With the increase of K, the couple stress coefficient, m_ω decreases. In the same Figure, for all values of the vortex viscosity parameter K, there exists a local maximum of the couple stress coefficient, m_ω. These maximum values of the couple stress coefficient, m_ω, are noticed to be 0.59832, 0.52276, 0.46347, and 0.41697 at $\tau = 6.4$ for K = 0.50, 1.0, 1.5, and 2.0 respectively. At $\tau = 6.4$, the shear stress decreases by 12.62, 22.53 and 30.30 percent, respectively, as K increases from 0.50 to 1.0, 1.5 and 2.0.

5.4.3 Effect of micropolar heat conduction parameter, N^* on transient velocity profiles, temperature profiles and angular velocity profiles

The effects of varying N^* on the velocity profiles, temperature profiles and angular velocity profiles against η are depicted in Fig. .10. It is clear from the figures that the velocity profiles, temperature profiles and angular velocity profiles increase with an increase in N^*. We also observe that there is local maximum for velocity profiles and temperature profiles while angular velocity always decreases as η increases. Fig. 5.10(a) illustrates velocity profiles, $u(0, \eta)$, against η for different values of the heat conduction parameter N^* (= 0.25, 0.50, 0.75, and 1.0). As N^* increases, the velocity profiles, $u(0, \eta)$, increase . In Fig. 5.10(a), for all values of the heat conduction parameter N^*, there exists a local maximum of the velocity profiles, $u(0, \eta)$. These maximum values of the velocity profiles, $u(0, \eta)$, are 0.36891, 0.38174, 0.39588, and 0.411529 at η = 1.53 for N^* = 0.5,1.0, 1.5, and 2.0, respectively. At η = 1.53, the velocity profile increases by 3.47, 7.31 and 11.55 percent, respectively, when N^* increases from 0.25 to 0.50, 0.75 and 1.0. Fig. 5.10(b) also shows the temperature profiles, $\theta(0, \eta)$, against η for different values of the micropolar heat conduction parameter N^*(= 0.25, 0.50, 0.75, and 1.0). The temperature profiles decrease along η for all values of the heat conduction parameter N^*. Fig. 5.10(c) depicts the angular velocity profiles, $N(0, \eta)$, against η for different values of the heat conduction parameter N^* (= 0.25, 0.50, 0.75 and 1.0). As N^* increases, the angular velocity profiles, $N(0, \eta)$, increase. In the same figure, it is seen that for all values of the heat conduction parameter N^*, there exists a local maximum of the angular velocity profiles, $N(0, \eta)$. These maximum values of the angular velocity profiles, $N(0, \eta)$, are 0.214790, 0.22260, 0.23209, and 0.24973 at η = 1.83 for N^* = 0.25, 0.50, 0.75, and 1.0, respectively. Again at η = 1.83, the

angular velocity increases by 3.63, 8.05 and 12.07 percent, respectively, when N^* increases from 0.25 to 0.50, 0.75, and 1.0.

5.3.4 Effect of vortex viscosity parameter, K on transient velocity profiles, temperature profiles and angular velocity profiles

Fig. 5.11 exhibits the velocity profiles, temperature profiles and angular velocity profiles against η for different values of the vortex viscosity parameter, K.

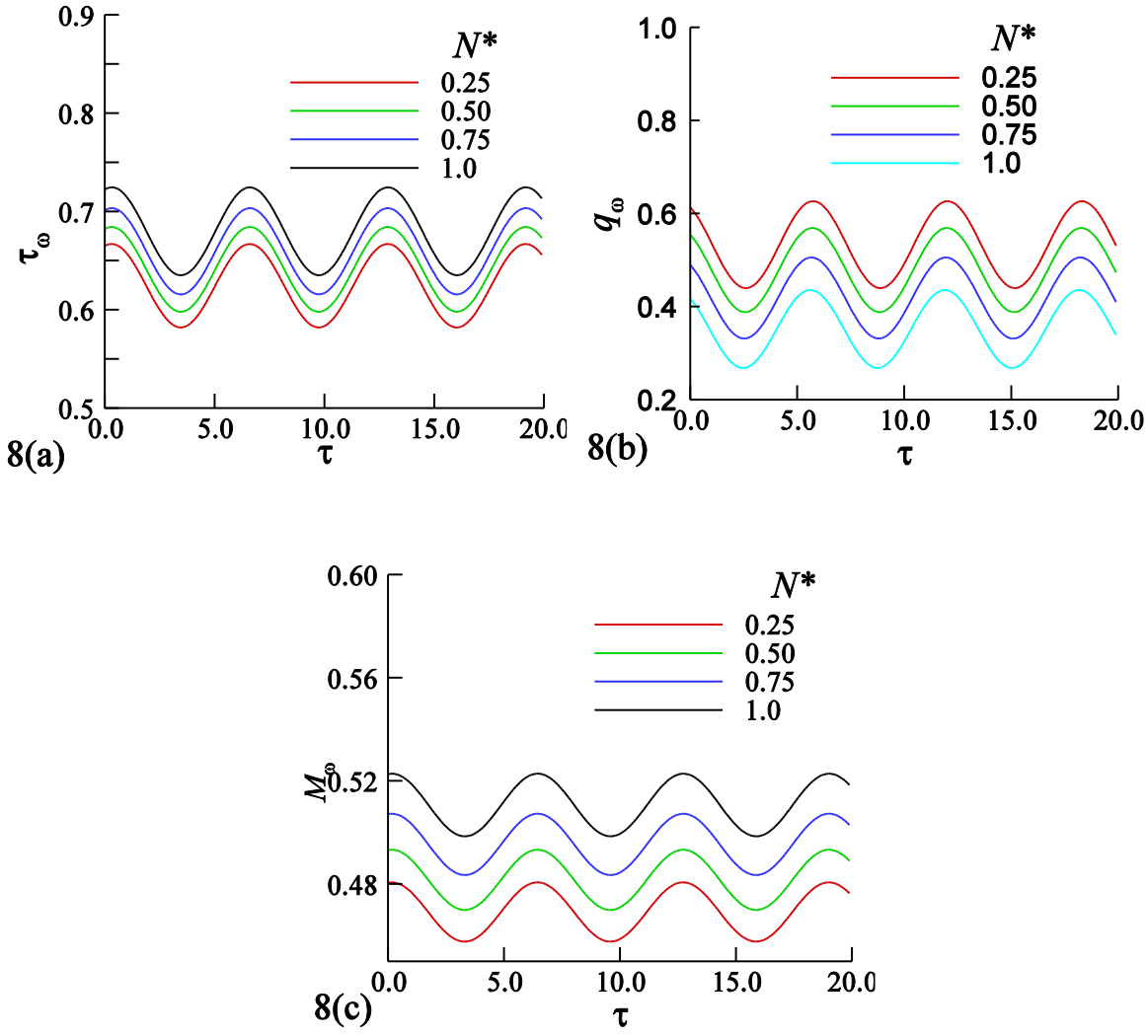

Fig. 5.8: Numerical values of (a) surface shear stress (b) heat transfer coefficient and (c) couple-stress for different values of N^* against τ while Pr = 9.0 and ω = 1.

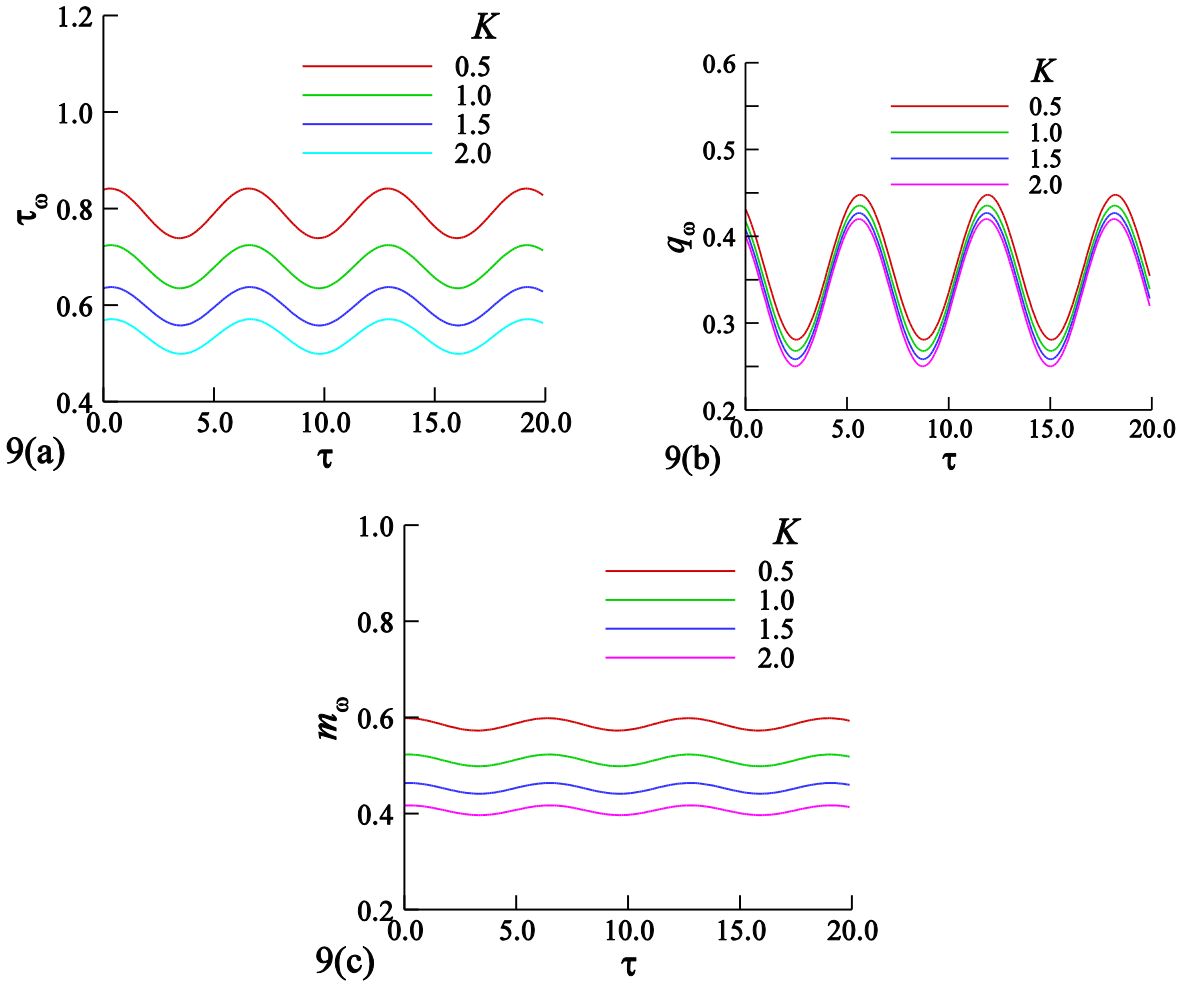

Fig. 5.9: Numerical values of (a) shear stress (b) surface heat transfer coefficient and (c) couple-stress for different values of K against values of τ while Pr = 9.0 and ω = 1.

It is seen from the Fig. 5.11 that the velocity profiles attain a maximum value while temperature profiles and angular velocity profile decrease monotonically with the increase of η. Fig. 5.11(a) illustrates the velocity profiles, $u(0, \eta)$, against η for different values of the vortex viscosity parameter K (= 0.5, 1.0, 1.5, and 2.0). These figures display the effect of K on the velocity profiles, $u(0, \eta)$. As K increases, the velocity profiles, $u(0, \eta)$, increase. In the same fig., for each value of the vortex viscosity parameter K, there exists a local maximum of the corresponding velocity profile, $u(0, \eta)$. These maximum values of velocity profiles, $u(0, \eta)$, are 0.48234, 0.411529, 0.360379, and 0.322369 at η = 1.56 for K = 0.5, 1.0, 1.5, and 2.0 respectively. Also η = 1.56, the velocity profiles increases by 14.68, 25.28 and 33.16 percent,

respectively, as *K* increases from 0.5 to 1.0, 1.5, and 2.0.

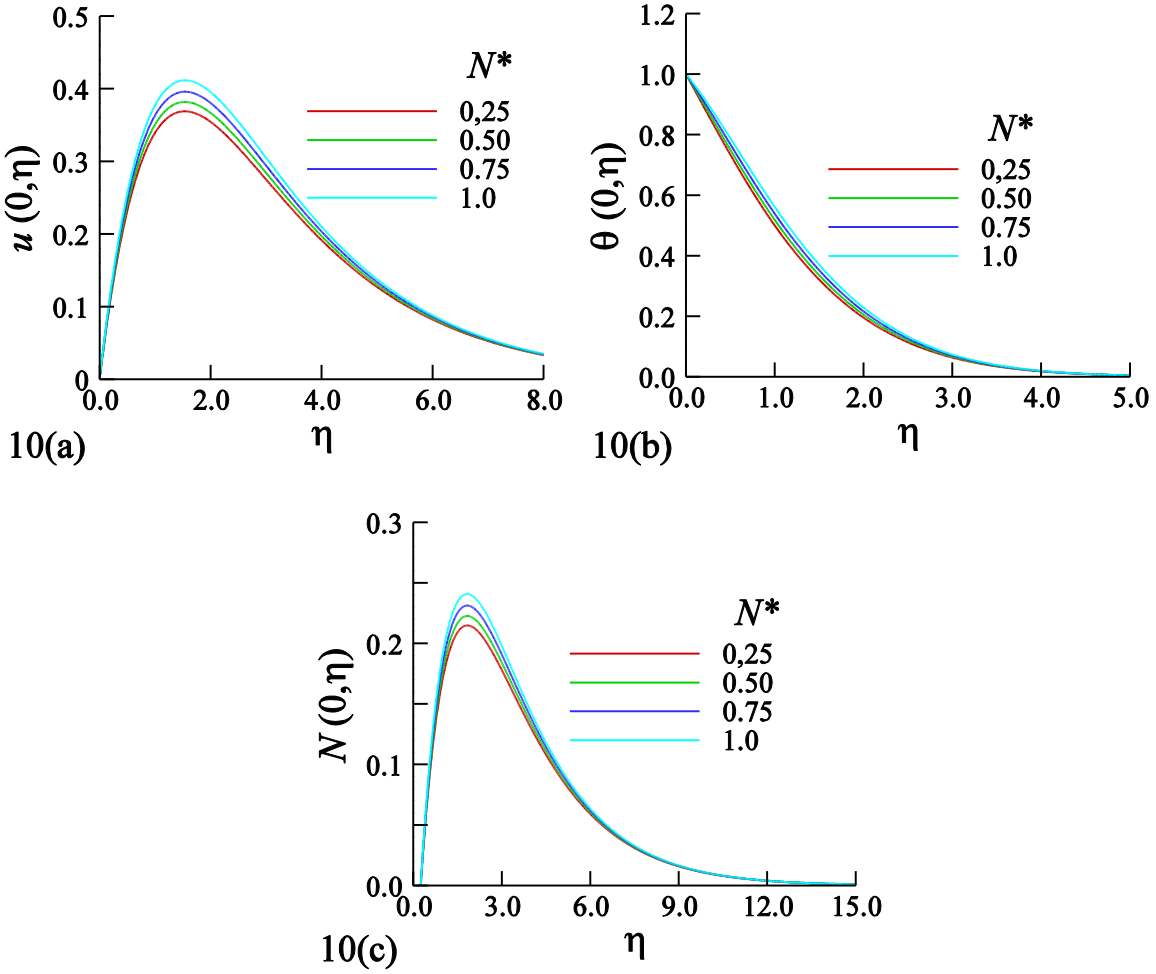

Fig. 5.10: Numerical values of (a) velocity profiles (b) temperature profiles and (c) angular velocity profiles for different values of N* against η while Pr = 9.0 and ω = 1.

Fig. 5.11(b) shows temperature profiles, θ(0, η), against η for different values of the micropolar heat conduction parameter *K* (= 0.5, 1.0, 1.5, and 2.0). The temperature profile decreases along η for all values of the vortex viscosity parameter *K*. Fig. 5.11(c) also depicts the angular velocity profile, *N*(0, η), against η for different values of the vortex viscosity parameter *K* (= 0.5, 1.0, 1.5, and 2.0). As *K* increases, the angular velocity profile, *N*(0, η), also increases. Finally, Fig. 5.11(c) shows that for every value of the vortex viscosity parameter, *K*, there exists a local maximum of the angular velocity profile, *N*(0, η). These maximum values of the angular velocity profile, *N*(0, η), are 0.27360, 0.24073, 0.214149, and

0.193509 at η = 1.83 for K = 0.5, 1.0, 1.5, and 2.0, respectively. At η = 1.83, the angular velocity increases by 12.01, 21.72 and 29.27 percent, respectively, as K increases from 0.5 to 1.0, 1.5, and 2.0.

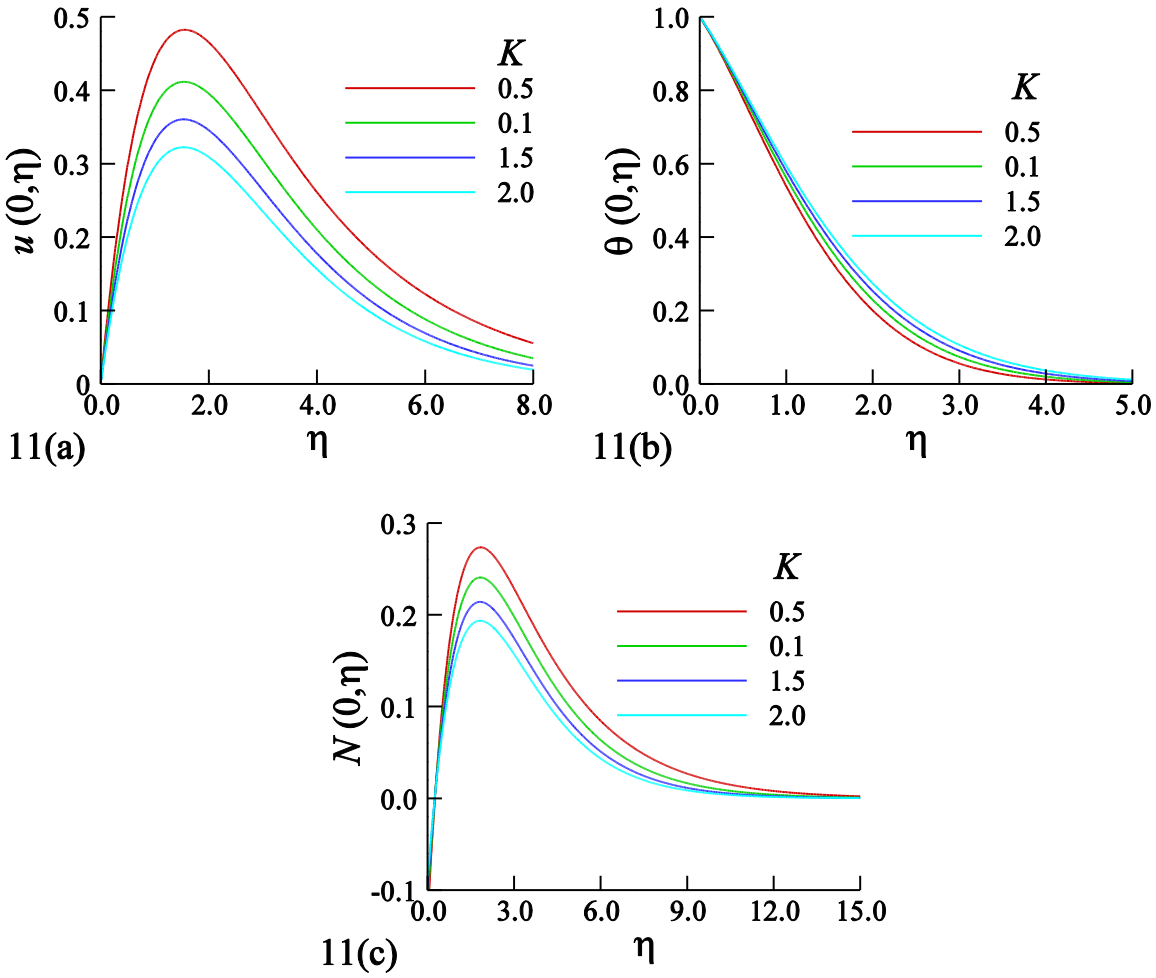

Fig. 5.11: Numerical values of (a) velocity profiles (b) temperature profiles and (c) angular velocity profiles for different values of K against η while Pr = 9.0 and ω = 1.

Chapter Six
Free convection flow of a thermomicropolar fluid along a vertical surface with sinusoidal surface temperature

6.1 Introduction

The paper studies the problem of two-dimensional steady free convection about a vertical plate with the combined effect of stream wise sinusoidal variations of the surface temperature in a micropolar fluid flow with classical Newtonian fluid. Under these assumptions, the governing boundary layer equations are analyzed numerically by a straight forward finite difference method.

The space of various the material parameters contains the micro polar heat conduction parameter, N^*, the vortex viscosity parameter, K, and the amplitude of surface temperature, a, as well as the shear stress, τ, the surface heat transfer, q, and the couple-stress, m, are plotted graphically and discussed.

Also, it was found that, the effects of non-dimensional physical parameters are obtained by the isolines of temperature, isolines of the species concentration and streamlines.

6.2 Mathematical Formalisms

The two-dimensional steady free convection laminar boundary layer flow of a thermo-micropolar viscous incompressible fluid along a vertical flat plate is considered. The temperature of the ambient fluid and the surface are assumed to be $\overline{T}_\infty$ and $\overline{T}_w$ respectively. The coordinate system and the flow configuration are shown in Fig. 7.1.

In this figure δ_M, δ_T and δ_N represent approximate momentum, thermal and micro rotation boundary layer thickness, respectively.

Free convection flow of a thermomicropolar fluid along a vertical surface with sinusoidal surface temperature

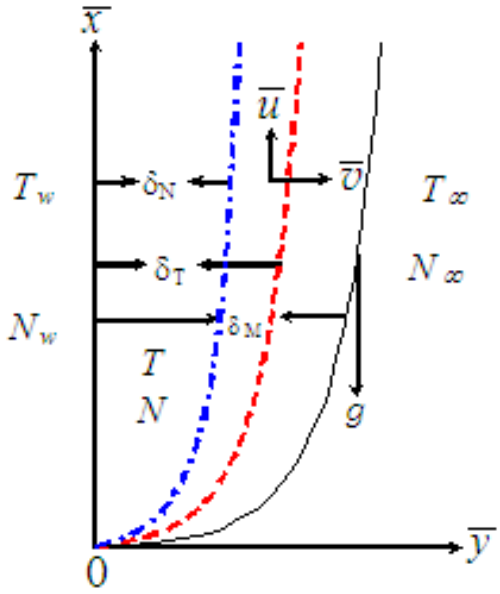

Fig. 6.1: Flow configuration and coordinate system.

Under the usual Boussinesq approximation the governing equations of conservation of mass, momentum, angular velocity and energy that govern the flow are given as

$$\frac{\partial \bar{u}}{\partial \bar{x}} + \frac{\partial \bar{v}}{\partial \bar{y}} = 0 \tag{6.1}$$

$$\rho\left(\bar{u}\frac{\partial \bar{u}}{\partial \bar{x}} + \bar{v}\frac{\partial \bar{u}}{\partial \bar{y}}\right) = (\mu + k)\frac{\partial^2 \bar{u}}{\partial \bar{y}^2} + k\frac{\partial \bar{N}}{\partial \bar{y}} + \rho g\beta\left(\bar{T} - \bar{T}_\infty\right) \tag{6.2}$$

$$\rho j\left(\bar{u}\frac{\partial \bar{N}}{\partial \bar{x}} + \bar{v}\frac{\partial \bar{N}}{\partial \bar{y}}\right) = \gamma\frac{\partial^2 \bar{N}}{\partial \bar{y}^2} - k\left(2\bar{N} + \frac{\partial \bar{u}}{\partial \bar{y}}\right) \tag{6.3}$$

$$\bar{u}\frac{\partial \bar{T}}{\partial \bar{x}} + \bar{v}\frac{\partial \bar{T}}{\partial \bar{y}} = \alpha\frac{\partial^2 \bar{T}}{\partial \bar{y}^2} + \frac{\alpha_c}{\rho c_p}\left(\frac{\partial \bar{T}}{\partial \bar{x}}\frac{\partial \bar{N}}{\partial \bar{y}} - \frac{\partial \bar{T}}{\partial \bar{y}}\frac{\partial \bar{N}}{\partial \bar{x}}\right) \tag{6.4}$$

The boundary conditions to be satisfied are

$$\bar{u}(\bar{x},0) = 0,\quad \bar{v}(\bar{x},0) = 0,\quad \bar{N} = -\frac{1}{2}\frac{\partial \bar{u}}{\partial \bar{y}},\ \bar{T}(\bar{x},0) = \bar{T}_\infty + \left(\bar{T}_w(\bar{x}) - \bar{T}_\infty\right)\left(1 + a\sin\left(\pi\frac{\bar{x}}{L}\right)\right) \text{ at } \bar{y} = 0$$

$$\bar{u} \to 0,\quad \bar{v} = 0,\quad \bar{N} \to 0,\quad \bar{T} \to 0 \quad \text{as} \quad \bar{y} \to \infty \tag{6.5}$$

Here, $\bar{x}$, $\bar{y}$ are the dimensional coordinates parallel with and perpendicular to the flat surface, $\bar{u}$, $\bar{v}$ are the dimensional velocity component, ρ the fluid density, μ the dynamic viscosity, κ the thermal conductivity, $\bar{N}$ the dimensional angular velocity, g the acceleration due to gravity, β the coefficient of volume expansion, $\bar{T}$ the dimensional temperature, $\bar{T}_w(x)$ the

mean surface temperature of the fluid in the surface, $\bar{T}_\infty$ the temperature of the ambient fluid, j the micro inertia per unit mass, γ the spin-gradient viscosity, c_p the specific heat capacity, α the thermal diffusivity, α_c the micro polar conductivity and a is amplitude of oscillation in the surface temperature.

We introduce the following dimensionless variables

$$x=\frac{\bar{x}}{L},\quad y=\frac{\bar{y}}{L}\left(\frac{g\beta\Delta TL^3}{\alpha^2}\right)^{1/4},\quad \bar{u}=\frac{\alpha}{L}\left(\frac{g\beta\Delta TL^3}{\alpha^2}\right)^{1/2}u,\quad \bar{v}=\frac{\alpha}{L}\left(\frac{g\beta\Delta TL^3}{\alpha^2}\right)^{1/4}v$$
$$\bar{N}=\frac{\alpha}{L^2}\left(\frac{g\beta\Delta TL^3}{\alpha^2}\right)^{3/4}N,\quad \theta=\frac{\bar{T}-\bar{T}_\infty}{\Delta\bar{T}},\quad \bar{T}_w(\bar{x})-\bar{T}_\infty=\Delta\bar{T}\theta_w(x). \tag{6.6}$$

where L is the wave length, N is the dimensionless angular velocity, θ is the dimensionless temperature.

Thus the dimensionless equations of conservation of mass, momentum, angular velocity and energy that govern the flow are given as

$$\frac{\partial u}{\partial x}+\frac{\partial v}{\partial y}=0 \tag{6.7}$$

$$u\frac{\partial u}{\partial x}+v\frac{\partial u}{\partial y}=\Pr(1+K)\frac{\partial^2 u}{\partial y^2}+\Pr K\frac{\partial N}{\partial y}+\theta \tag{6.8}$$

$$u\frac{\partial N}{\partial x}+v\frac{\partial N}{\partial y}=\Pr\left(1+\frac{K}{2}\right)\frac{\partial^2 N}{\partial y^2}-BK\left(2N+\frac{\partial u}{\partial y}\right) \tag{6.9}$$

$$u\frac{\partial \theta}{\partial x}+v\frac{\partial \theta}{\partial y}=\frac{\partial^2\theta}{\partial y^2}+N^*\left(\frac{\partial\theta}{\partial x}\frac{\partial N}{\partial y}-\frac{\partial\theta}{\partial y}\frac{\partial N}{\partial x}\right). \tag{6.10}$$

The boundary conditions are

$$u=0,\ v=0,\ N=-\frac{1}{2}\frac{\partial u}{\partial y},\ \theta=\theta_w(x)\left[1+a\sin(\pi x)\right]\ \text{at}\ y=0$$
$$u\to 0,\ v\to 0,\ N\to 0,\ \theta\to 0\quad \text{as}\ y\to\infty \tag{6.11}$$

In equations (6.8)-(6.10), $K=\kappa/\mu$ is termed as vortex viscosity parameter, $\Pr=\nu/\alpha$ is the Prandtl number, $\gamma=(\mu+\kappa/2)j$ is the gyro-viscosity coefficient and $N^*=\alpha_c(g\beta\Delta TL^3)^{1/2}/(L^2\rho c_p\alpha)$ is the micropolar heat conduction parameter, $B=L^2(g\beta\Delta TL^3/\alpha^2)^{-1/2}/j$ is the material parameter. Finally, $\theta_w(x)$ defined in equation (6.11) is assumed to be proportional to a linear function of x. From application point of view, we need to find the values of shear stress, $\bar{\tau}$, the couple-stress, $\bar{m}$, and the rate of heat transfer, $\bar{q}$, at the surface of the plate, that may be obtained by the relations given below:

$$\bar{\tau} = (\mu + k)\left(\frac{\partial \bar{u}}{\partial \bar{y}}\right)_{\bar{y}=0}, \quad \bar{q} = -k\left(\frac{\partial \bar{T}}{\partial \bar{y}}\right)_{\bar{y}=0}, \quad \bar{m} = \gamma\left(\frac{\partial \bar{N}}{\partial \bar{y}}\right)_{\bar{y}=0} \tag{6.12}$$

Using the relation (6.6) on (6.12), we obtain

$$\tau = (1+K)\left(\frac{\partial u}{\partial y}\right)_{y=0}, \quad q = -\left(\frac{\partial \theta}{\partial y}\right)_{y=0}, \quad m = \left(1+\frac{K}{2}\right)\left(\frac{\partial N}{\partial y}\right)_{y=0} \tag{6.13}$$

Where τ, m and q are the dimensionless shear stress, couple-stress and rate of heat transfer, respectively, which are defined by

$$\tau = \frac{\bar{\tau}\alpha^{1/2}}{\mu L^{1/4}}, \quad q = \frac{\bar{q}\left(\alpha^2 L\right)^{1/4}}{\Delta \bar{T}\left(g\beta\Delta T\right)^{1/4}}, \quad m = \frac{\bar{m}\alpha}{\mu j g \beta \Delta T}.$$

6.3 Method of Solution

The set of equations (6.7)-(6.10) with the boundary conditions (6.11) can be integrated by straight forward finite difference method. For integration, we set the following group of transformation for the dependent and independent variables:

$$u = XU,\ v = V,\ x = X,\ \ y = Y,\ \ N = XG,\ \ \theta = X\Theta \tag{6.14}$$

Therefore the equations (6.7)-(6.10) are transformed into

$$U + X\frac{\partial U}{\partial X} + \frac{\partial V}{\partial Y} = 0 \tag{6.15}$$

$$U\left(U + X\frac{\partial U}{\partial X}\right) + V\frac{\partial U}{\partial Y} = \Pr(1+K)\frac{\partial^2 U}{\partial Y^2} + \Pr K\frac{\partial G}{\partial Y} + \Theta \tag{6.16}$$

$$UG + XU\frac{\partial G}{\partial X} + V\frac{\partial G}{\partial Y} = \Pr\left(1+\frac{K}{2}\right)\frac{\partial^2 G}{\partial Y^2} - KB\left(2G + \frac{\partial U}{\partial Y}\right) \tag{6.17}$$

$$U\Theta + X\left(U - N^*\frac{\partial G}{\partial Y}\right)\frac{\partial \Theta}{\partial X} + \left[V + N^*\left(G + X\frac{\partial G}{\partial X}\right)\right]\frac{\partial \Theta}{\partial Y} + N^*\frac{\partial G}{\partial Y}\Theta = \frac{\partial^2 \Theta}{\partial Y^2} \tag{6.18}$$

The boundary conditions to be satisfied by the above equations are by the equations (6.11)

$$\begin{aligned} &U = 0,\ V = 0,\ G = -\frac{1}{2}\frac{\partial U}{\partial Y},\ \ \Theta = 1 + a\sin(\pi X) \quad \text{at} \quad Y = 0 \\ &U \to 0,\ V \to 0,\ \ G \to 0,\ \ \ \Theta \to 0 \quad \text{as} \quad Y \to 0 \end{aligned} \tag{6.19}$$

Here $\theta_w(X) = X$

Now, equations (6.15)-(6.17) subject to the boundary conditions (6.19) are discredited by central difference scheme for the diffusion terms and backward-difference scheme for the convective terms. The resulting tridiagonal algebraic system is obtained as follows:

For the momentum equation, we have

$$A_1 U_{i-1,j} + B_1 U_{i,j} + C_1 U_{i+1,j} = D_1 \tag{6.20}$$

where

$$A_1 = \Pr\frac{1+K}{\Delta Y^2} + \frac{V_{i,j}}{2\Delta Y}, \quad B_1 = \left\{ -\Pr\frac{2(1+K)}{\Delta Y^2} - U_{i,j} - \frac{X_j}{\Delta X} U_{i,j} \right\}, \quad C_1 = \Pr\frac{1+K}{\Delta Y^2} - \frac{V_{i,j}}{2\Delta Y}$$

$$\text{and} \quad D_1 = -\Pr K\left(\frac{G_{i+1,j} - G_{i-1,j}}{2\Delta Y}\right) - \Theta_{i,j} - \frac{X_j}{\Delta X} U_{i,j} U_{i,j-1}.$$

For the angular velocity equation, we get

$$A_2 G_{i-1,j} + B_2 G_{i,j} + C_2 G_{i+1,j} = D_2 \tag{6.21}$$

$$\text{whear } A_2 = \Pr\frac{(1+K/2)}{\Delta Y^2} + \frac{V_{i,j}}{2\Delta Y}, \quad B_2 = -\Pr\frac{2(1+K/2)}{\Delta Y^2} - U_{i,j} - 2KB - \frac{X_j}{\Delta X} U_{i,j},$$

$$C_2 = \Pr\frac{(1+K/2)}{\Delta Y^2} - \frac{V_{i,j}}{2\Delta Y} \quad \text{and} \quad D_2 = KB\left(\frac{U_{i+1,j} - U_{i-1,j}}{2\Delta Y}\right) - \frac{X_j}{\Delta X} U_{i,j} U_{i,j-1}.$$

Finally, for the energy equation, we obtain

$$A_3 \Theta_{i-1,j} + B_3 \Theta_{i,j} + C_3 \Theta_{i+1,j} = D_3 \tag{6.22}$$

Where $A_3 = \frac{1}{\Delta Y^2} + \frac{1}{2\Delta Y} V_{i,j} + N^*\left[G_{i,j} + X_j\left(\frac{G_{i,j} - G_{i,j-1}}{\Delta X}\right)\frac{1}{2\Delta Y}\right]$

$$B_3 = -\frac{2}{\Delta Y^2} - U_{i,j} - X_j \frac{1}{\Delta X} U_{i,j} + X_j N^*\left(\frac{G_{i+1,j} - G_{i-1,j}}{2\Delta Y}\right)\frac{1}{\Delta X} - N^*\left(\frac{G_{i+1,j} - G_{i-1,j}}{2\Delta Y}\right)$$

$$C_3 = \frac{1}{\Delta Y^2} - \frac{1}{2\Delta Y} V_{i,j} - N^*\left[G_{i,j} + X_j\left(\frac{G_{i,j} - G_{i,j-1}}{\Delta X}\right)\frac{1}{2\Delta Y}\right]$$

$$D_3 = -X_j \frac{\Theta_{i,j-1}}{\Delta X} U_{i,j} + X_j N^*\left(\frac{G_{i+1,j} - G_{i-1,j}}{2\Delta Y}\right)\frac{\Theta_{i,j-1}}{\Delta X}.$$

The implicit tridiagonal algebraic system of equations (6.20)-(6.22) is solved using the Gaussian elimination method for the unknown *U*, *W*, and Θ independently. In the computation, the continuity equation is used to directly measure the normal velocity vector *V* from the following expression:

$$V_{i,j} = V_{i-1,j} - \frac{\Delta Y}{\Delta X} X_j \left(U_{i,j} - U_{i,j-1}\right) + \frac{\Delta Y}{2}\left(U_{i,j} + U_{i-1,j}\right). \tag{6.23}$$

The effects of the physical parameters, such as, the micropolar heat conduction parameter, N^*, the vortex viscosity parameter, K, the amplitude of surface temperature, a, are discussed in terms of the coefficients of the shear stress, τ, rate of heat transfer, q, and couple stress, m, from the following expressions:

$$\tau = (1+K)\,X\left(\frac{\partial U}{\partial Y}\right)_{Y=0}, \quad q = -X\left(\frac{\partial \Theta}{\partial Y}\right)_{Y=0}, \quad m = \left(1+\frac{K}{2}\right)X\left(\frac{\partial G}{\partial Y}\right)_{Y=0} \tag{6.24}$$

6.4 Results and discussion

In this study we have analyzed numerically the natural convection flow of viscous incompressible fluid along a vertical flat surface with streamwise variations of the surface temperature. The dimensionless equations are solved using the straight forward finite difference method. Results have been presented in terms of the coefficients of the shear stress, rate of heat transfer and couple stress. We also investigate the effects of physical parameters on the isolines of temperature, isolines of angular velocity and the streamlines in the boundary layer regimes.

In order to validate the numerical solutions, a comparison is made in Table 1. From the table, it is seen that the present solutions are good agreement with Jena and Mathur [8].

Table 6.1: Numerical values of $U'(0,0)$ and $G'(0,0)$ for Pr = 9.0, a = 0.0, K =0.1, B = 500.0 and N^* = 1.0

$U'(0,0)$		$G'(0,0)$	
Jena and Mathur [8]	Present	Jena and Mathur [8]	Present
0.1558	0.15574	0.0365	0.03650

6.4.1 Effect of the physical parameters on coefficients of shear stress, τ, rate of heat transfer, q, and couple stress, m

The effects of the micropolar heat conduction parameter, N^*, on the coefficients of the shear stress, rate of heat transfer and couple-stress are shown in figures 6.2(a)-6.2(c). From the figures 6.2(a) and 6.2(c) it is seen that the amplitudes of oscillation of the surface shear stress and couple-stress decrease slowly, while figure 6.2(b) indicate that the amplitude of heat transfer coefficient increases with x as the value of N^* increases.

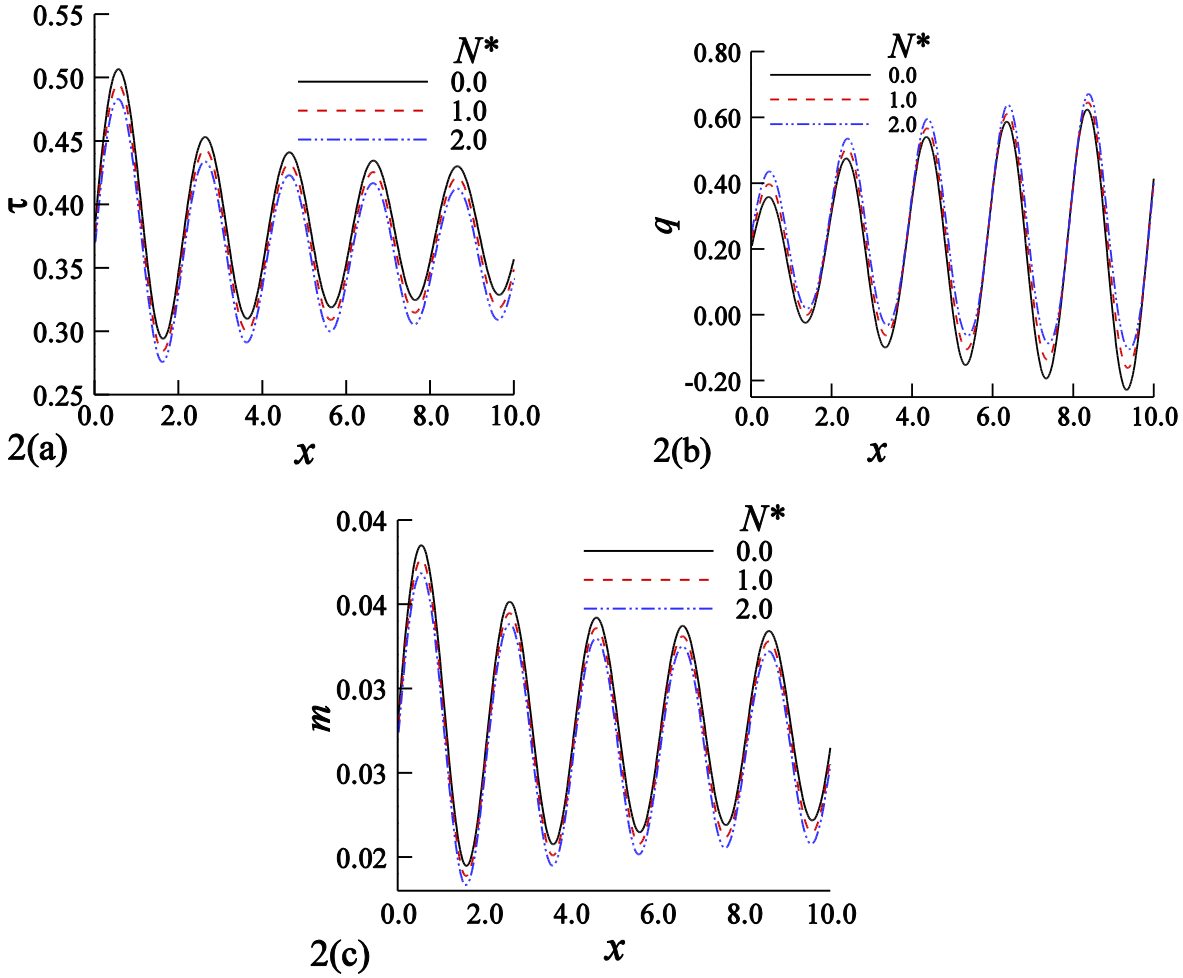

Fig. 6.2: Numerical values of (a) the shear stress (b) rate of heat transfer and (c) couple-stress against x for different values of N^* while Pr = 9.0, K=5.0, a = 0.5.

Figures 6.3(a)-(c) depict the effects of varying the vortex viscosity parameter, K, on the shear stress, rate of heat transfer and couple-stress. Figures suggest that the amplitude of oscillation of the shear stress, rate of heat transfer and couple-stress is higher for lower values of K. The reason for such an increase in the amplitude is that the value of K is higher for lower viscous fluid or higher vortex viscosity paraetemr.

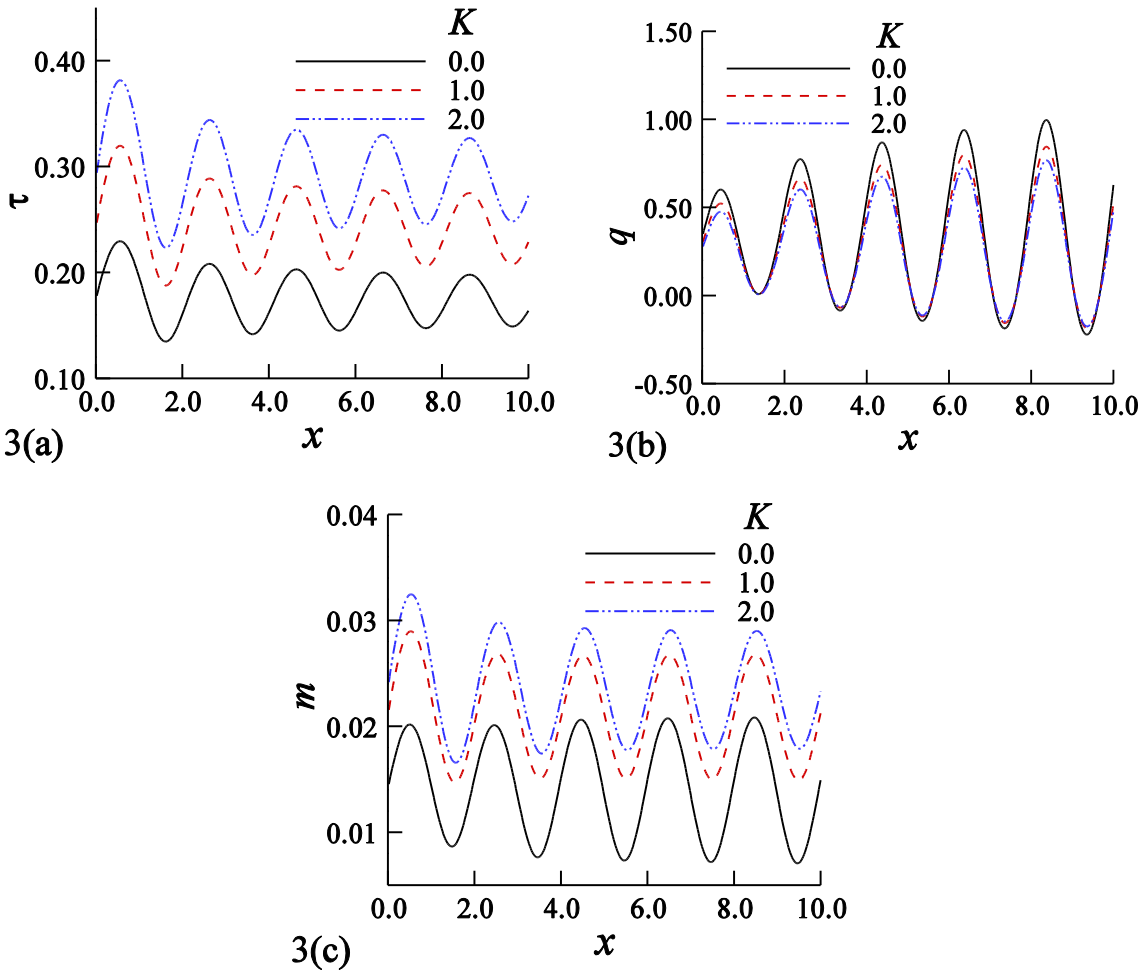

Fig. 6.3: The coefficients of (a) the shear stress (b) coefficient of heat transfer and (c) couple-stress against x for different values of K while Pr = 9.0, N^*=1.0, a = 0.5.

The influence of the amplitude of the surface temperature on the surface shear stress, rate of heat transfer and couple-stress is shown in figures 6.4(a)-(c). Evidently, the surface shear stress, the rate of heat transfer and the couple-stress are found to be higher with an increase of the amplitude of the surface temperature oscillation. It is due to strong influence of heat transfer from the surface.

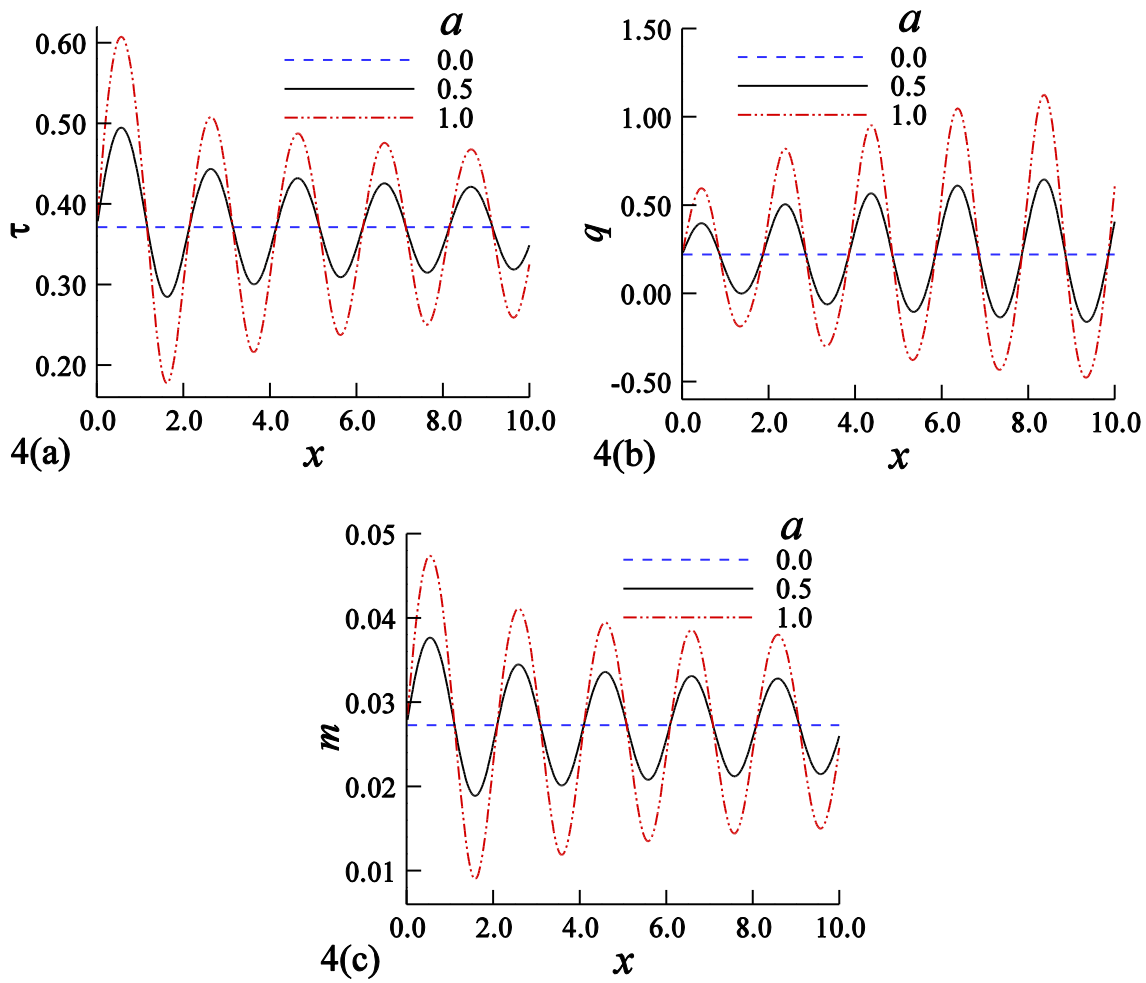

Fig. 6.4: Numerical values of (a) the shear stress (b) rate of heat transfer and (c) couple-stress against x for different values of a while Pr = 9.0, N*=1.0, K=5.0.

6.4.2 Effect of the physical parameters on the isolines of temperature, isolines of angular velocity and on streamlines

In this section we discuss the effects of the micropolar heat conduction parameter, N^*, the vortex viscosity parameter, K, and the amplitude of surface temperature, a, on the isolines of temperature, isolines of angular velocity as well as the streamlines in the boundary layer regimes.

Figures 6.5(a)-(c) demonstrate the effects of N^* on the isolines of temperature, isolines of angular velocity and the streamlines. Results indicate that for higher values of N^* the thermal and momentum boundary layers become wider but the isolines of angular velocity reduces. Also it is found that there develops near wall layers within the main boundary layers of temperature and isolines of angular velocity fields. These layers increase when N* increases.

Moreover, the oscillation in the fluid flow is observed due to streamwise variations of the surface temperature.

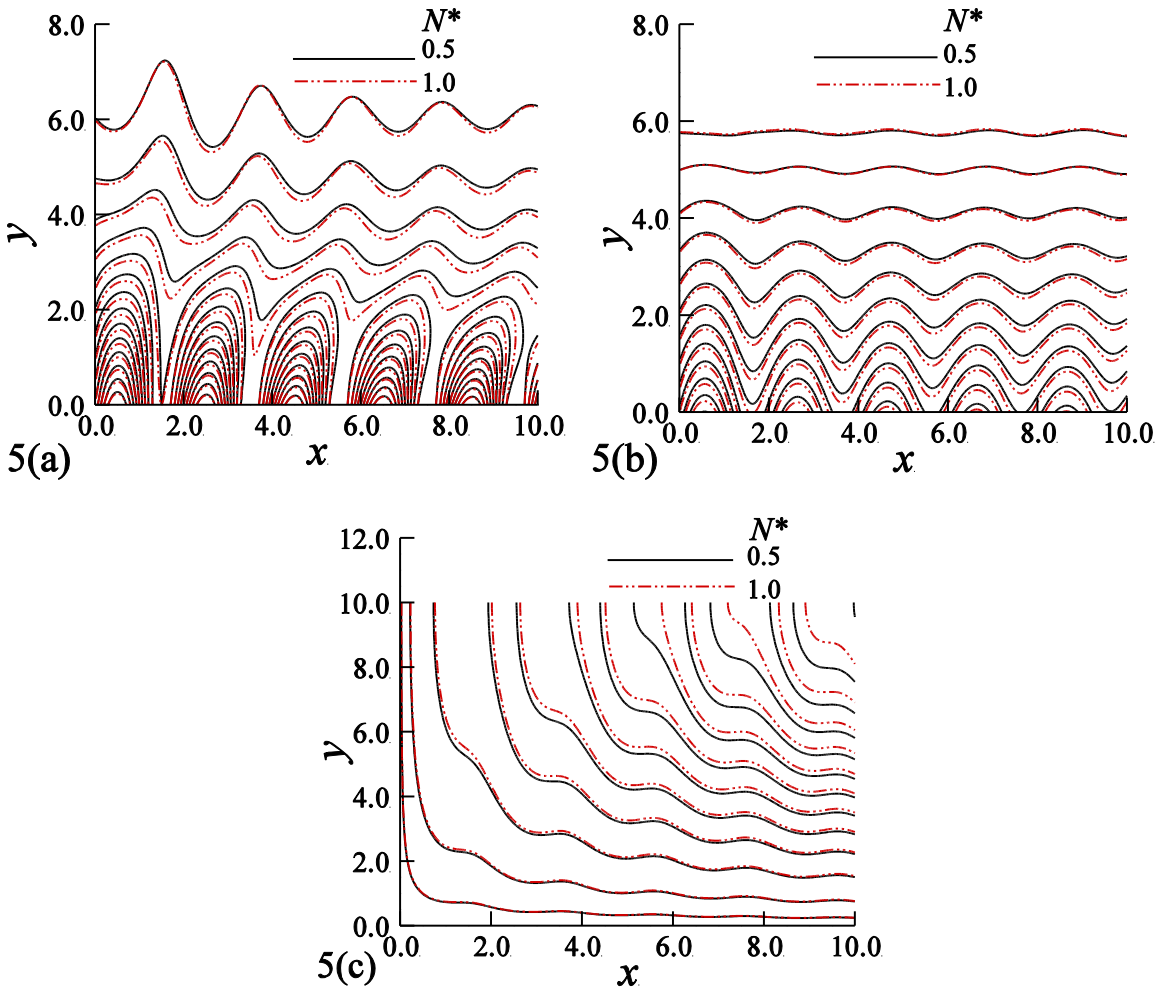

Fig. 6.5: (a) Isolines of temperature (b) isolines of angular velocity and (c) streamlines in the boundary layer for different values of N^* while Pr = 9.0, K=5.0, a = 0.5.

The influences of the variation of vortex viscosity parameter, K, on the isolines of temperature, isolines of angular velocity and the streamlines are depicted in figures 6.6(a)-(c). The thicknesses of the momentum and thermal boundary layers and the isolines of angular velocity become wider with the increase of K. It is because the vortex viscosity or the fluid viscosity significantly affects the fluid flow and heat transfer.

Figures 6.7(a)-(c) exhibit the effects of the amplitude of oscillation, a, on the isolines of temperature, isolines of angular velocity and the streamlines. It is observed that the momentum and thermal boundary layer thicken and the isolines of angular velocity is higher for higher values of the amplitude of oscillation, a. Due to high amplitude of oscillation in the

surface temperature, the fluid flow and heat transfer are seen to be oscillating with larger amplitude.

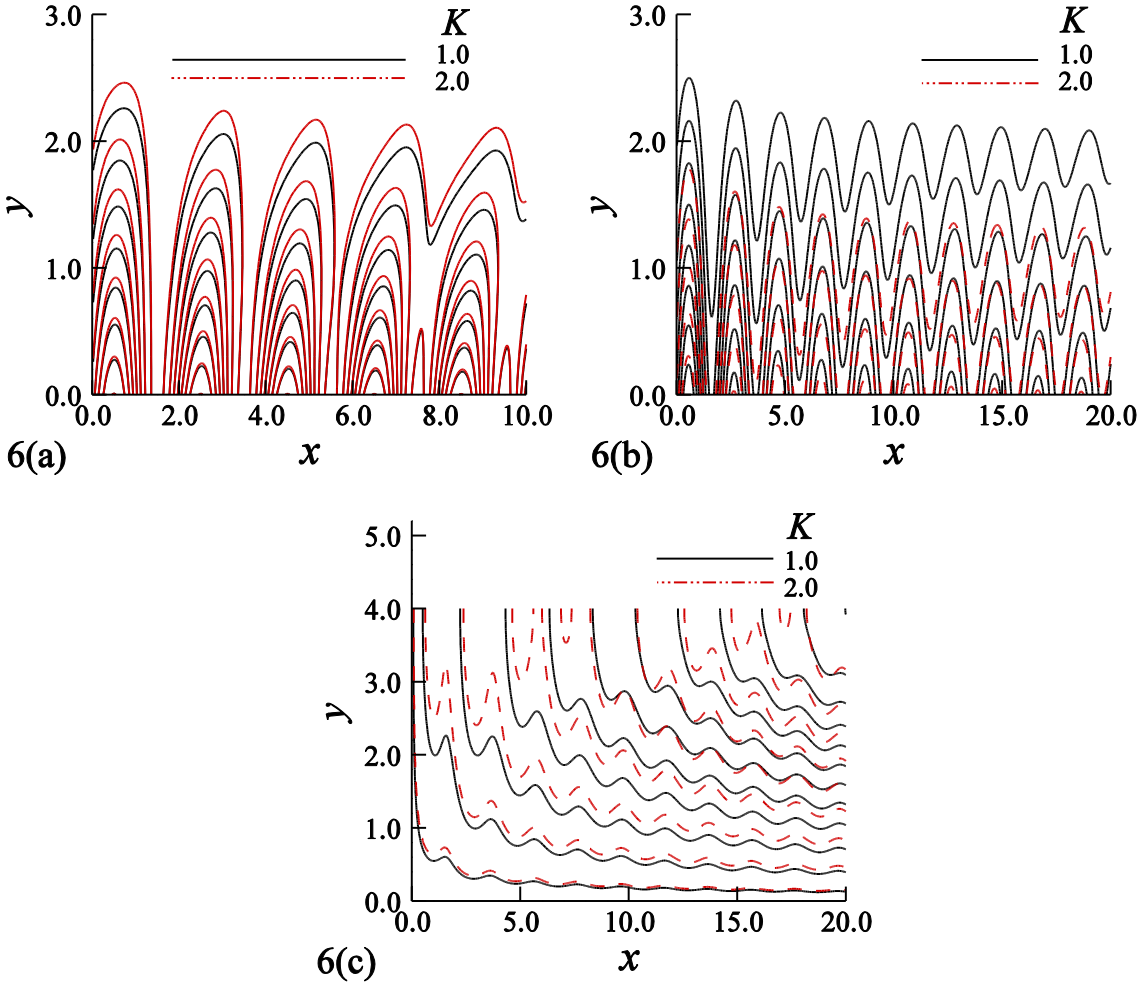

Fig. 6.6: (a) Isoclines of temperature (b) isoclines of angular velocity and (c) streamlines in the boundary layer for different values of K while Pr = 9.0, N^* =1.0, a = 0.5.

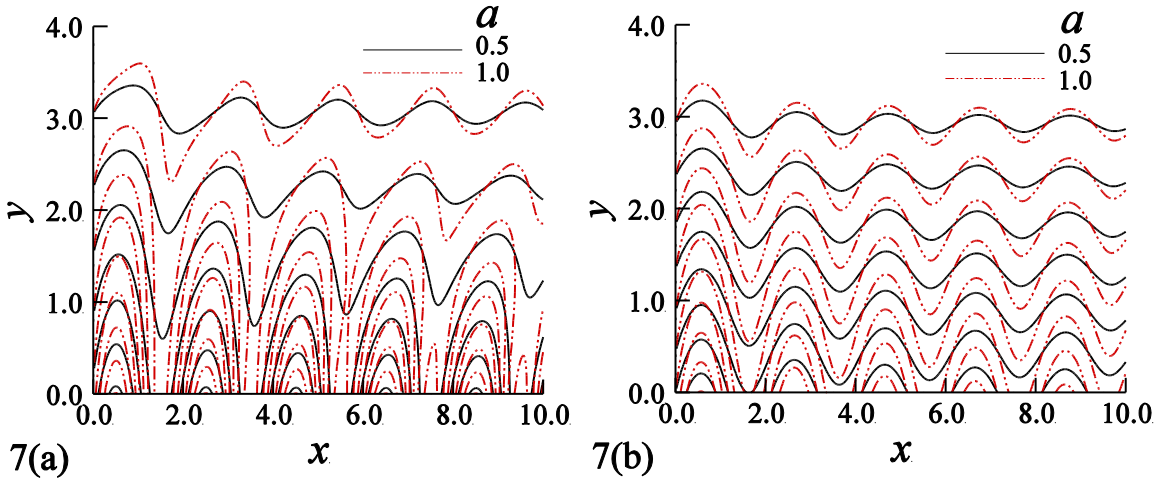

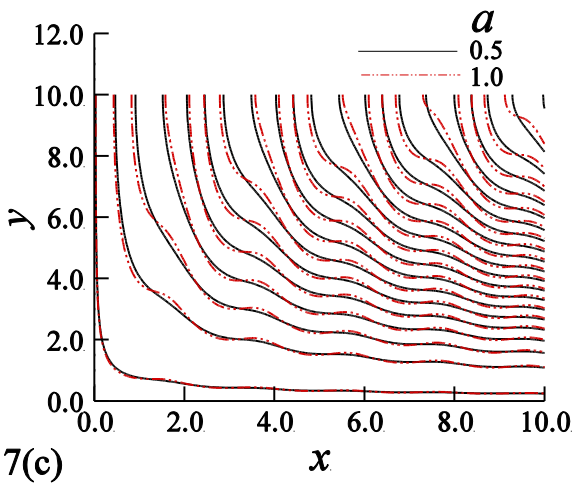

Fig. 6.7: (a) Isolines of temperature (b) isolines of angular velocity and (c) streamlines in the boundary layer for different values of a while Pr = 9.0, N^* =1.0, K = 5.0.

Chapter Seven
Summary and Future Work

The present dissertation deals with the effect of heat transfer of a steady free convection flow of Newtonian fluids along a uniform surface heat flux. We start by introducing a similarity transformation and the governing non-linear partial differential equations have been transformed into a system of non-linear ordinary differential equations which are locally similar and solved them numerically using shooting iterative technique.

From the present study we have investigated the effects of the vortex viscosity parameter, K , and the transpiration parameter, s , on laminar mixed convection boundary layer flow of a micropolar fluid past a vertical permeable flat plate. The governing boundary layer equations have been simulated employing four distinct methods, namely: (1) the series solution for small ξ, (2) the asymptotic solution for large ξ, (3) the implicit finite difference method together with Keller-box scheme and (4) the primitive-variable formulation method for all ξ. Results are expressed in terms of the surface shear stress, the couple-stress and heat transfer rate. From the present investigation it may be concluded that:

(i) Agreement between the solutions of the stream-function formulation and the primitive-variable formulation found to be excellent.

(ii) An increase in the value of the vortex viscosity parameter, K , leads to an increase in the value of the surface shear stress, the heat transfer rate and the local couple-stress.

(iii) Values of the surface shear stress, the heat transfer rate or the couple-stress increases due to increase in the rate of increase in fluid injection parameter s.

In this article we have investigated an unsteady free convection boundary layer flow of a thermo-micropolar fluid along a heated vertical plate, considering the presence of micropolar heat conduction. The reduced governing equations that are valid for entire time regimes are solved using explicit finite difference method. Asymptotic solutions for small and large time are also obtained. The results thus obtained are compared and found in excellent agreement. From the present investigation we may conclude the following:

1. The micropolar heat conduction, α^* leads to decrease the shear stress as well as the heat transfer; whereas, this leads to increase in the couple stress.
2. There is decrease in the value of shear stress and the couple stress and increase in the surface heat transfer owing to increase in the value of the vortex viscosity.

3. Both the axial velocity and angular velocity along with temperature profile increase due to increase in the micropolar thermal conductivity, α^*.

4. Increase in the vortex viscosity leads to decrease in the momentum boundary layer thickness; but leads to reduce the angular momentum boundary layer thickness.

In this Thesis, the unsteady free convection boundary layer flow of a thermo-micro polar fluid along a vertical plate has been discussed. It is assumed that the temperature of the plate is oscillating about a constant mean temperature, θ_w, with small amplitude, ε. The governing boundary layer equations are analyzed using, straight forward finite difference method for the entire values of locally varying variable, x. The effects of the material parameters such as angular velocity, N^*, the vortex viscosity parameter, K, on the shear stress, surface heat transfer and the couple-stress have been investigated. Through the present investigation it is found that micro polar fluids have a greater resistance (resulting from dynamic viscosity and vortex viscosity) to the fluid motion compared to Newtonian fluids.

The steady two-dimensional flow of an incompressible micropolar fluid about a vertical plate with the effect of stream wise sinusoidal variations of the surface temperature has been investigated. The governing boundary layer equations are solved numerically using the straight forward finite difference method. It is found that the vortex viscosity parameter and the amplitude of surface temperature strongly affect the shear stress, rate of heat transfer and couple stress while the influence of the micropolar heat conduction parameter is rather weak. The thicknesses of the momentum, thermal and angular velocity are found to be wider owing to an increase of the micropolar heat conduction parameter, the vortex viscosity parameter and the amplitude of surface temperature. But the exception is that the isoclines of angular velocity become lower for higher values of the micropolar heat conduction parameter.

Scope of possible future works

The results of this study may be made applicable in different fields of science, technology and industry. The possible extensions of the present study are indicated below:

- The present investigation can be extended for three dimensional studies.
- This work can be applied for other non -Newtonian micro polar fluid.
- Different numerical techniques can be applied to analyze this study and compare with existing methodologies.
- Better knowledge of this work will be helpful in designing of related equipment.
- The present analysis can be extended to study the influences of different parameters by changing the boundary conditions.
- This problem can be extended to nano fluid flow with an objective to explore how nano particles with volume fraction as parameter, affect the velocity and particularly temperature field.
- The future work can be carried out generalizing the geometry of the bearing shape, using different types of lubricants, types of loading and variation of magnetic field applied.
- Further this can be extended by applying Finite Volume Method.
- Velocity, temperature and concentration profiles for different variations of the parameters. This study may be helpful to do the two dimensional problems of unsteady MHD free convective flows.
- Also this study may be helpful in investigating the nature of flows.

Bibliography

[1] A. C. Eringen, Theory of micropolar fluids, J. Math. Mech., Vol. 16, p. 1–18 (1966).

[2] A.C. Eringen, Theory of thermomicropolar fluids, J. Math. Anal. Appl. Vol. 38, p. 480–496 (1972).

[3] M.M. Khonsari, On the self-excited whirl orbits of a journal in a sleeve bearing lubricated with micropolar fluids, Acta Mech. Vol. 81, p. 235–244 (1990).

[4] M. M. Khonsari, D. Brewe, On the performance of finite journal bearing lubricated wit micropolar fluids, STLE Tribology Trans., Vol. 32, p. 155–160 (1989).

[5] B. Hadimoto, T. Tokioka, Two-dimensional shear flows of linear micropolar fluids, Int. J. Eng. Sci. Vol. 7, p. 515–522 (1969).

[6] F. Lockwood, M. Benchaita, S. Freberg, Study of polyotropic liquid crystals in viscometric flow and elastohydrodynamic contact, ASLE Tribology Trans., Vol. 30, p. 539 (1987).

[7] J. D. Lee and A. C. Eringen, Boundary effects of orientation of nematic liquid crystals, J. Chem. Phys., Vol. 55, p. 4509–4512 (1971).

[8] T. Ariman, M.A. Turk and N.D. Sylvester, Microcontinum fluid mechanics-a review, Int. J. Eng. Sci., Vol. 11, p. 905–930 (1973).

[9] V. Kolpashchikov, N.P. Migun, P.P. Prokhorenko, Experimental determinations of material micropolar coefficients, Int. J. Eng. Sci., Vol. 21, p.405–411 (1983).

[10] T. Ariman, M.A. Turk, N.D. Sylvester, Application of microcontinum fluid mechanics, Int. J. Eng. Sci., Vol. 12, p. 273–293 (1973).

[11] G. Ahmadi, Self-similar solution of incompressible micropolar boundary layer flow over a semi-infinite plate, Int. J. Eng. Sci., Vol. 14, p. 639–646 (1976).

[12] D. A. S. Rees and Andrew P. Bassom, The Blasius boundary-layer flow of a micropolar fluid, Int. J. Eng. Sci., Vol. 34, p. 113–124 (1996).

[13] S. K. Jena and M. N. Mathur, Similarity solutions for laminar free convective flow of a thermomicropolar fluid past a non-isothermal vertical plate, Int. J. Eng. Sci., Vol. 19, p. 1431–1439 (1981).

[14] S. K. Jena and M. N. Mathur, Free convection in the laminar boundary layer

flow of thermomicropolar fluid past a non-isothermal vertical plate with suction/injection, Acta Mech., Vol. 42, p. 227–238 (1982).

[15] R. S. R. Gorla, Combined forced and free convection in micropolar boundary layer flow on a vertical flat plate, Int. J. Eng. Sci., Vol. 26, p. 385 (1983).

[16] M.A. Hossain, and M.K. Chowdhury and H.K. Takhar, Mixed convection flow of micropolar fluids with variable spin gradient viscosity along a vertical plate, J. Theo. And Appl. Fluid Mech., Vol. 1, p. 64 (1995).

[17] Y. Muri, Buoyancy effects in forced laminar convection flow over a horizontal flat plate, J. Heat Transfer, Vol. 83, p. 479 (1961).

[18] C.-P. Chiu, H.-M. Chou, Free convection in boundary layer flow of a micropolar fluid along a vertical wavy surface, Acta Mech., Vol. 101, p. 161 (1993).

[19] M.A. Hossain and M.K. Chowdhury, Mixed convection flow of micropolar fluid over an isothermal plate with variable spin gradient viscosity, Acta Mechanica, Vol. 131, p. 139–151 (1998).

[20] M.A. Hossain, M.K. Chowdhury and Ram Subba Reddy Gorla, Natural convection of thermomicropolar fluid from an isothermal surface inclined at a small angle to the horizontal, Int. J. of Num. Meth. Heat and Fluid Flow, Vol. 9, p. 814–832 (1999).

[21] R. Eichhorn, The effect of mass transfer on free convection, ASME J. Heat Transfer, Vol. 18, p. 260–263 (1960).

[22] E.M. Sparrow,and R.D. Cess, Free convection with blowing and suction, Int. J. Heat Mass Transfer, Vol. 23, p. 387 (1961).

[23] J.H. Merkin, Free convection with blowing and suction, Int. J. Heat Mass Transfer, Vol. 15, p. 989 (1972).

[24] J.H. Merkin, The effect of blowing and suction on free convection boundary layer, Int. J. Heat Mass Transfer, Vol. 18, p. 237 (1975).

[25] P.G. Perikh, R. Moffat, W. Kays, and D. Bershader, Free convection over a vertical porous plate with transpiration, Int. J. Heat Mass Transfer, Vol. 14, p. 205 (1971).

[26] J.P. Hartnett, and E.R.G. Eckert, Mass transfer cooling in a laminar boundary layer with constant fluid properties, ASME J. Heat Transfer, Vol. 79, p. 247 (1975).

[27] E.M. Sparrow and J.B. Starr, The transpiration cooling flat plate with various thermal and velocity boundary condition, Int. J. Heat Mass Transfer, Vol. 9,p. 508 (1966).

[28] T.T. Kao, Laminar incompressible forced convection along a flat plate with arbitrary suction or injection at the wall, ASME J. Heat Transfer, Vol. 97, p. 484 (1975).

[29] T.T. Kao, Locally non-similar solution for free convection along a flat plate with arbitrary suction or injection at the wall, ASME J. Heat Transfer, Vol. 97, p. 484 (1976).

[30] M. Vedhanayagam, R.A. Altenkirch and R. Echhorn, A transformation of the boundary layer equation for free convection flow past a vertical flat plate with arbitrary blowing and wall temperature variation, Int. J. Heat Mass Transfer, Vol. 23, p. 1236 (1980).

[31] Yucel, A. Mixed convection micropolar fluid flow over horizontal plate with surface mass transfer. Int. J. Eng. Sci., Vol. 27, pp. 1593 (1989).

[32] H. A. Attia, Investigation of non-Newtonian micropolar fluid flow with uniform suction/blowing and heat generation, Turkish J. Eng. Env. Sci. Vol. 30, p. 359 – 365 (2006).

[33] A. Ishak, R. Nazar, I. Pop, MHD boundary-layer flow of a micropolar fluid past a wedge with variable wall temperature, Acta Mech., Vol. 196, p. 75–86 (2008).

[34] S. K. Jena and M. N. Mathur, Mixed convection flow of a micropolar fluid from an isothermal vertical surface, Comp & Math. with Appl. Vol. 10, p. 291–304 (1984).

[35] M.A. Hossian, M.K. Chowdhury, R. S. R. Gorla, Free convection flow of thermo- micropolar fluid along a vertical plate with non-uniform surface temperature and surface heat flux, Int. J. Numerical Methods for heat and Fluid Flow, Vol. 9, p. 568–585 (1999).

[36] M. Mosharof Hossain, N. C. Roy, and M. A. Hossain; Boundary layer fow and heat transfer in a micropolar fuid past a permeable flat plate; Theoret. Appl. Mech., Vol. 40, p. 403–425 (2012).

[37] Gorla, R. S. R. and Takhar, H. S., Unsteady mixed convection boundary layer flow of a micropolar fluid near the lower stagnation point on a cylinder, Int. J.

Eng. Fluid Mech., Vol. 4, p. 337–351 (1991).

[38] M. Kumari and G. Nath; Unsteady incompressible boundary layer flow of a micropolar fluid at a stagnation point, Int. J. Engng Sci., Vol. 22, No. 6, p. 168, (1984).

[39] Y.Y. Lok, N. Amin, I. Pop, Unsteady boundary layer flow of a micropolar fluid near the rear stagnation point of a plane surface, Int. J. Thermal Sci. Vol. 42, p. 995–1001 (2003).

[40] H. Xu, S. J. Liao, Shanghai, China, and I. Pop, Series solutions of unsteady boundary layer flow of a micropolar fluid near the forward stagnation point of a plane surface; Acta Mechanica Vol. 184, p. 87–101 (2006).

[41] M. Kumari and G. Nath; Unsteady mixed convection flow of a thermomicropolar fluid on a long thin vertical cylinder, Int. J. Engng Sci. Vol. 27, No. 12, p. 1507–1518 (1989).

[42] C. C. Wang, C. K. Chen, Transient force and free convection along a vertical wavy surface in micropolar fluids, Int. J, Heat Mass Transfer, Vol. 44, p. 3241–3251 (2001).

[43] H. P. Rani and Chang Nyung Kim; A transient natural convection of micropolar fluids over a vertical cylinder; Heat Mass Transfer, Vol. 46, p. 1277–1285(2010).

[44] M. Mosharof Hossain, N.C. Roy, A. C. Mandal and M. A. Hossain; Fluctuating Flow of Thermomicropolar Fluid past a vertical surface, Appl. Applied Mathematics, Vol. 8, p. 128–150 (2013).

[45] M.A. Hossain, S. Bhowmick, R.S.R. Gorla, Unsteady mixed-convection boundary layer flow along a symmetric wedge with variable surface temperature, Int. J. Eng. Sci., Vol. 44, p. 607–620 (2006).

[46] S.M. Mahfooz, M.A. Hossain, R. S. R. Gorla, Radiation effects on transient MHD natural convection flow with heat generation, Int. J. Thermal Sci., Vol. 58, p. 79–91 (2012).

[47] M. J. Lighthill, The response of laminar skin-friction and heat transfer to fluctuations in the stream velocity, Proc.. Royl. Soci., Vol. A 224, p. l–23 (1954).

[48] R. S. Nanda and V. P. Sharma, Free convection laminar boundary layers in oscillatory flow, J. Fluid Mech., Vol. 15, p. 419–428 (1963).

[49] S. Eshghy, V. S. Arpaci and J. A Clark, The effect of longitudinal oscillation on free convection from vertical surface, J. Appl. Mech. Vol. 32, p.183–191 (1965).

[50] P. K. Muhuri and M. K. Maiti, Free convection oscillatory flow from a horizontal plate, Int. Heat Mass Transfer, Vol. 10, p. 717–732 (1967).

[51] R. L. Verma, Free convection fluctuating boundary layer on a horizontal plate, J. Appl. Math. Mech., Vol. 63, p.483–487 (1982).

[52] M. D. Kelleher and K. T.,Yang, Heat transfer response of laminar free-convection boundary layers along a vertical heated plate to surface-temperature oscillations, J. App. Math. Phys., Vol. 19, p. 31–44 (1968).

[53] M. A. Hossain, S. K. Das and I. Pop, Heat transfer response of mhd free Convection flow along a vertical plate To surface temperature oscillations, Int. J. Non-Linear Mech.Vol. 33,p. 541– 553 (1998a).

[54] M. A. Hossain, S. K. Das and D. A. S. Rees, Heat transfer response of free convection flow from a vertical heated plate to an oscillating surface heat flux, Acta Mechanica, Vol. 126, p.101–113 (1998b).

[55] M. Ashraf, S. Asghar and M. A. Hossain, Fluctuating hydromagnetic natural convection flow Past a magnetized vertical surface in the presence of thermal radiation, Thermal Sci., Vol. 16, pp. 1081–1096 (2012).

[56] M. K. Jaman and M. A. Hossain, Effect of Fluctuating Surface Temperature on Natural Convection flow over cylinders of Elliptic Cross Section, Transport Phenomena Journal, Vol. 2, p. 35–47 (2010).

[57] M. D. Kelleher and K. T. Yang, Heat transfer response of laminar free-convection boundary layers along a vertical heated plate to surface-temperature oscillations. J. App. Math. Phys., Vol. 19, pp. 31–44(1968).

[58] R.S.R. Gorla, H.S. Takhar, A. Slaouti, MHD free convection boundary layer flow of a thermomicropolar fluid over a vertical plate, Int. J.Eng.Sci. Vol. 36, p. 315–327 (1998).

[59] M. Mosharof Hossain, N.C. Roy, M.A. Hossain, Transient natural convection flow of thermo-micropolar fluid of micropolar thermal conductivity along a non-uniformly heated vertical surface, Advances in Mechanical Engineering, 10.1155/2014/141437 (2014).

[60] D.A.S. Rees, The effect of steady streamwise surface temperature variations on

vertical free convection, Int. J. Heat Mass Transfer, Vol. 42, p. 2455–2464 (1999).

[61] N.C. Roy and M.A. Hossain, Numerical solution of a steady natural convection flow from a vertical plate with the combined effects of streamwise temperature and species concentration variations, Heat Mass Transfer Vol. 46, p. 509–522 (2010).

[62] Md. Mamun Molla, Md. Anwar Hossain, Rama Subba Reddy Gorla, Natural convection laminar flow with temperature dependent viscosity and thermal conductivity along a vertical wavy surface , Int. J. Fluid Mechanics Research, Vol. 36, p. 272–288 (2009).

[63] H. Pohlhausen, Der Warqneaustausch Warqneaustausch zwischen festen korpern and Flussigkeiten mit kleiner Reibung and Kleiner Warmeleitung ZAMN Vol. 1, p.115–121 (1921).

[64] S. Ostrach, An analysis of laminar free convection flow and heat transfer along a flat plate parallel to the direction of the generating body force, NACA Report Vol., p. (1953).

[65] E.M. Sparrow, R. Eichor and J.L. Gregg, Combined forced and free convection in a boundary layer flow, Physics Fluids, Vol. 2, p. 319–328 (1959).

[66] J.H. Merkin, The effect of buoyancy forces on the boundary layer flow over a semi-infinite vertical flat plate in a uniform stream, J. Fluid Mech., Vol. 35, p. 439–450 (1969).